Coastal and Hydraulics Laboratory

US Army Corps of Engineers®
Engineer Research and
Development Center

Camp Marmal Flood Study

Jeremy A. Sharp, Steve H. Scott, Mark R. Jourdan, and Gaurav Savant

March 2012

Camp Marmal Flood Study

Jeremy A. Sharp, Steve H. Scott, Mark R. Jourdan, and Gaurav Savant

Coastal and Hydraulics Laboratory
U.S. Army Engineer Research and Development Center
3909 Halls Ferry Road
Vicksburg, MS 39180

Final report

Abstract

The ERDC-CHL conducted the Camp Marmal Flood Study at the request of the Afghanistan District. Major flooding at the camp occurs from upland sources. The purpose of the study was to determine the effectiveness of flood mitigation alternatives. The AdH 2-D shallow water finite element model was implemented for the study. Boundary conditions for AdH were generated with HEC-HMS. The HEC model used local rainfall data to generate the routed run-off hydrograph from upstream watersheds. Existing conditions were simulated with the generated hydrographs to determine the potential flood characteristics of the facility and for the comparison of the alternatives. Additionally, a sensitivity analysis was conducted to determine the effect of variations in Manning's n and run-off return periods. The 20 year, 24 hour event was selected for simulation in the alternatives. The District provided three alternatives for evaluation in the model. Alternative 1 provided minimum protection. Alternative 2 showed increased protection, but there were several issues of concern that made it less ideal. Alternative 3 potentially provided the most flood mitigation. However, prior to construction of any alternative it is recommended that the final design be simulated in the AdH model.

Contents

Report Documentation Page

Figures and Tables

Figures

Tables

Preface

This study was conducted for the U.S. Army Engineer District, Afghanistan under project identification "Camp Marmal Flood Study." The technical monitors were Martin L. Ahmann and John J. Heitstuman.

The work was performed by the River Engineering Branch of the Flood and Storm Protection Division, U.S. Army Engineer Research and Development Center – Coastal and Hydraulics Laboratory. At the time of publication, Lisa Hubbard was Chief of the River Engineering Branch; Bruce Ebersole was Chief of the Flood and Storm Protection Division; and Bill Curtis was the Technical Director for Flood and Coastal Storm Damage Reduction. The Deputy Director of CHL was Jose E. Sanchez and the Director was Dr. William Martin.

COL Kevin J. Wilson was the Commander and Executive Director of ERDC, and Dr. Jeffery P. Holland was the Director.

Unit Conversion Factors

Multiply	By	To Obtain
feet	0.3048	meters
yards	0.9144	meters

1 Introduction

Camp Marmal and the Mazar-e Sharif airfield, located in northeast Afghanistan, provide support to coalition operations in the area. The airfield is located on an alluvial fan with steep and flat terrain and currently has issues with flooding. Flood waters flow out of upland sources and inundate the camp. After upstream events, flooding occurs both in the camp and the airfield. Once flooded, the airfield loses part or all of its operational readiness compromising the usability of the airfield. With expansions to the camp planned in the future, continued issues with flooding are expected. Measures are necessary to reduce or eliminate flooding at the camp and airfield.

Current flood mitigation measures include a diversion ditch to direct low magnitude flows around the facility. Additionally, a security wall upstream of the ditch impedes flow, reducing the peak flow experienced by the diversion ditch. Internal to the camp is a system of culverts and ditches that handles on-Base drainage, but is not intended to accommodate upland sources.

The Afghanistan District, Trans Atlantic North (TAN), requested the assistance of the ERDC-CHL to evaluate flood mitigation alternatives. A two-dimensional (2-D) depth-averaged model, Adaptive Hydraulics (AdH), was applied for analysis to evaluate flood mitigation plans. Initially, the model was used to simulate the existing condition to determine the possible flood extents for the current airbase configuration. Proposed TAN alternatives were then implemented in the model to determine their respective effectiveness for eliminating flooding on the Airbase. The existing conditions were compared to the alternatives, based on design criteria provided by TAN.

2 Approach

A three-phase approach was implemented to evaluate and determine the most appropriate mitigation measure at Camp Marmal and the Mazar-e Sharif airfield. Existing conditions currently in place were evaluated for a basis of comparison. Once established, the existing condition was used to determine the sensitivity of the model. The sensitivity analysis provided a systematic approach of selecting the design event simulated in the three alternatives. Once simulated, the three alternatives were compared to the existing condition to determine the most effective flood mitigation measure.

Each simulation, including the existing condition and the three alternatives, were established on the same mesh. The base mesh was the existing simulation mesh, which was constructed using lidar data provided by TAN. Additionally, key features, i.e. airfield, tarmac, and security wall, were located and delineated with aerial images. Modifications were then made to the base mesh to construct the TAN provided alternatives. These modifications included new ditches, basins, and berm profiles. The new features required modified topography and mesh resolution.

The model applied in this study was the 2-D Adaptive Hydraulics model (AdH) Savant et al. (2011). It is an ERDC-developed model that has been used for estuaries, rivers, dam breaks, and overland flow scenarios. AdH is an implicit, conservative model that uses an unstructured finite element mesh. It can simulate both super and subcritical flow, and wetting and drying, which is critical for the Camp Marmal simulations. Finally, as the name implies, the model can be adapted both spatially and temporally. The AdH model provided the means to simulate the flow spreading aspects of the study both in the channel and overland.

Model boundary conditions were simulated using simulated hydrographs. The hydrographs were based on local rainfall data. The rainfall data were routed through the upstream watersheds with HEC-HMS (http://www.hec.usace.army.mil/software/hec-hms/) which generated an outlet hydrograph applicable for the AdH model. Seven 24-hour return periods were simulated over twelve delineated watersheds in the HEC model.

Existing conditions were simulated using the generated hydrographs, resulting in inundation of the camp and airfield. Upstream flow is routed from the southern mountains and foothills. The flow is first intercepted by the southern security wall. This wall acts as a retention basin as the flow is backed up. Once against the wall, the flow begins to pass through culverts and gates. Passing through the openings in the wall, the flow floods the eastern portion of the camp and the majority of the airfield. For all simulations, the internal drainage system of the camp is not included since it is not intended to carry upstream flow volumes.

Simulations of alternative measures consisted of three different flood ditch configurations. In addition, there was an alternative simulated that had been recommended by the German Command. The German alternative proposed using the existing wall to impound water. The first alternative evaluated the effectiveness of an anti-vehicle ditch on the western portion of the camp. The second and third alternatives evaluated two different berm and ditch alignments along with a retention basin to minimize downstream flooding.

3   Mesh Construction

3.1   Mesh configuration

The construction of an existing condition mesh was achieved based on current landscape elevations. The existing mesh is comprised of 323,166 nodes and 645,327 elements. The domain outline is shown in Figure 1 with the brown color. The mesh is shown in the inset. The average element size in the area of interest ranges from $2 - 100$ m². Delineated within the mesh is the air-field and camp along with the flood diversion ditch and wall south of the camp, shown in red (Figure 1).
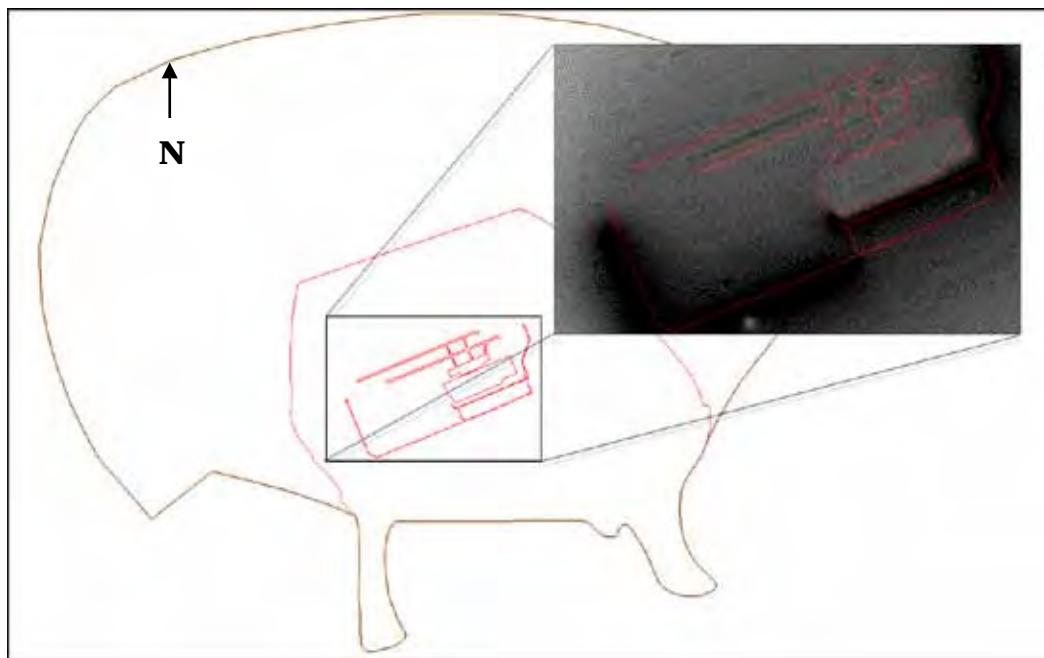
Figure 1. Existing mesh setup with exploded view of airfield and camp.

Each element is assigned a material type (Figure 2). The material type identifier defines the skin friction in terms of the Manning's n roughness coefficient and the eddy viscosity. There are six materials defined in the existing mesh configuration, representing the area surrounding the airfield and camp, the diversion ditch to the south, the solid wall to the south, airfield, and the camp. These five materials represent the landscape features as defined by aerial imagery. The sixth material, shown in green, represents a continued length to the downstream boundary (Figure 3). This provides a stable tailwater boundary while eliminating backwater conditions.
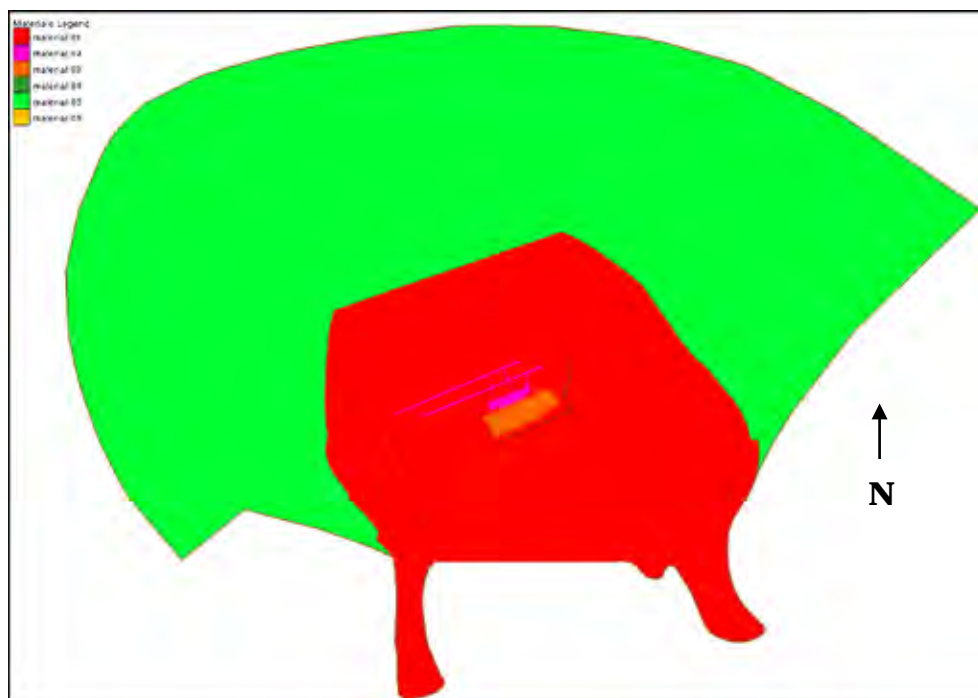
Figure 2. Material view of existing condition mesh.
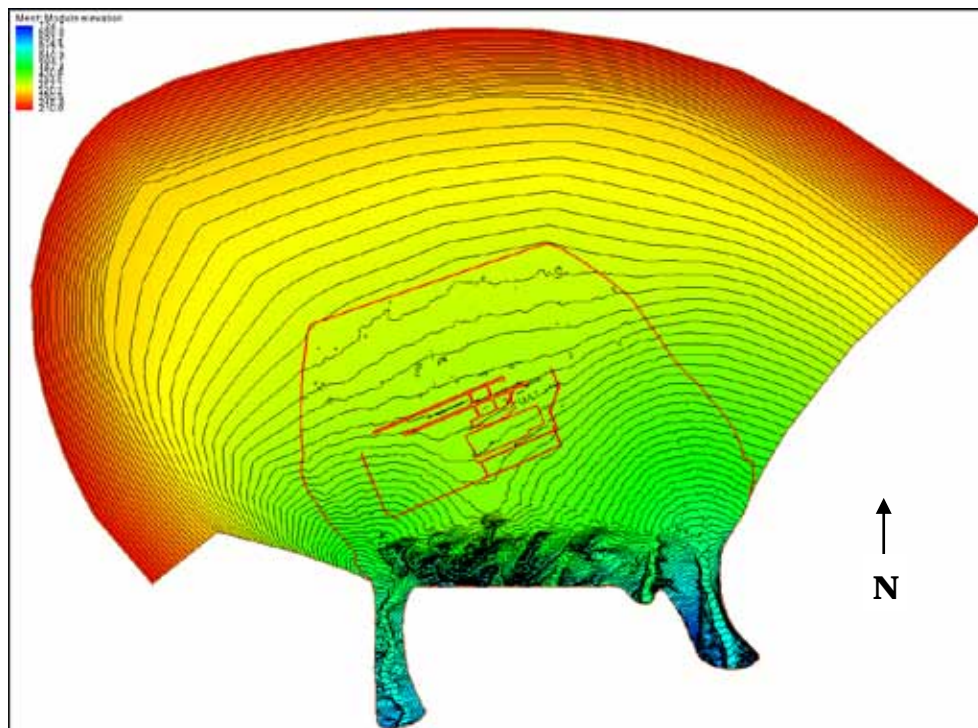
Figure 3. 5 m elevation contours in existing condition mesh.

Topographic data shown in Figures 3 and 4 were provided by TAN. The source of the data was a lidar survey, and is referenced to UTM Zone 42 WGS 1984.
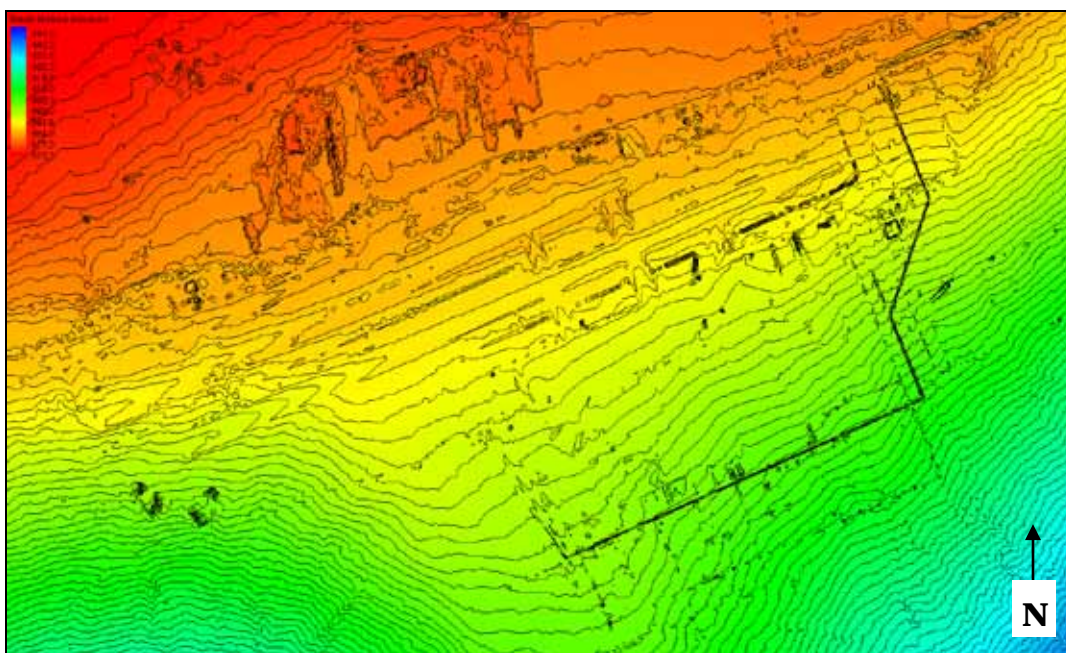
Figure 4. 1 m contours of mesh in the camp.

3.2 Boundary conditions

The model's upstream boundary conditions are driven with runoff from the surrounding watersheds directed through five major wadies. The model defines the wadies as inflow boundaries. To conservatively account for all contributing flow to Camp Marmal, runoff south of the camp is directed through these five boundaries (Figure 5). Watersheds in the domain that are south of the airfield are denoted as interior watersheds (Figure 7) and those outside and south of the domain are exterior watersheds (Figure 8). Watersheds to the north are downstream and considered non-contributing.

Combining interior and exterior watersheds (Table 1) required the calculation of lag times to adjust the interior watersheds to the boundary. Typical lag times were estimated by velocities calculated in the model along with the measured travel distance. These velocities ranged from 2 – 4 m/sec with the travel distance measured along a straight path. The straight path is used because it is difficult to define a flow path with overland flow. The lag times varied from 900 – 1,800 seconds. Of the contributing sources, although stream 5 was the largest, it did not contribute to flooding on the camp; stream 4 produced the largest volume of flooding to the camp (Figure 6). Other contributors to camp flooding are streams 2 and 3.

Figure 5. Location of boundary conditions.

Table 1. Combined interior and exterior watersheds for corresponding stream number.

	Exterior Watershed	Interior Watershed
Stream 1	1-B	11, 12
Stream 2	na	14, 13
Stream 3	na	15
Stream 4	2-B	16, 17, 18
Stream 5	3-B	19

3.3 Adaptive hydraulics model (AdH)

The equations solved in AdH are the 2-D non-linear shallow water equations. Although not applicable for turbulent flow or where vertical acceleration is present, these equations have proven successful in describing non-breaking conditions (Reeve et al. 2008). Fundamentally, the equations are derived on the assumption that the vertical velocity component is negligible. For this study, the primary application is to simulate a flood surge, and it is assumed that the equations are applicable for the given conditions.
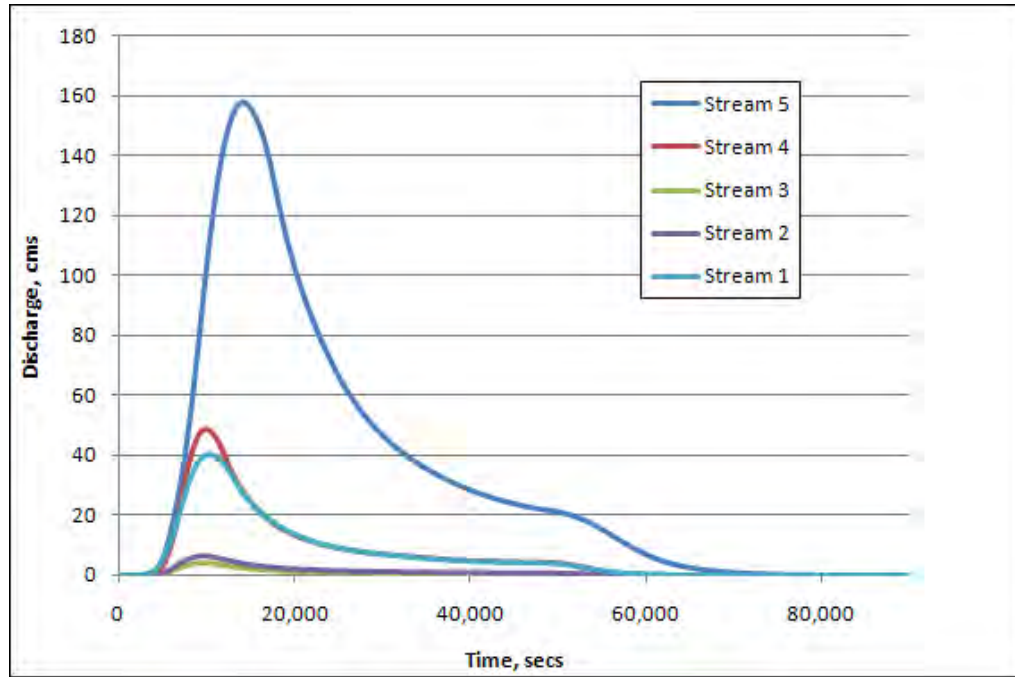
Figure 6. Combined watershed runoff for 20-yr event.

Neglecting shear stress and fluid pressure at the free surface, the 2-D shallow water equations as implemented within AdH are written as:

$$\frac{\partial Q}{\partial t} + \frac{\partial F_x}{\partial x} + \frac{\partial F_y}{\partial y} + H = 0 \tag{1}$$

where

$$Q = \begin{Bmatrix} h \\ uh \\ vh \end{Bmatrix} \tag{2}$$

$$F_x = \begin{Bmatrix} uh \\ u^2 h + \frac{1}{2}gh^2 - h\dfrac{\sigma_{xx}}{\rho} \\ uvh - h\dfrac{\sigma_{yx}}{\rho} \end{Bmatrix} \tag{3}$$

$$F_y = \left\{ \begin{array}{c} vh \\[2mm] uvh - h\dfrac{\sigma_{yx}}{\rho} \\[3mm] v^2 h + \dfrac{1}{2} gh^2 - h\dfrac{\sigma_{yy}}{\rho} \end{array} \right\} \tag{4}$$

and

$$H = \left\{ \begin{array}{c} 0 \\[2mm] gh\dfrac{\partial z_b}{\partial x} + n^2 g\dfrac{u\sqrt{u^2 + v^2}}{h^{1/3}} \\[3mm] gh\dfrac{\partial z_b}{\partial y} + n^2 g\dfrac{v\sqrt{u^2 + v^2}}{h^{1/3}} \end{array} \right\} \tag{5}$$

The Reynolds stresses (σ), where the first subscript indicates the direction and the second indicates the face on which the stress acts, are due to turbulence. The Reynolds stresses are determined using the Boussinesq approach to the gradient in the mean currents:

$$\sigma_{xx} = 2\rho v_t \frac{\partial u}{\partial x} \tag{6}$$

$$\sigma_{yy} = 2\rho v_t \frac{\partial v}{\partial y} \tag{7}$$

and

$$\sigma_{xy} = \sigma_{yx} = 2\rho v_t \left(\frac{\partial u}{\partial y} + \frac{\partial v}{\partial x} \right) \tag{8}$$

Here v_t = kinematic eddy viscosity, which varies spatially where turbulence closure is achieved through the algebraic eddy viscosity formulation described by Rodi (1993).

The equations are discretized using the finite element method in which u, v, and h are represented as linear polynomials on each element.

The set of partial differential equations represented in Equation 1 solved with the finite element method using the approach of Petrov-Galerkin that incorporates a combination of a Galerkin test function and a non-Galerkin component to control oscillations due to convection (Berger 1997).

AdH utilizes a Pseudo-Transient Continuation and Switched Evolution Relaxation inspired time step size selection algorithm (Savant et al. 2010). This technique computes the optimal time step size dependent on the L2 norm of the system of equations. This selection algorithm provides an efficient technique for temporally accurate solution of rapidly varying hydrodynamic and sediment flows. Additional information about the AdH model can be accessed at www.adh.usace.army.mil.

4   Hydrograph Development

Mazar-e Sharif receives most of its precipitation between early December and late April. During May through November, precipitation is very light and rare during the summer. The annual average precipitation is about 200 mm per year. On average, the wettest months are February, March, and April when typically about 40 mm is expected each month. These three months account for 60 percent of the annual total.

The heaviest precipitation occurs during the late winter and spring months when strong transitory weather systems move across Afghanistan and produce heavier precipitation. Usually, heavy precipitation does not persist for more than a couple of days.

Daily Tropical Rainfall Measuring Mission (TRMM) data from January 1998 through November 2010 were sorted by the maximum for each year, and then a rainfall intensity algorithm was applied. The TRMM data generally agrees in intensity with the observed climate data provided by the Air Force Climate Center.

The climate chart is based on Air Force Climate Center data and TRMM data. The location is in a relatively flat region and at an elevation of 378 meters (~1240 feet). Much higher terrain rises quickly to the south and if river flow from these mountains is important, the effects of terrain must be accounted for due to dramatically increased precipitation, snow, and snow cover.

Using the precipitation amounts from Table 2, design hydrographs were developed for flows that could potentially affect the airfield. Figure 7 illustrates watersheds contributing from south of the computational domain. Note that the domain is slightly different than that of the final domain used. Figure 8 illustrates those watersheds that contribute flow that are at least partially, if not completely, within the computational domain. These watersheds were delineated from Level 2 Digital Terrain Elevation Data (DTED) using the USACE Watershed Modeling System (WMS).

Hydrographs for the selected return periods were developed using the WMS and the HEC-HMS model. Three hydrographs were generated with

their associated curve numbers listed in Table 3. Based on the overall objective and understanding of the problem, Hydrograph 2 is currently recommended by ERDC-CHL for simulation of the existing condition and mitigating alternatives. Hydrograph 3 is only implemented for model sensitivity analysis. Figure 9 depicts Hydrographs 2 for Basin 2B, a main contributor to camp flooding.

Table 2. Precipitation amounts for selected return periods.

Return Period (yr)	24 hour Precipitation (mm)
2	27.4
5	36.7
10	42.9
25	50.7
50	56.5
100	62.3
4 inch	102.0
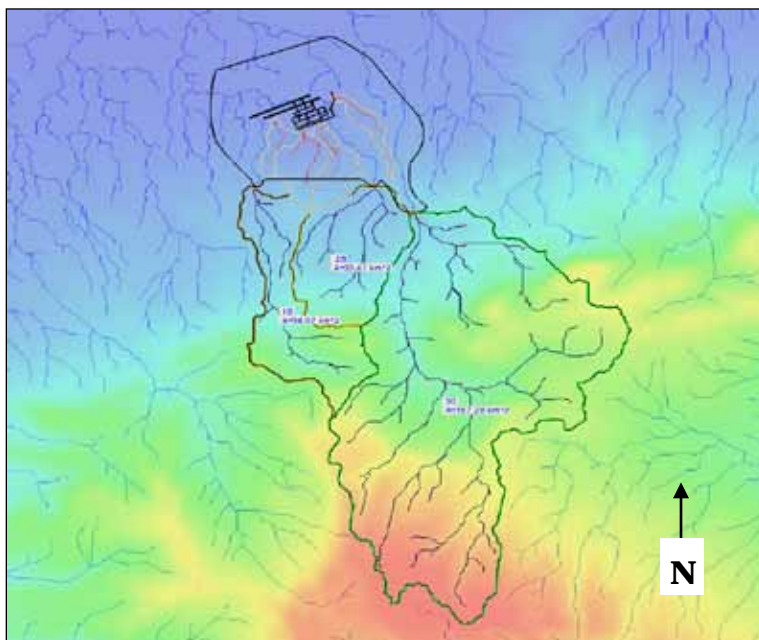
Figure7. Exterior to the domain contributing watersheds.
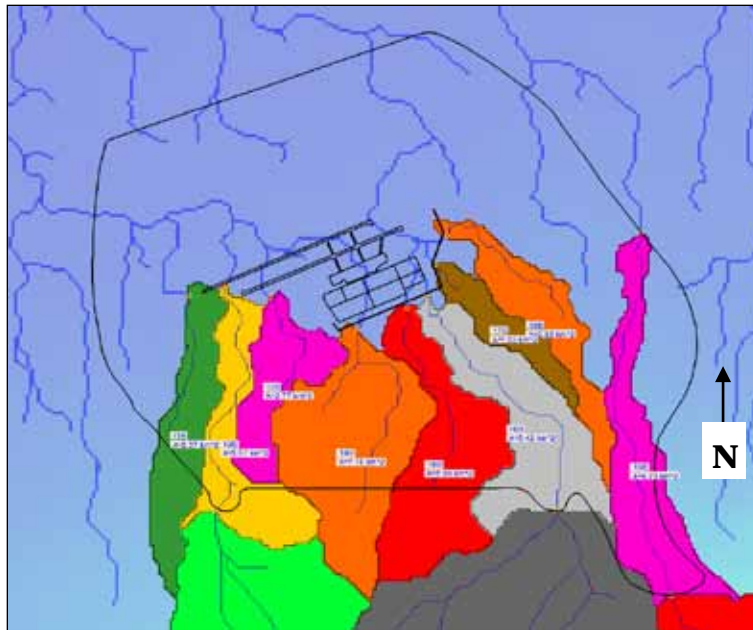
Figure 8. Interior to the domain contributing watersheds.

Table 3. Curve numbers for associated basin and hydrograph.

	Basin	Hydrograph 1	Hydrograph 2	Hydrograph 3
Exterior Watershed	1-B	98.0	82.3	76.3
	2-B	98.0	78.6	70.6
	3-B	98.0	83.2	75.2
Interior Watershed	11	98.0	72.5	64.5
	12	98.0	74.5	66.5
	13	98.0	75.1	67.1
	14	98.0	77.3	69.3
	15	98.0	77.4	69.4
	16	98.0	77.8	69.8
	17	98.0	76.1	68.1
	18	98.0	77.3	69.3
	19	98.0	83.4	75.4

Figure 9. Typical hydrograph for contributing watersheds.

5   Existing Condition Simulations

5.1   Sensitivity analysis

ERDC conducted a sensitivity analysis to determine the impact of varying model parameters. This was necessary since no validation data were available. Model sensitivity was evaluated by varying three parameters; surface friction, magnitude, and infiltration. From these parameters twelve runs were set up and executed. Table 4 shows the twelve sensi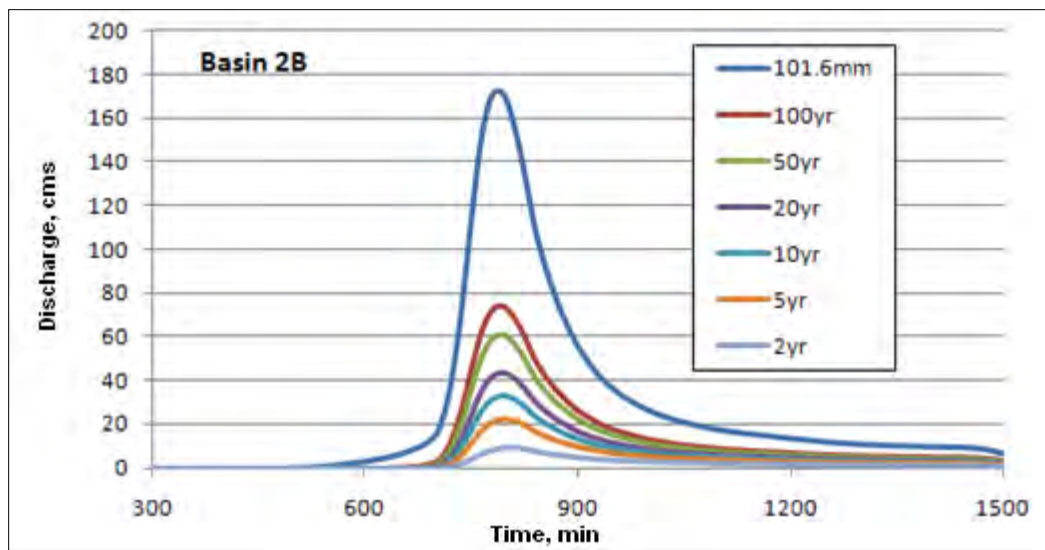tivity runs and their respective parameters. Although this is not a comprehensive sensitivity analysis, it does serve to illuminate model variability and potential shortcomings.

Table 4. Run matrix for sensitivity analysis of existing condition runs.

	Hydrograph 2			Hydrograph 3
Return Period, yr	n = 0.03	n = 0.025	n = 0.02	n = 0.03
100	Completed	Completed	Completed	Completed
50	Completed	Completed	Completed	Completed
20	Completed	Completed	Completed	Completed

Skin friction in AdH is specified as a Manning's n roughness coefficient. Selection of the value is based on recommendations from Chow (1959). In addition to varying skin friction, two of the three hydrographs, 2 and 3, were simulated for sensitivity evaluation. Overall, the model varied the most with flood storm frequency.

Figures 10 – 18 show the extent of maximum inundation depth in hydrograph 2, for the various sensitivity runs. It is clearly illustrated that the extents of flood inundation for the 100 year return period are more significant than the 50 year and 20 year events. Also as expected, Hydrograph 2 produced greater flooding than Hydrograph 1 simulations, and was thus selected as the desired design scenario. Additionally, it was shown that increased skin friction retards the flow resulting in greater flooding. Note that sensitivity runs were not simulated with the solid wall located to the south of the camp, as seen in Figure 1. The wall was left out of the simulation to better visually determine the flooding characteristics of the model.

5.1.1 Manning's n = 0.03:

Figure 10. Maximum depth for 20 year runoff event, m.

Figure 11. Maximum depth for 50 year runoff event, m.

Figure 12. Maximum depth for 100 year runoff event, m.
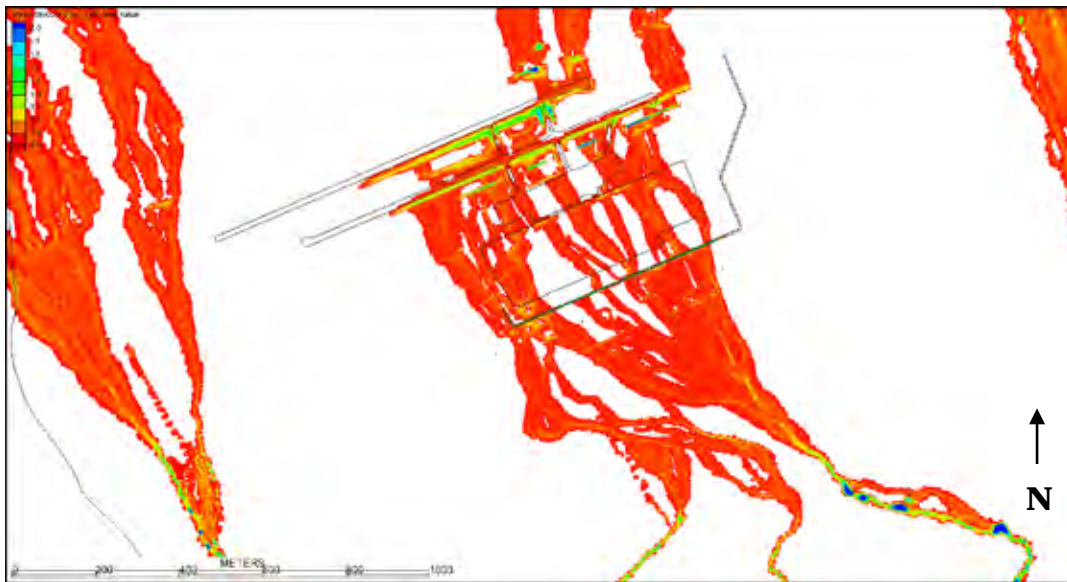
5.1.2 Manning's n = 0.025:

Figure 13. Maximum depth for 20 year runoff event, m.
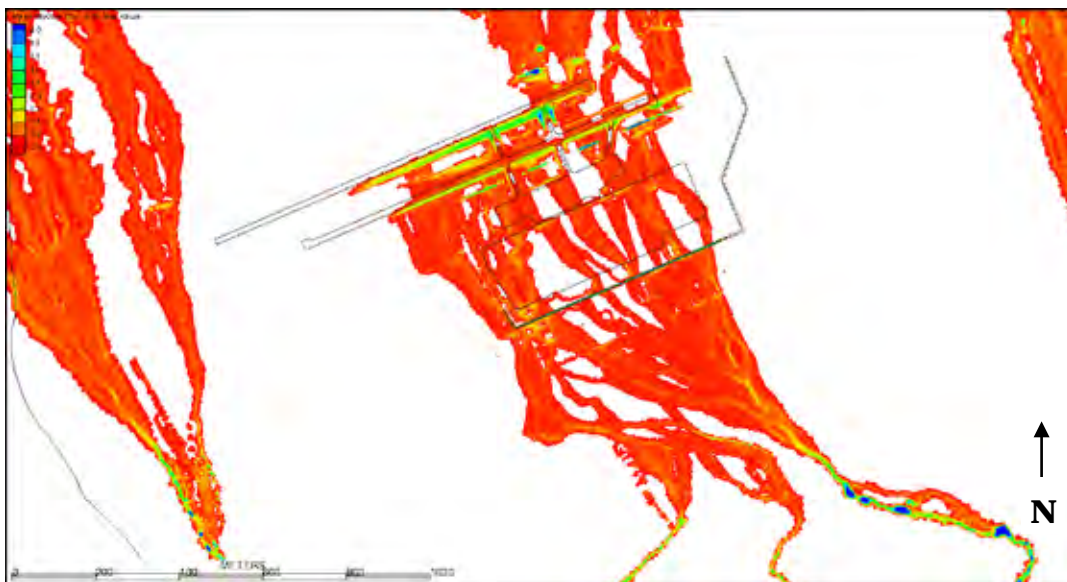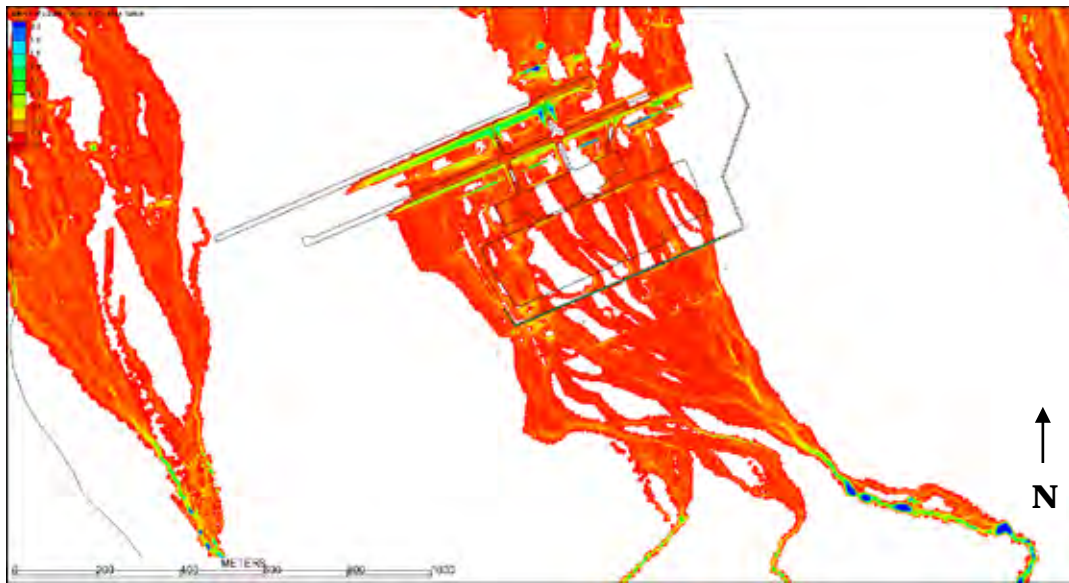
Figure 14. Maximum depth for 50 year runoff event, m.

Figure 15. Maximum depth for 100 year runoff event, m.
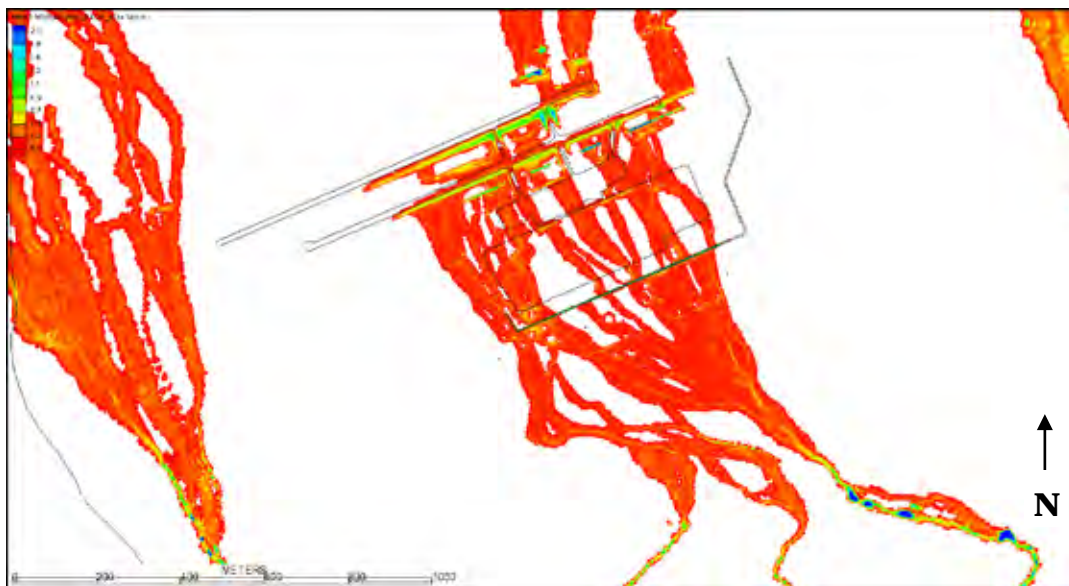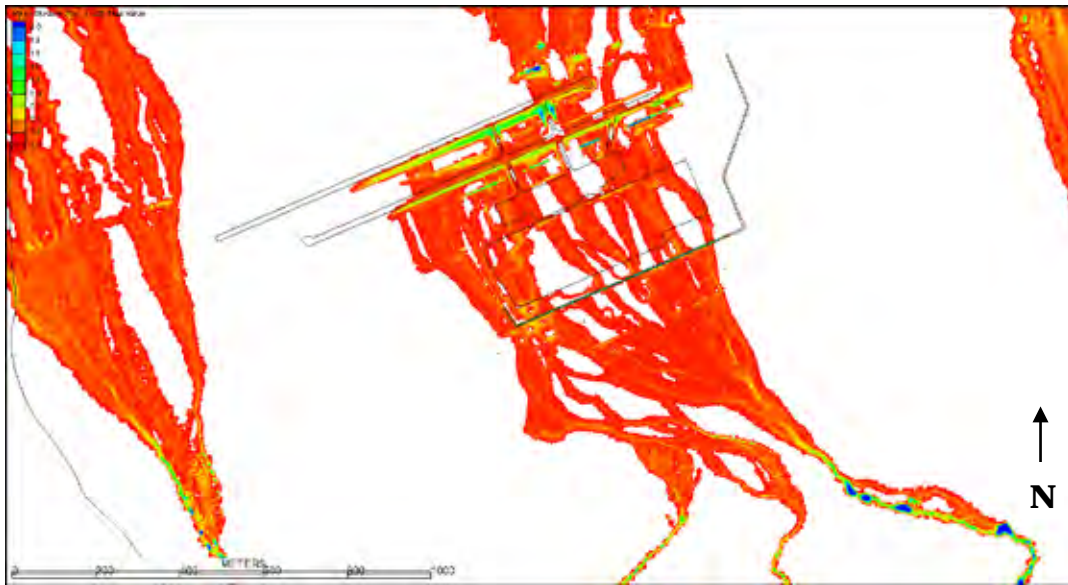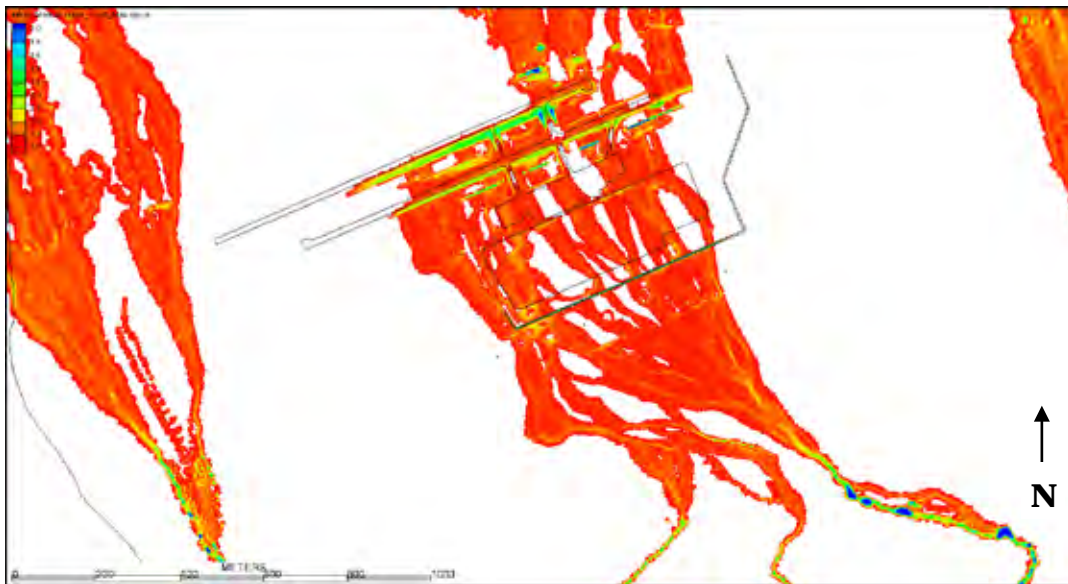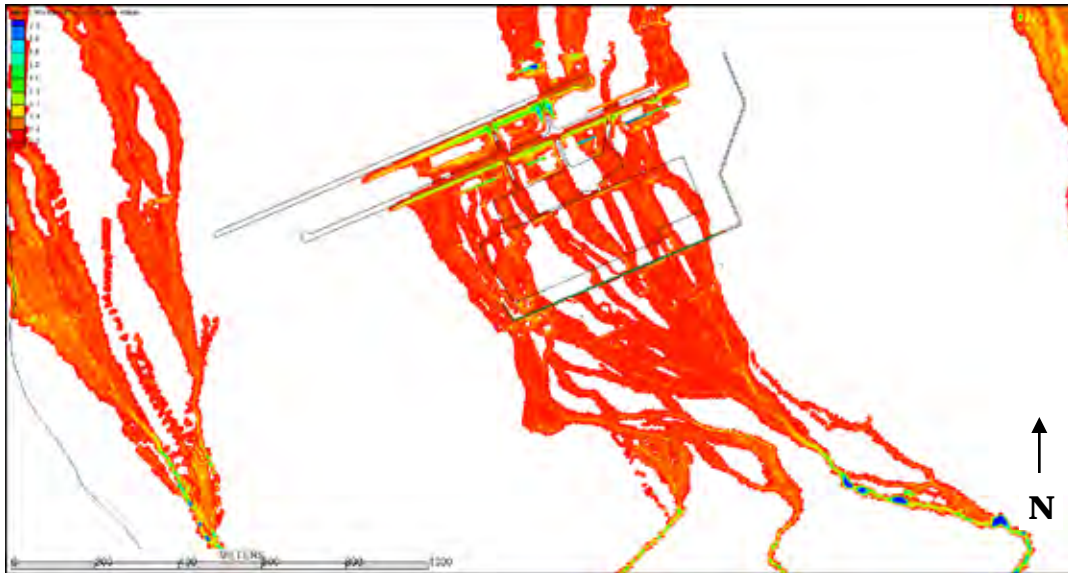
5.1.3   MANNING'S n = 0.02:

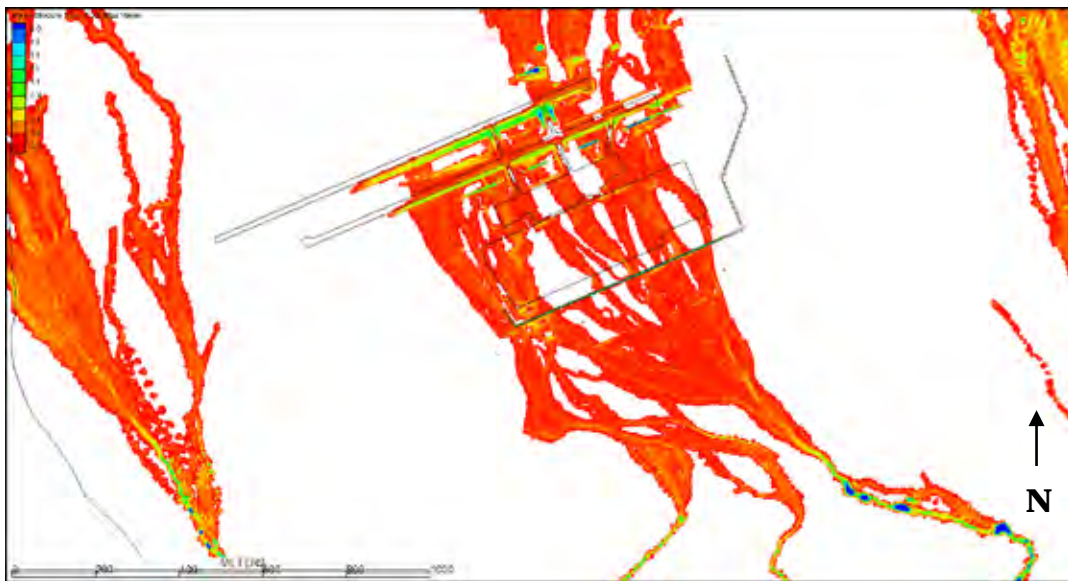Figure 16. Maximum depth for 20 year runoff event, m.

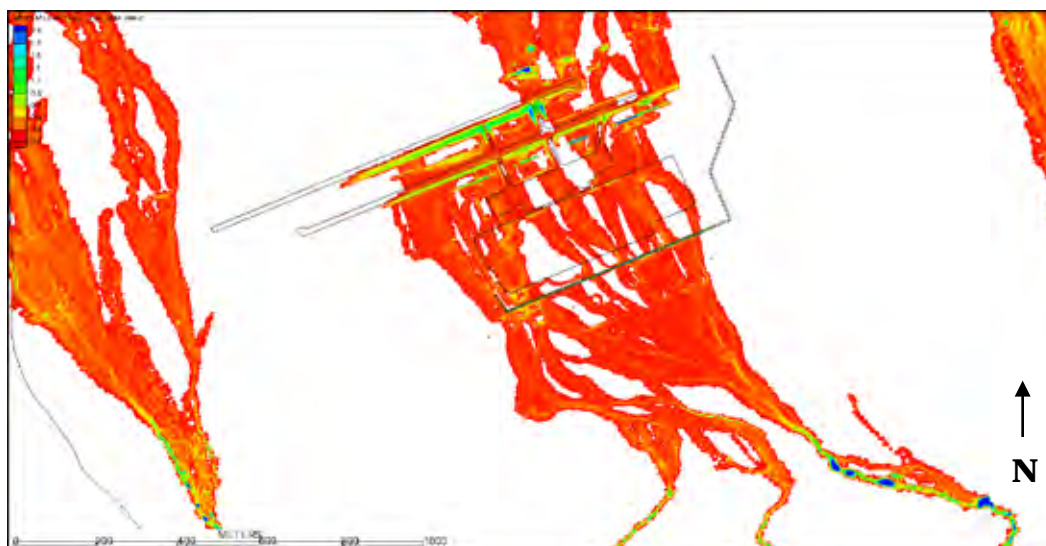Figure 17. Maximum depth for 50 year runoff event, m.

Figure 18. Maximum depth for 100 year runoff event, m.

The sensitivity simulation results provided the basis for selection of the final model configuration for the three alternative runs. A Manning's n of 0.03 and hydrograph 2 for a 20 year event were chosen for the alternative simulations. The selection provided a configuration that produces a conservative estimate for flooding conditions while providing a statistically reasonable estimate for design parameters.

5.2 Existing conditions

For evaluation of the field conditions at Camp Marmal, a series of existing condition simulations were conducted. The existing conditions were based on the camp configuration shown in Figure 19. The three return period floods of 20, 50, and 100 years were applied. The existing conditions deviated from the sensitivity runs due to the inclusion of the solid wall around the southwest and southeast portion of the facility. The wall re-directs flow as shown in Figure 20.

The existing condition model indicates significant flooding in the central and eastern portion of the facility. The source of flooding to the facility is three wall openings, see Figure 19. Two openings, those on the east side, are meant to pass flow and are a series of culverts. There were no detailed data available to size the flow openings. Therefore, there is no boundary control in the model that attempts to pass the correct flow through the flow openings. The only control in the model is the width of the opening. The third opening, located to the west, is a gate. The gate passes a significant portion of the flow. Controlling and/or diverting flow at these openings is critical for mitigating flooding on the camp.
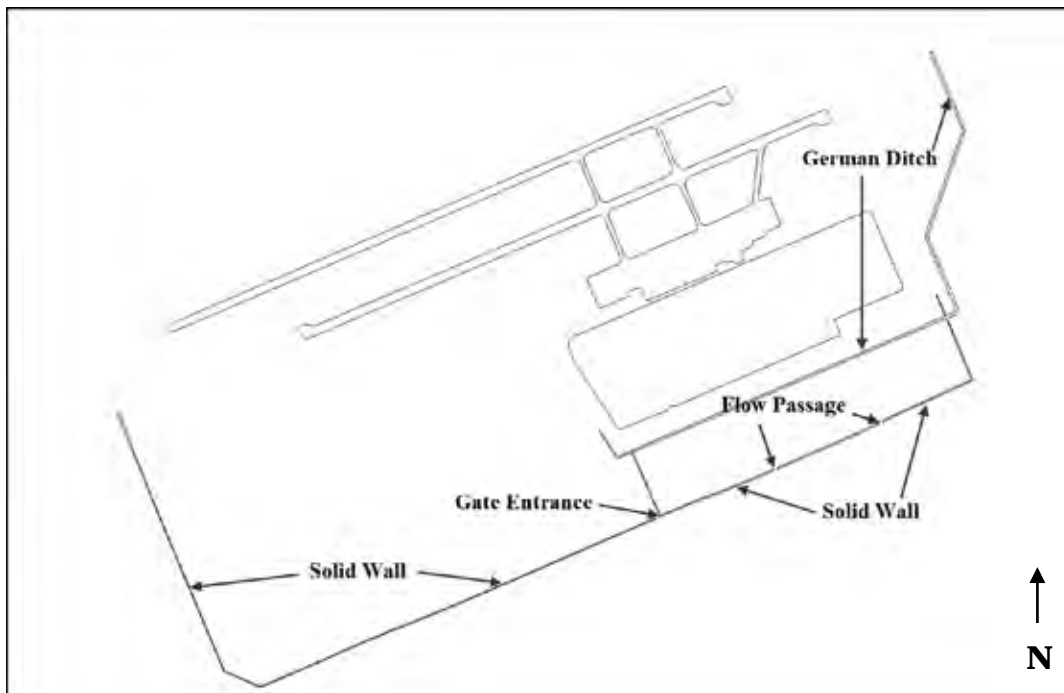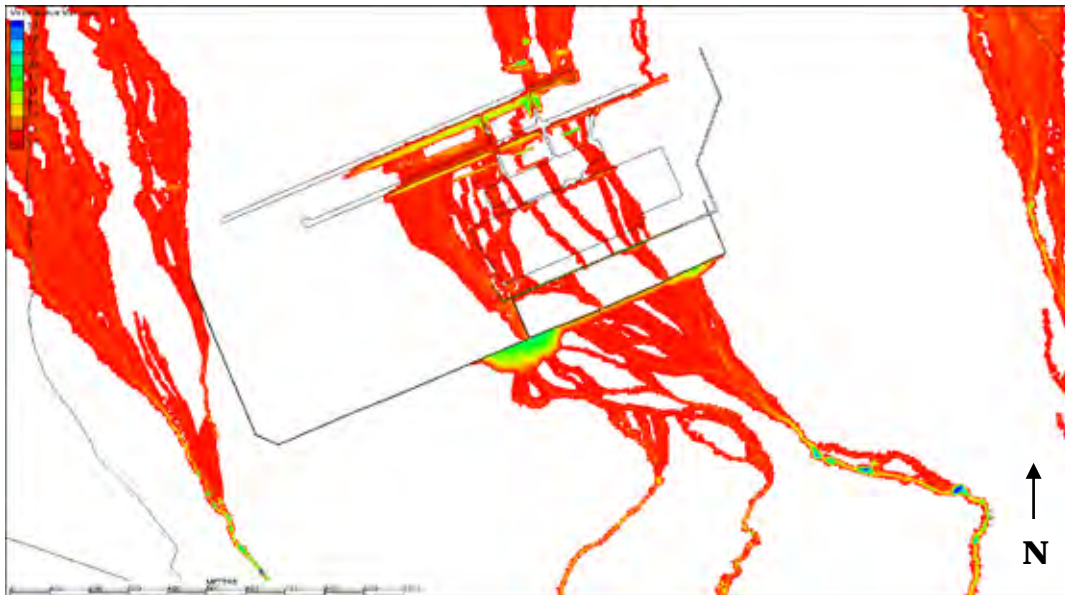
Figure 19. Existing configuration for camp.

Figure 20. 20 year flood inundation map for existing conditions, m.

6   Alternative Simulations

Three model alternatives were simulated for the evaluation of flood mitigation measures at Camp Marmal. In addition to the three original alternatives scoped, a fourth scenario was simulated. The fourth one was a recommendation by the German engineers. For all scenarios, the 20 year simulation was utilized to evaluate the potential flood mitigation.

6.1   Alternative 1

Alternatives 1-A and 1-B were modeled with and without the existing solid wall, respectively. This provided insight into the potential benefit and/or hindrance of the solid wall to flooding conditions defined by Alternative 1.

Alternative 1 was designed to evaluate future expansion plans of the camp. This included the assessment of an anti-vehicle ditch as a diversion channel starting at the southwest corner of the existing solid wall and running parrallel to the runway and wall, then turning back to the northwest where it is oriented perpendicular to the runway. Insertion of the channel into the model was implemented by discretizing the channel banks into the existing mesh. The channel geometry consists of a 4 m bottom width, 2 m depth, and 2:1 side slopes (see Figure 21). It is defined as a concrete lined channel with a Manning's n of 0.015.

For the implementation of Alternative 1, TAN provided a georeferenced drawing, as shown in Figure 22. The ditch alignment provided protection for the southwest portion of the camp that currently is unprotected from upstream flooding with the exception of the security wall. The new mesh is shown in Figure 23.

6.2   Alternative 2 and 3 recommendations

At the request of TAN, ERDC-CHL provided design guidance for Alternatives 2 and 3 to evaluate re-direction and retention of flow.
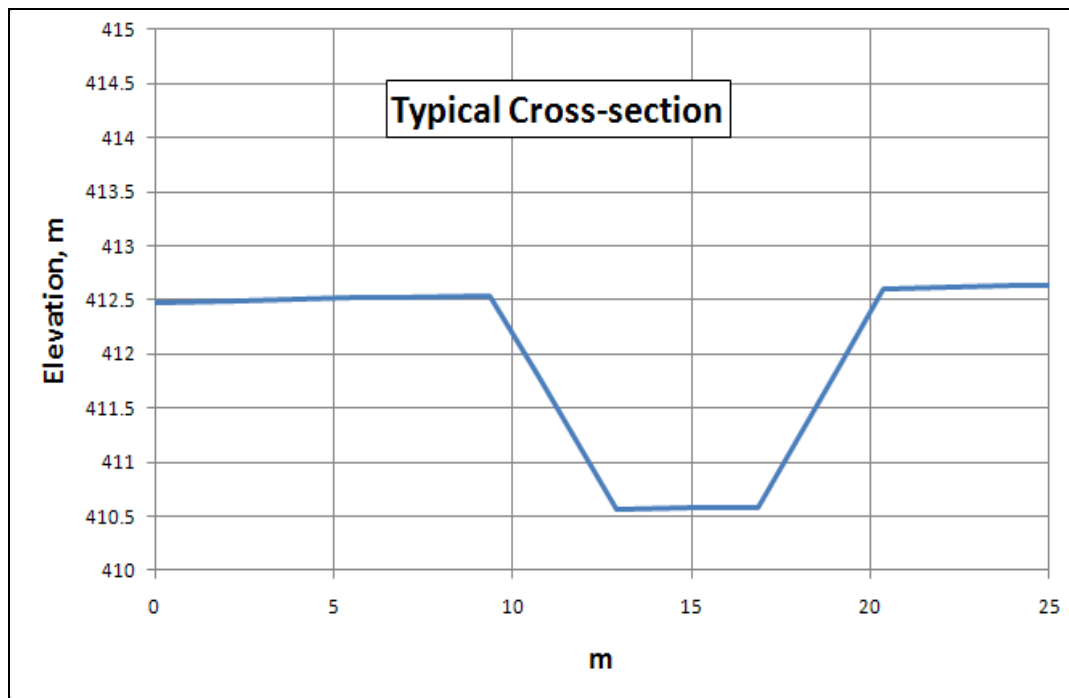
Figure 21. Typical cross-section for Alternative 1 diversion ditch.
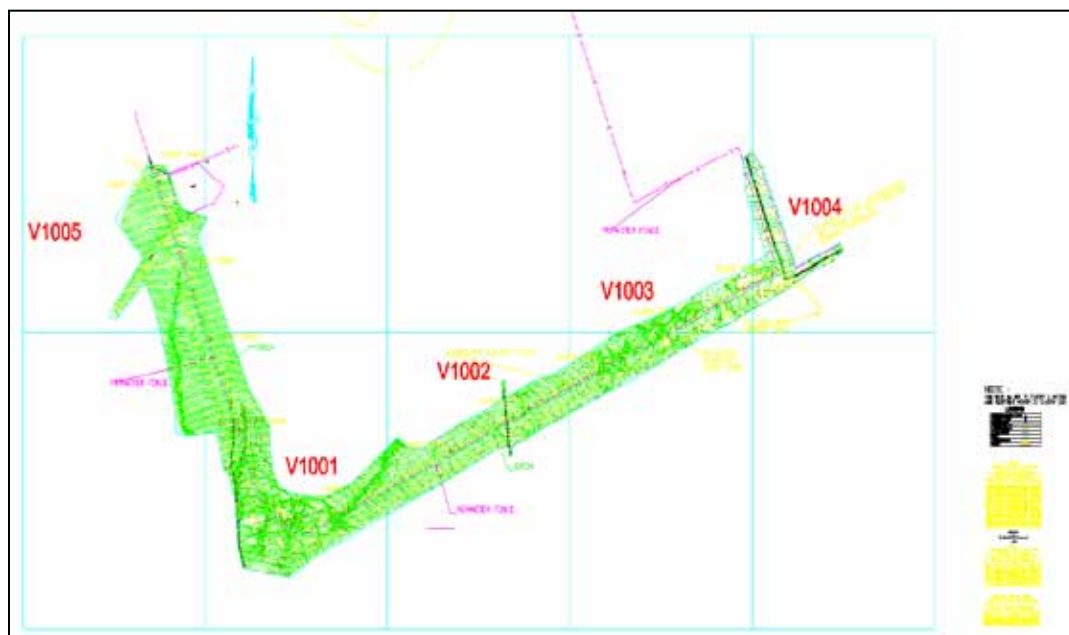

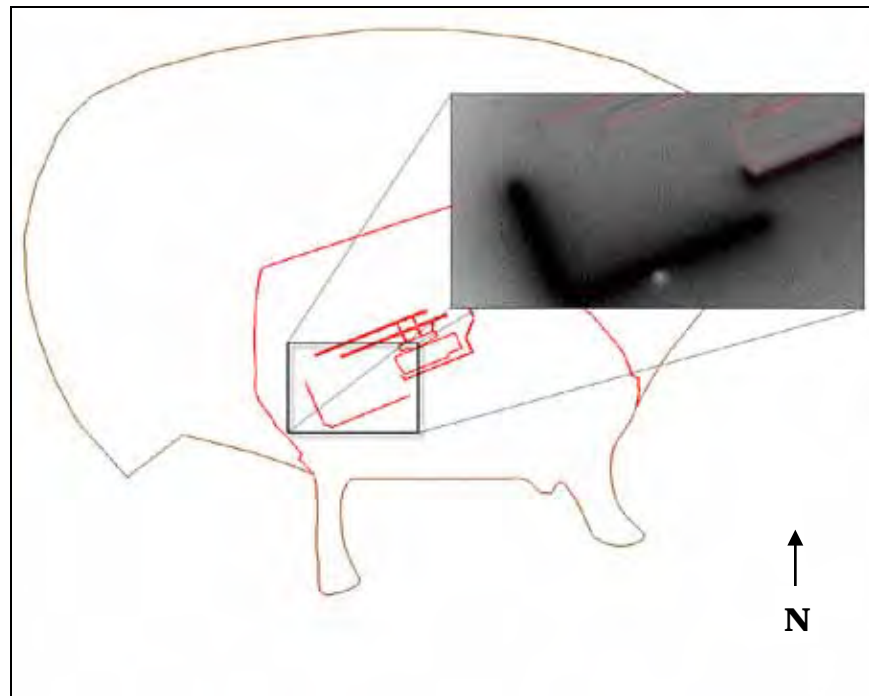Figure 22. TAN provided data for Alternative 1 ditch alignment.

Figure 23. Alternative 1 mesh setup with enlarged view of airfield and camp.

Re-direction of flow was investigated by including an extended ditch. Retention basins were included in the model to evaluate the impact of flow storage on flood extents. ERDC-CHL was provided a typical cross-section for implementation into the AdH model (Figure 24) for Alternatives 2 and 3. This configuration was used for the following calculations.

Alternative 1 was simulated with a ditch around the southwest area of the camp, and is shown in Figure 25 as a black line. The ditch extension for Alternative 2 is shown in red, and aligned based on the landscape slope. The approximate length of the combined Alternative 1 and Alternative 2 ditch is 6,400 m. The volume of flood flow is the primary criteria of flooding on the camp. Due to rapidly developing floods, flood defense measures quickly become overwhelmed. Thus, the requirement for Alternative 2 is to provide enough storage for the incoming flood flow to reduce peak discharge to the camp. This will allow other defensive measures such as the ditch and wall to re-route flow away from the camp.

Based on ditch length shown in Figure 25, the volume is 104,000 m³. However, as shown in Figure 26, the total volume entering the area of the ditch from the existing condition simulation for the 20 year event is 733,000 cubic meters.
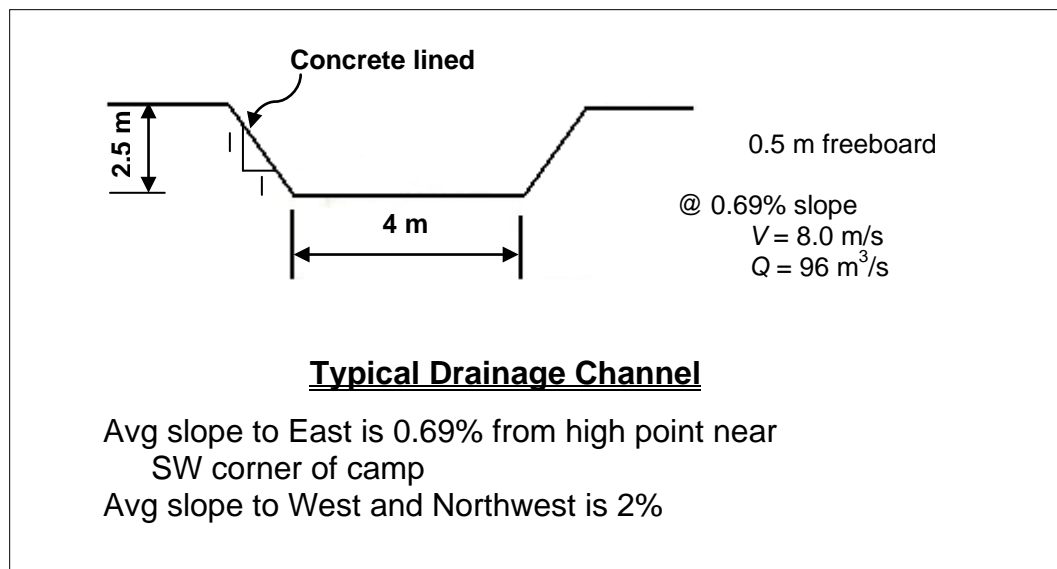
Concrete lined

2.5 m

4 m

0.5 m freeboard

@ 0.69% slope
$V = 8.0$ m/s
$Q = 96$ m^3/s

<u>Typical Drainage Channel</u>

Avg slope to East is 0.69% from high point near
SW corner of camp
Avg slope to West and Northwest is 2%

Figure 24. TAN typical drainage channel detail for Camp Marmal's ditch extension.

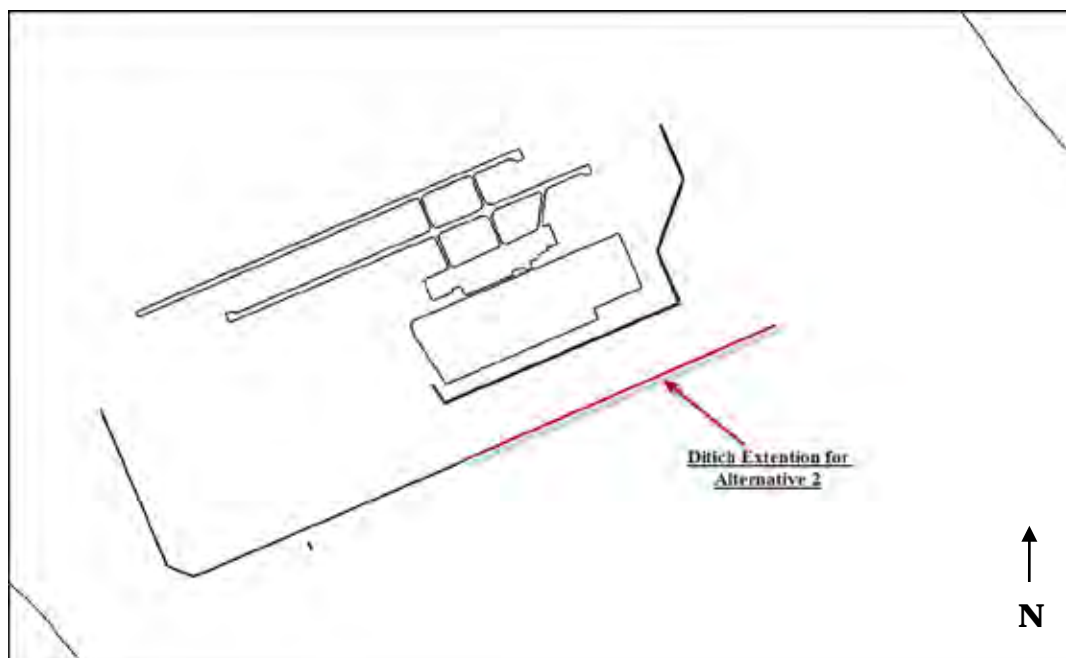
Ditch Extention for
Alternative 2

N

Figure 25. Recommended ditch alignment for Alternative 2.

Figure 26. Flux volumes for the 20 year event.

The Alternative 2 ditch configuration, as shown in Figures 24 and 25, does not sufficiently store and route the volume of flow from the camp. The model results indicate that the ditch is quickly overwhelmed with a lateral flow of 0.05 m³/m.

Based on the lateral flow estimates from the model, an estimate of the total capacity of the ditch is required. Regardless of where the flow enters the ditch, the capacity of the ditch must not be exceeded. For the following calculation, it is assumed that lateral flow entry into the ditch is uniform across its entire length. To account for variation in freeboard, a safety factor in addition to the ditch's freeboard was applied. Based on the ERDC/TAN calculation in Figure 24, the total capacity of the ditch is $75 - 95$ m³ depending upon Manning's n and the final grade slope. Assuming 77 m³ (Manning's n = 0.015, Slope = 0.007) and using the ditch length as defined in Figure 25, the permissible lateral flow as calculated by Equation 9 is 0.007 m³/m.

$$q = \frac{Q}{L}\frac{1}{S.F.} \tag{9}$$

where:

q = permissible lateral flow;
L = length of ditch;
Q = flow capacity of ditch;
SF = Safety Factor (recommend 2 to mitigate potential momentum issues).

Total discharge from all contributing sources with a factor of safety of 2 is estimated using Equation 10 as 37 m³.

$$Q_{S.F.} = qL \qquad (10)$$

As illustrated in Figure 26 the estimated total peak flow from all sources is estimated to be 55 - 65 m³, though it appears that the channel capacity will be exceeded at flows > 37 m³.

Three options are presented for mitigation of the excess flood flows. The first option is that a berm should be added to the current ditch configuration to increase capacity. The second option is to incorporate a retention pond into the design upstream of where the flow enters the ditch. The final option is to enlarge the ditch. The final two options will increase the construction cost, so the first option is more economically feasible. Additionally, the smaller ditch plus berm option can provide just as much protection as the larger ditch.

If a two meter high berm is constructed adjacent and parallel to the ditch, the volume of the combined ditch and berm can be estimated. Allowing for a 0.5 meter freeboard on the berm and assuming a landscape slope perpendicular to the channel of 4 percent, the combined cross-sectional area is 58 m². Then, multiplying the cross-sectional area by the ditch length results in a total storage volume of 370,000 m³. This represents approximately 50 percent of the total 24 hr, 20 year event as compared to only 10 percent of storage volume with the ditch, only.

The extended ditch and berm option was simulated for Alternative 2.

The main contributors to flow across the camp are streams 2, 3 and 4, as defined in Figure 5. Of the three streams, stream 4 is the largest and contributes approximately 85 percent of the total flow. The peak flow for the 20 year event is 50 m³. It was recommended that a retention pond be implemented on stream 4 for Alternative 3 in-line with the ditch.

Outflow of the stream 4 retention basin should not exceed the 24 hour, 2 year event where the peak discharge is approximately 15 m³. At this flow rate and in combination with streams 2 and 3, the total combined flow rate is 36 m³, which does not exceed the calculated design flow rate of 37 m³. Using a peak discharge of 15 m³ and linear reservoir routing, the total storage of the stream 4 pond needs to be 279,000 m³, as shown in Figure 27. This volume was calculated by integrating under the curves.
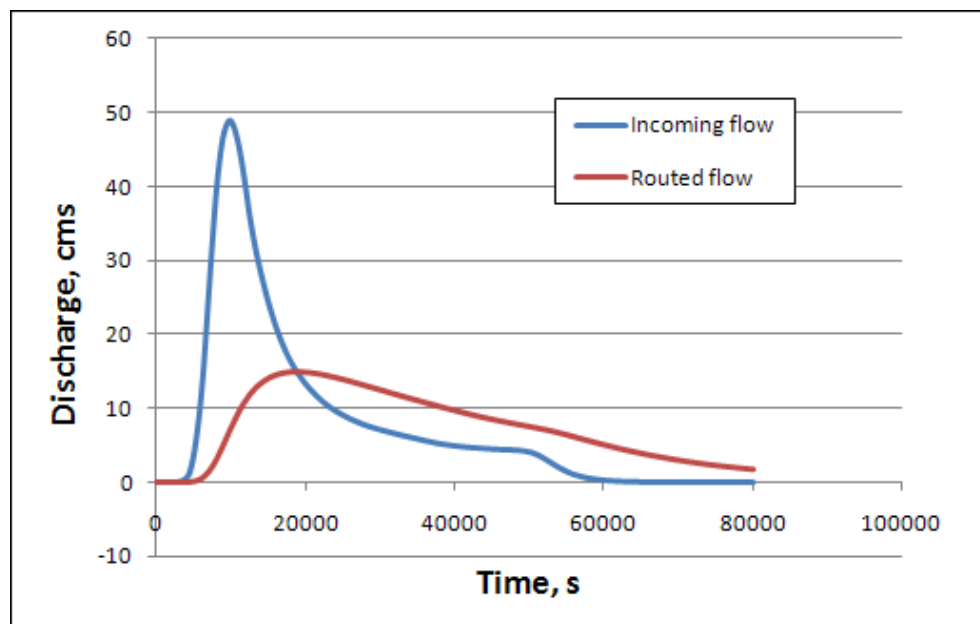
Figure 27. Original and routed hydrographs for stream 4.

6.3   Alternative 2

Based on the previous section's recommendations and further input from TAN, Alternatives 2-A and 2-B, with and without the berm, respectively, were simulated. The berm, shown in Figures 28 and 29, is an added measure of protection. Figure 28 indicates the flow direction based on ditch slope. The berm, as explained above, would drastically improve the protective ability of the ditch by increasing the storage volume. Shown in Figures 30 and 31 are the cross-section of the with and without the berm condition with their respective cut/fill volumes presented in Table 5.

6.4   Alternative 3

Three designs were simulated for Alternative 3. The design of Alternatives 3-A and 3-B were based on a derivation of Alternative 2. The western portion of the ditch is not needed, thus it was removed for Alternative 3 senerios. Alternative 3-A was simulated with a retention basin at the downstream end of the ditch, east of the camp (see Figure 32). For alternative 3-B, the basin was removed. A third alternative, 3-C, was simulated with a retention basin in-line with the ditch and a slightly different ditch alignment (see Figure 33). The purpose of this configuration was to reduce cut volume by locating the retention basin in a more ideal lanscape area.
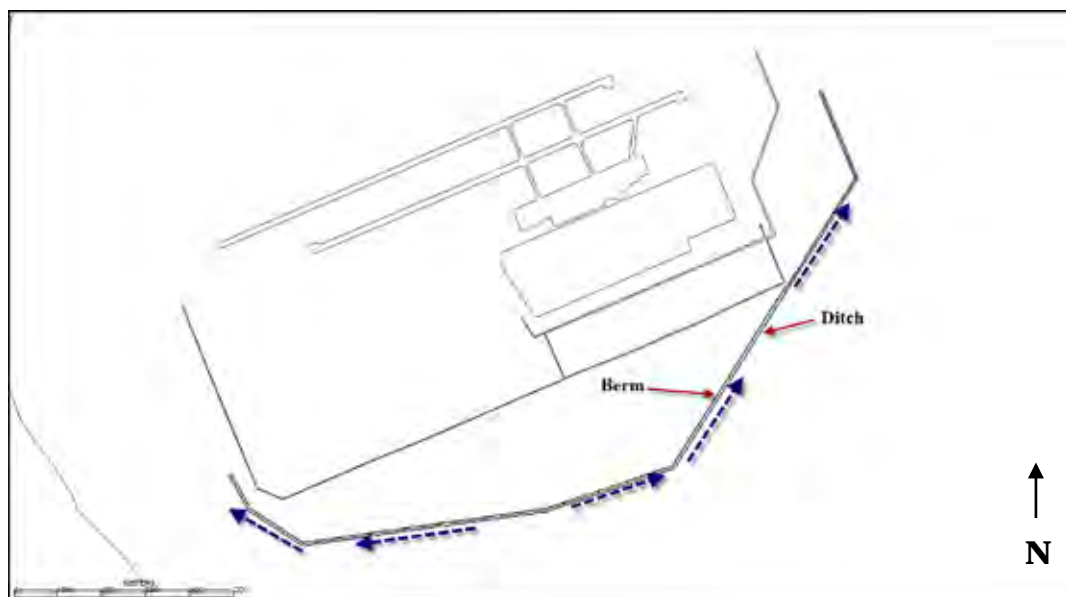
Figure 28. Alternative 2 shown with the berm and flow direction in ditch.
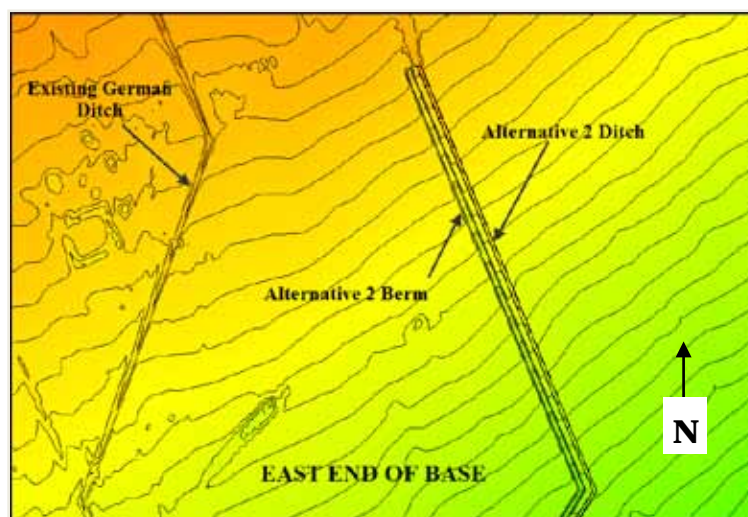
Figure 29. 1 m detail contours of Alternative 2 ditch and berm combination.

6.4.1 Alternative 3-A

A retention basin along with the removal of the western portion of the Alternative 2 ditch was simulated for Alternative 3-A (Figure 32). The basin was located at the downstream end of the ditch. The volume of storage in the retention basin basin was 280,000 m³. Length and width of the retention basin for 3-A were 435 m and 215 m, respectivly, with a depth of 3 m.
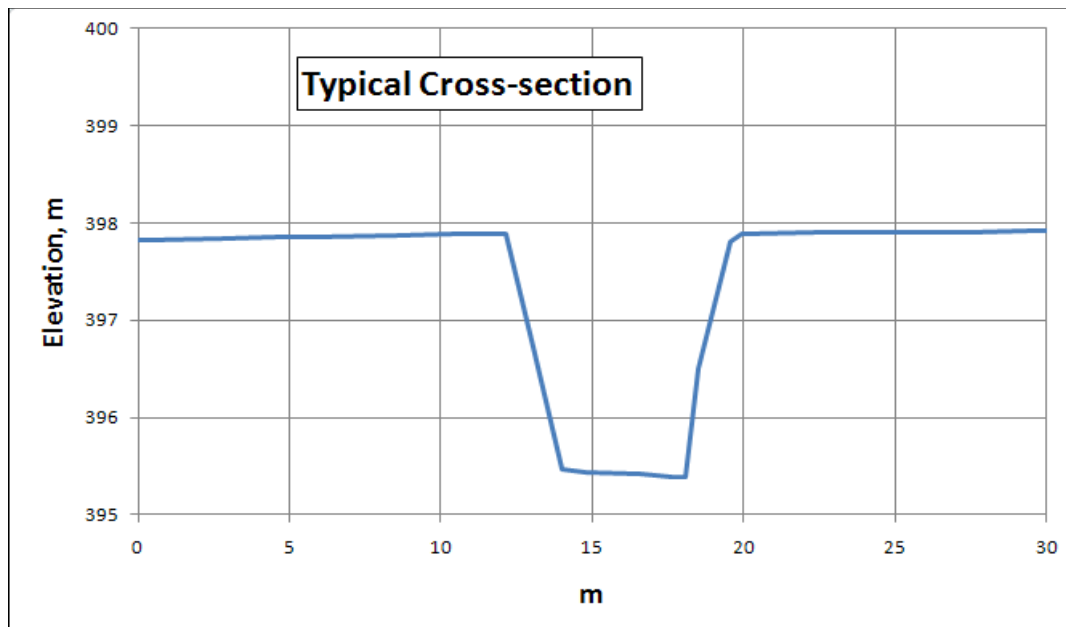
Figure 30. Alternative 2 typical cross-section with ditch, and without the berm.
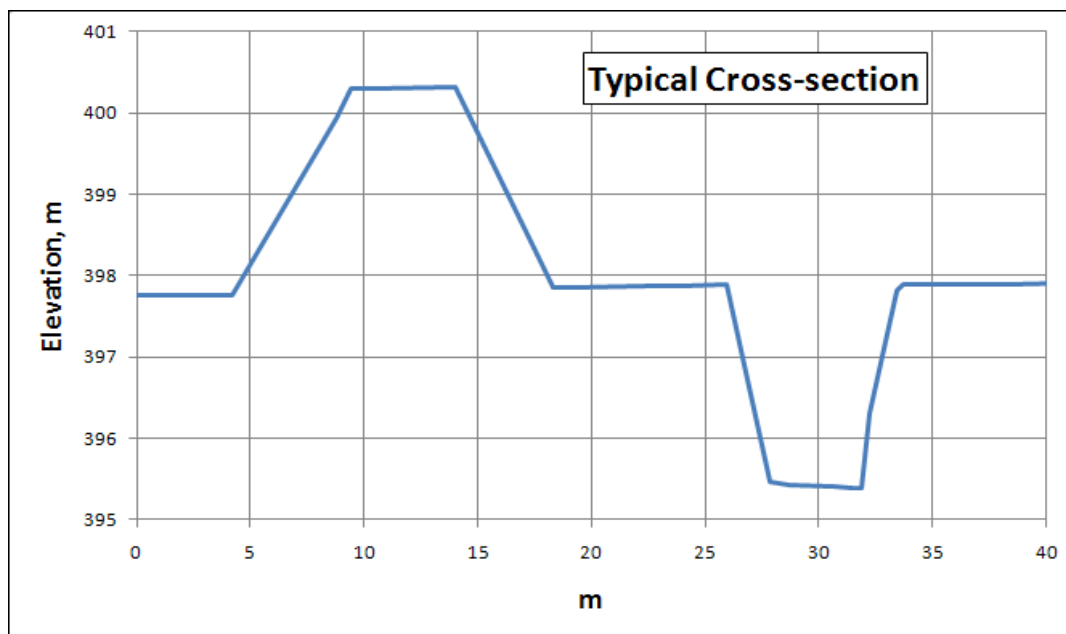
Figure 31. Alternative 2 typical cross-section with berm and ditch.

Table 5. Cut/Fill volumes for Alternative 2.

Alternative 2	
Feature	Cut/fill volume cm
Ditch	270,000
Berm	155,000
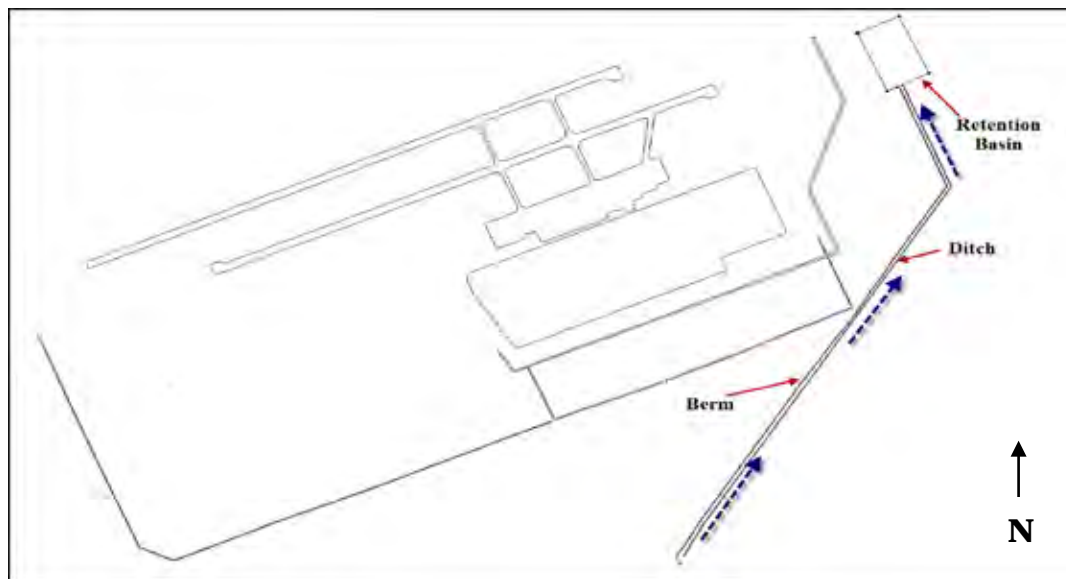
Figure 32. Alternative 3-A and 3-B layout.
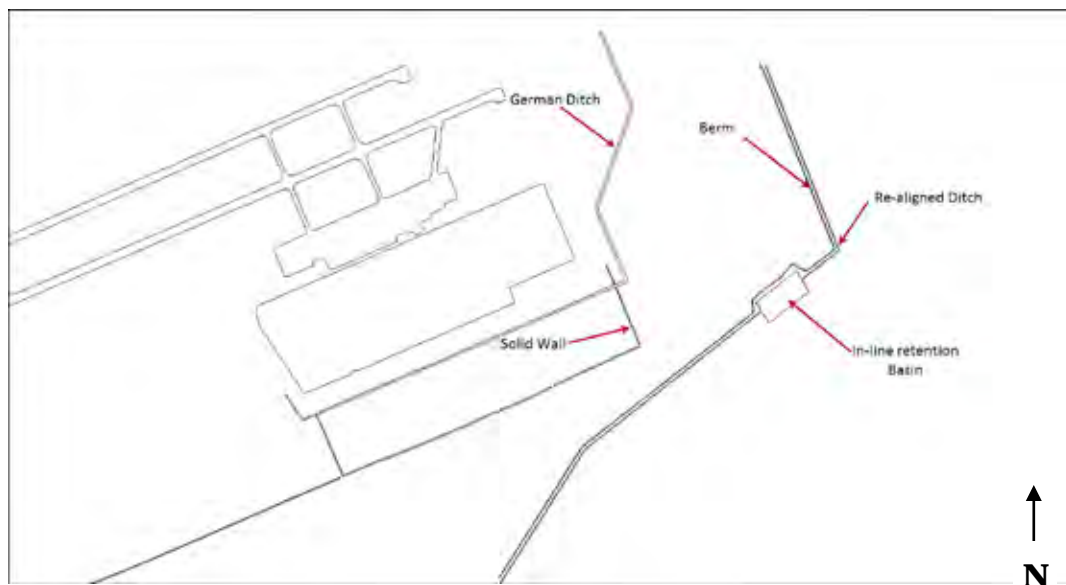
Figure 33. Configuration of Alternative 3-C.

Shown in Table 6 are the cut/fill volumes required for construction of these features.

6.4.2   Alternative 3-B

Alternative 3-B is simulated without the retention basin. This design provided insight into the potential flooding downstream of the camp.

Table 6. Cut/Fill volumes for Alternative 3-A and 3-B.

Alternative 3-A and 3-B	
Feature	Cut/fill volume cm
Ditch	165,000
Retention	815,000
Berm	80,000

6.4.3 Alternative 3-C

For Alternative 3-C, the ditch alignment is relocated, futher east, with an in-line retention basin, as shown in Figure 33. The new ditch alignment allows for camp expansion on the east side of the German Ditch. The length and width for the basin are 290 m and 144 m, respectivly, with a depth of 3 m. This provides a storage volume of 125,000 m^3, half of what was used in Alternative 3-B.

Thus, the retention basin in Alternative 3-C requires less excavation (see Table 7) than the retention basin in Alternative 3-A. However, the new ditch alignment does require more excavation than the alignment in Alternatives 3-A and 3-B. By placing the basin inline with the ditch, the most approriate landscape location can be selected to minimize cut volumes.

Table 7. Cut/Fill volumes for Alternative 3-C.

Alternative 3-C	
Feature	Cut/fill volume cm
Ditch	226,193
Retention	368,464
Berm	137,230

7   Results

7.1   Alternative 1

As shown in the existing condition runs (Figure 10) the site is quickly overwhelmed with the 20 year event. However, little flooding occurs in the expanded portion of the camp.

The Figure 34 inudation map demonstrates that Alternative 1-A is ineffective for reducing the majority of the flooding. Figures 35 – 41 present a series of time lapse contour plots illustrating the dynamic behavior of the flood during simulation of the design event.

7.2   Alternative 1-B

Alternative 1-B evaluated the impact of the solid wall on flood inundation . Figure 42 shows the maximum flood inundation depth for Alternative 1-B with the wall included.

Figures 43 – 49 present a series of time lapse contour plots illustrating the dynamic behavior of the flood event during simulation for Alternative 1-B.

Figure 34. Alternative 1-A maxiumum inundation depth, 20 year event, m.
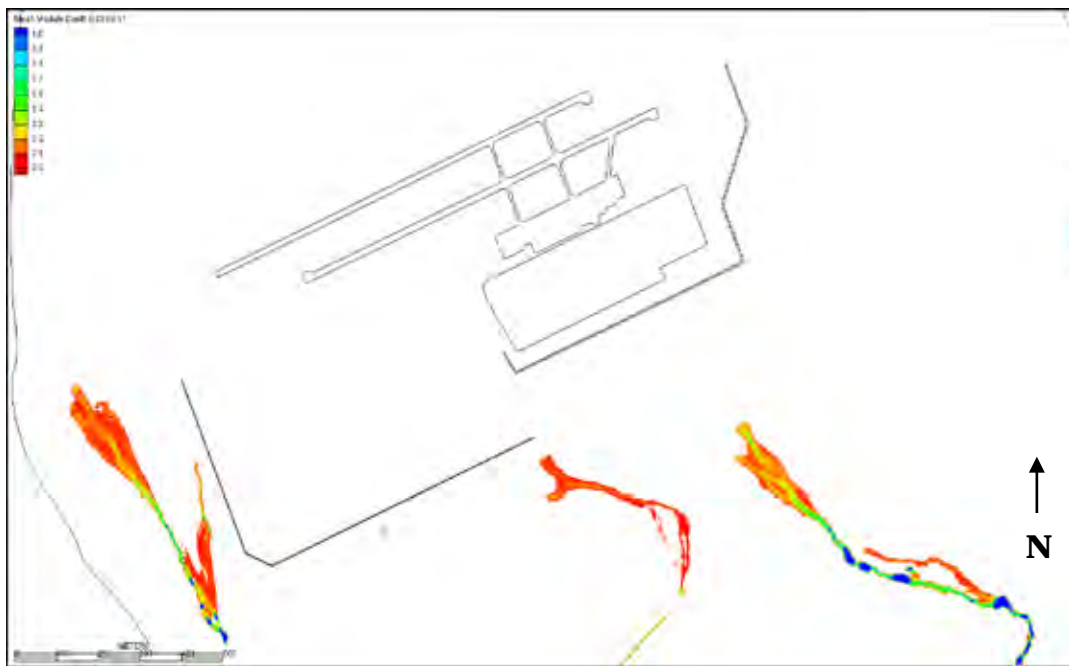
Figure 35. Alternative 1-A inundation depths, at 3 hours, m.

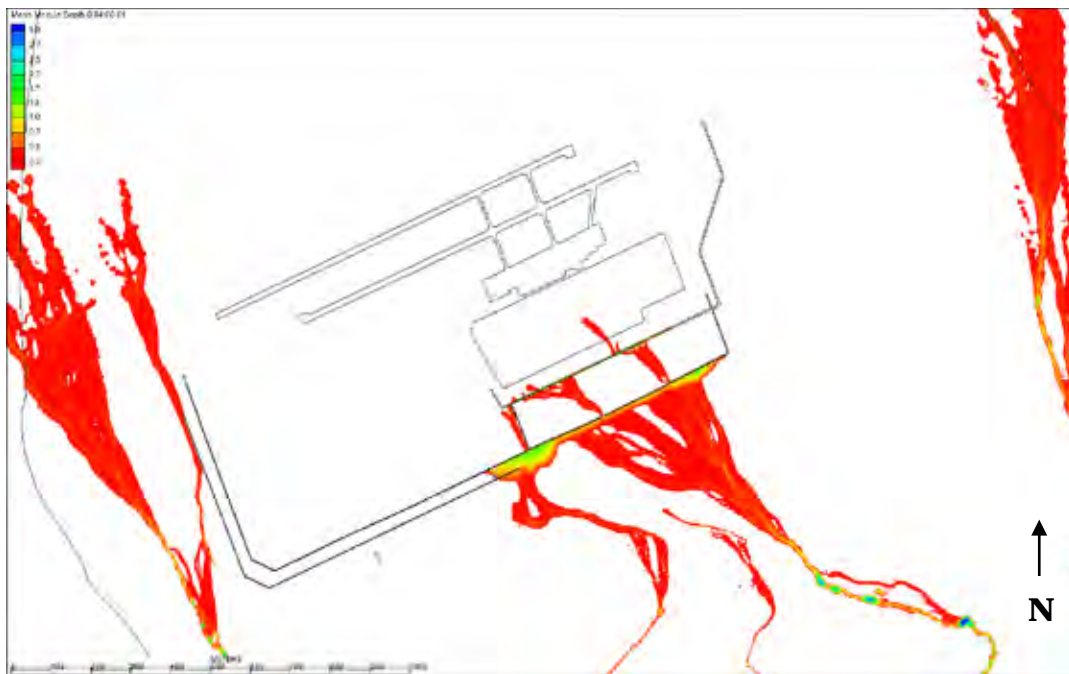Figure 36. Alternative 1-A inundation depths, at 3.5 hours, m.

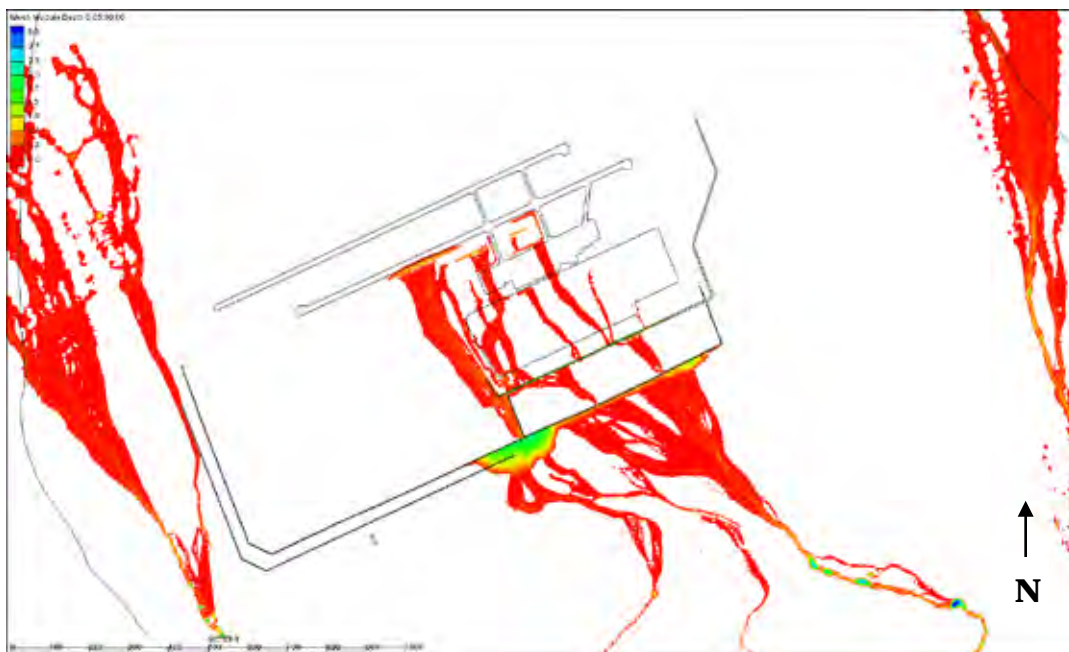Figure 37. Alternative 1-A inundation depths, at 4 hours, m.
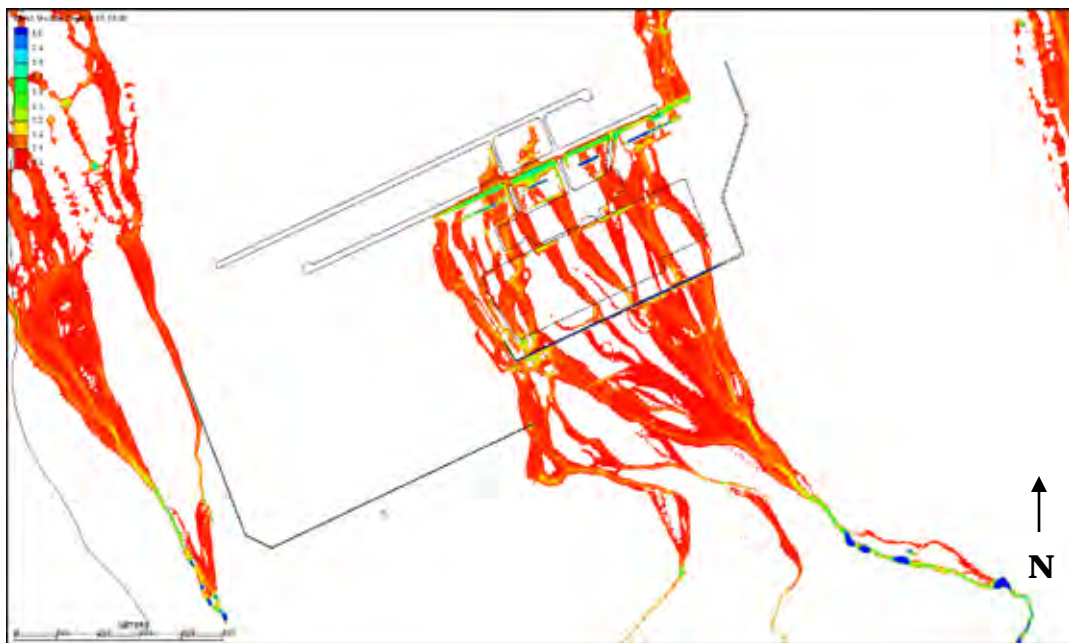
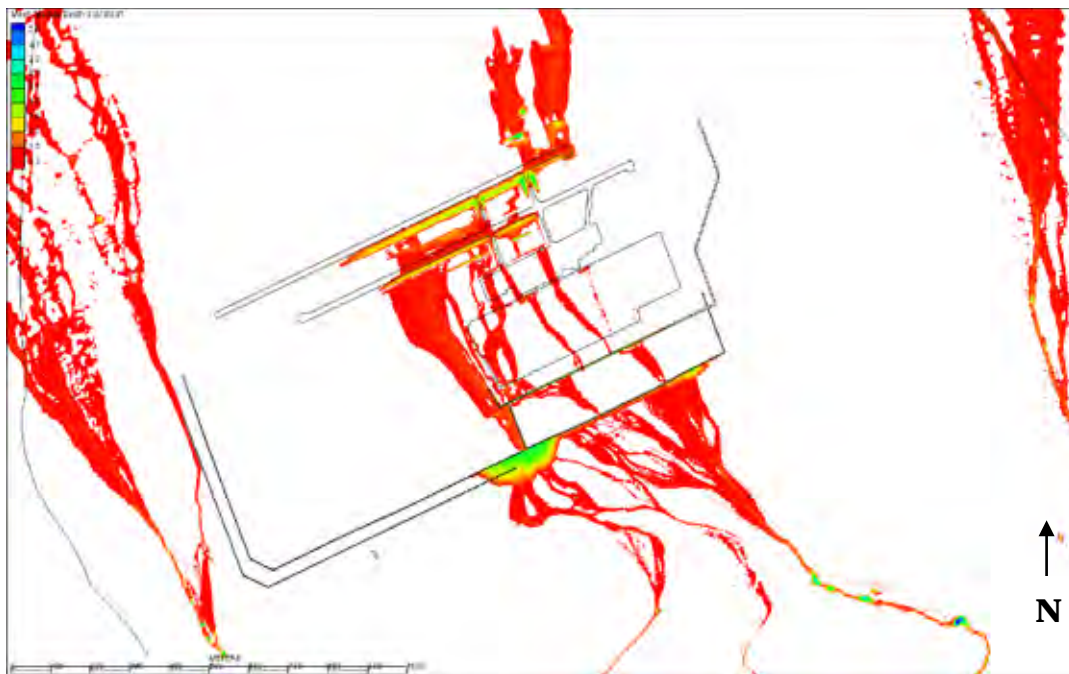Figure 38. Alternative 1-A inundation depths, at 5 hours, m.
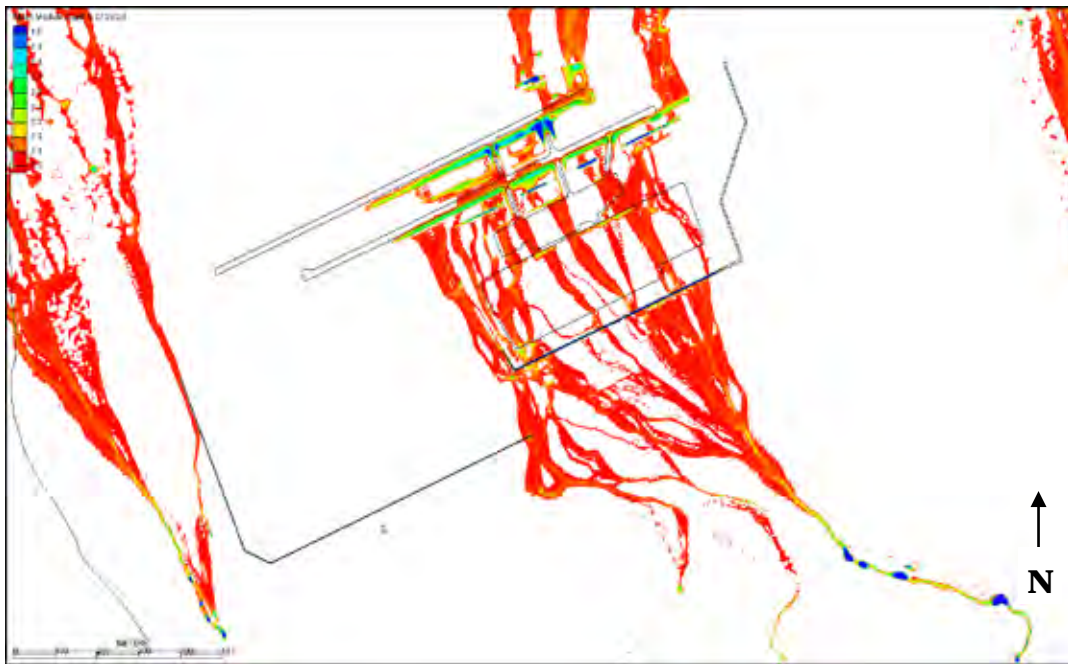
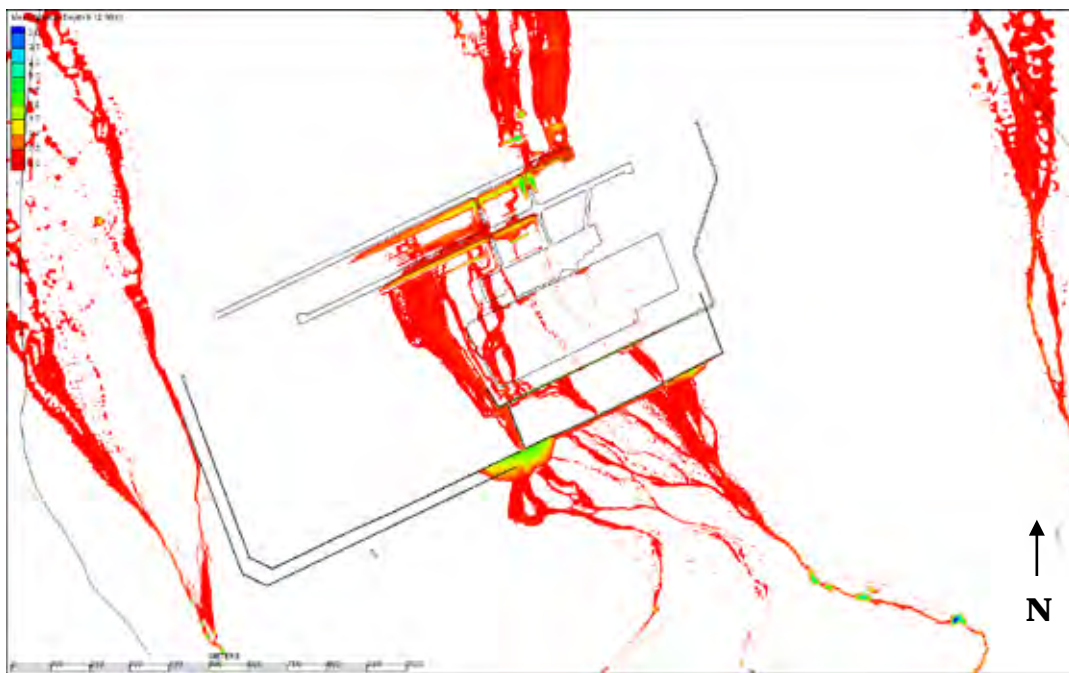Figure 39. Alternative 1-A inundation depths, at 7.5 hours, m.
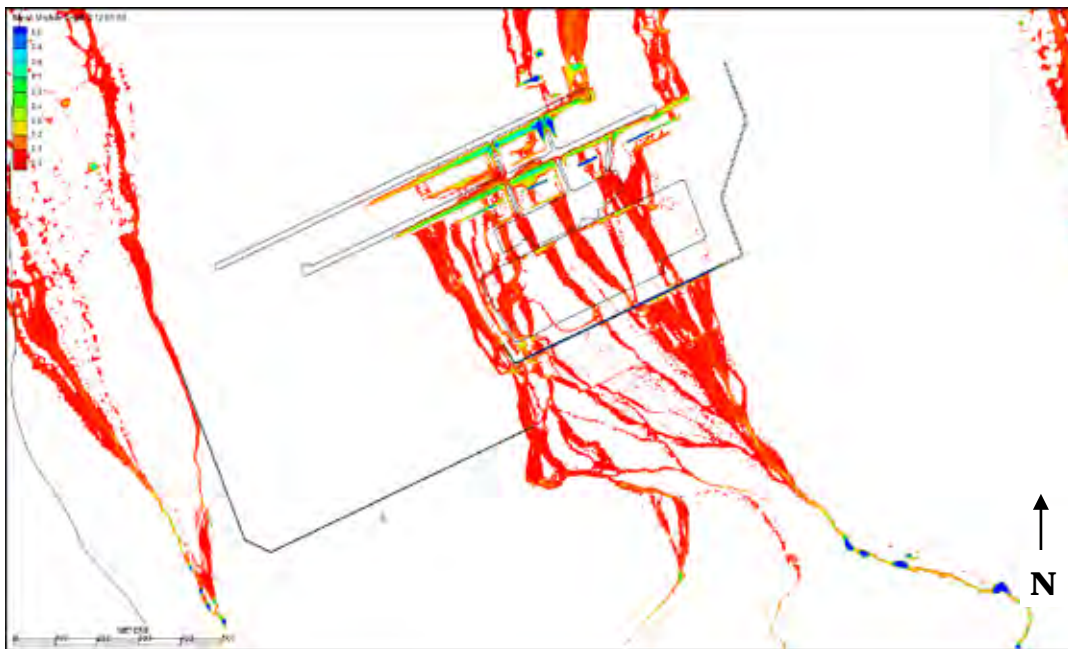
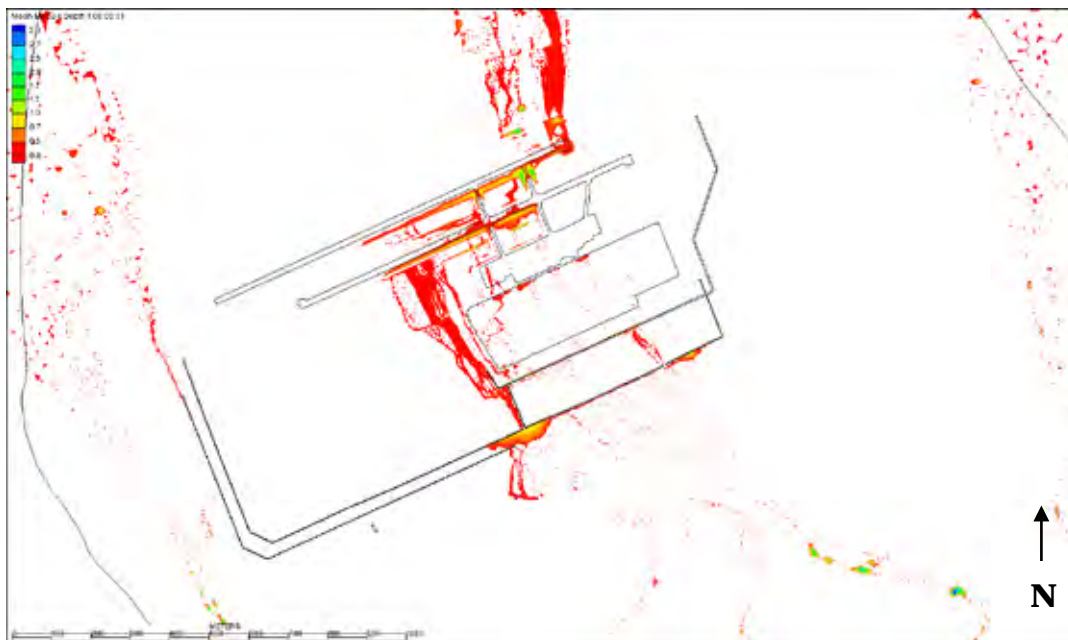Figure 40. Alternative 1-A inundatioln depths, at 12 hours, m.
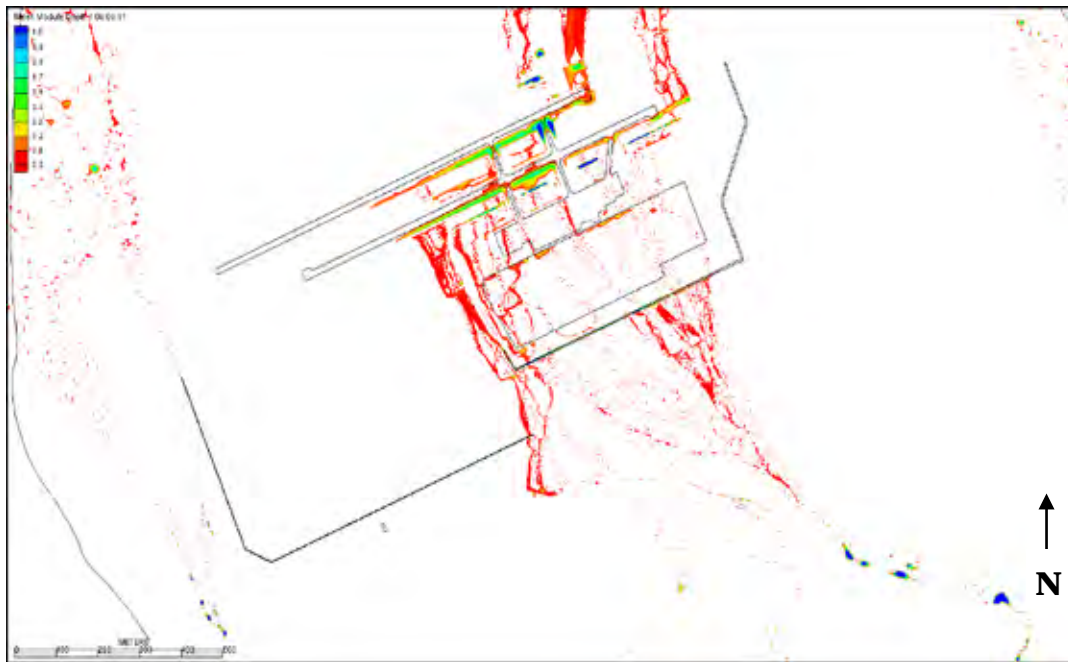
Figure 41. Alternative 1-A inundation depths, at 24 hours, m.
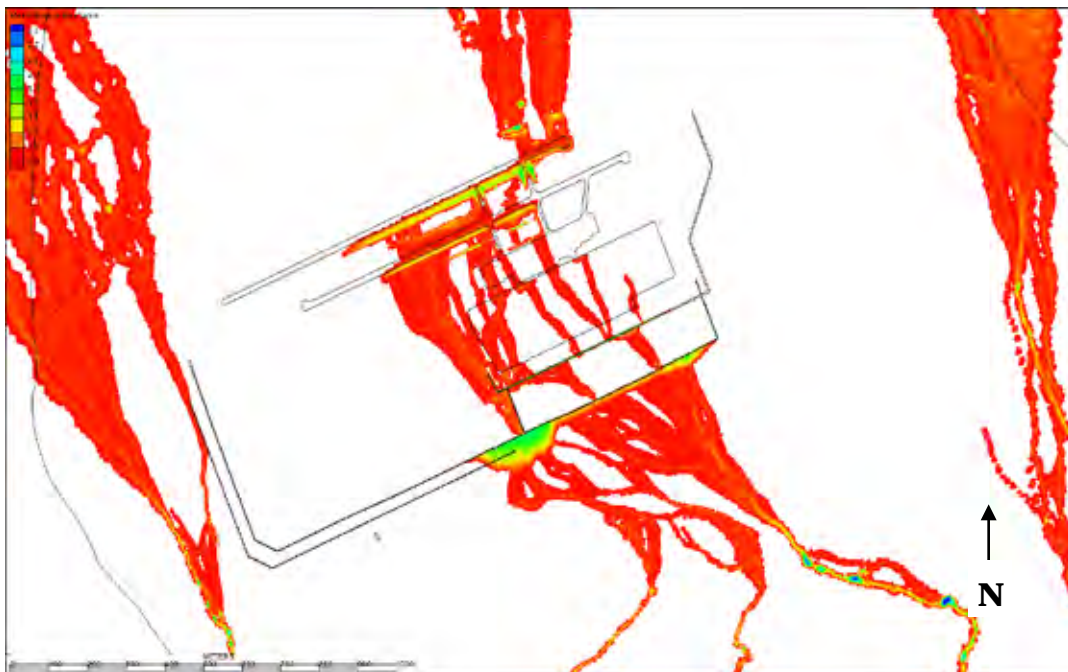
Figure 42. Alternative 1-B maxiumum inundation depth 20 year event, m.
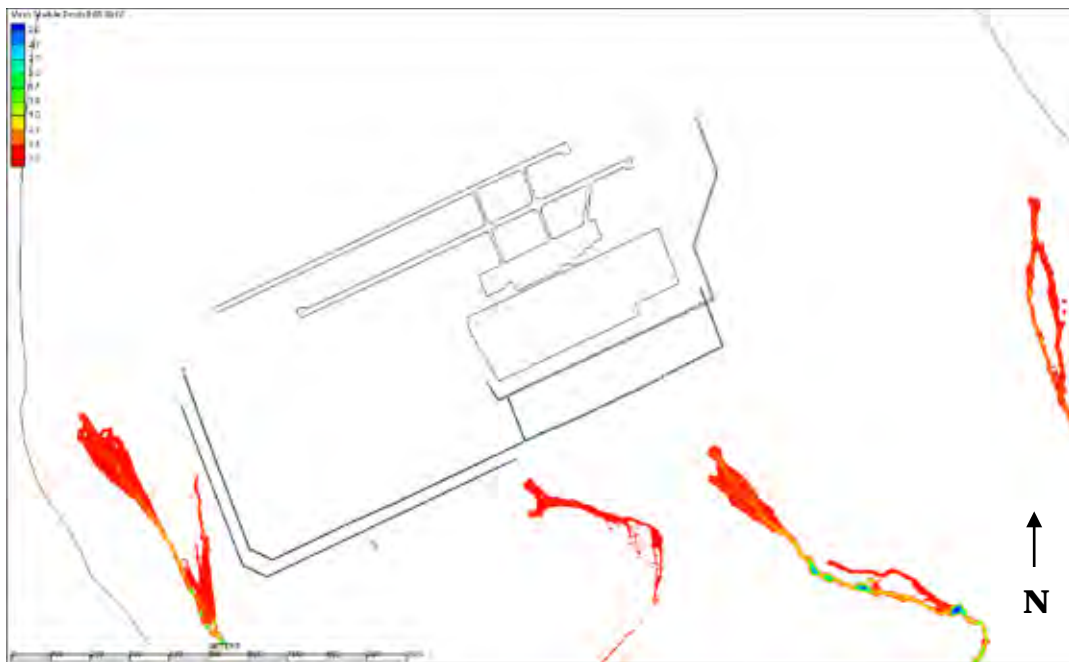
Figure 43. Alternative 1-B inundation depths, at 3 hours, m.

Figure 44. Alternative 1-B inundation depths, at 3.5 hours, m.

Figure 45. Alternative 1-B inundation depths, at 4 hours, m.

Figure 46. Alternative 1-B inundation depths, at 5 hours, m.

Figure 47. Alternative 1-B inundation depths, at7.5 hours, m.

Figure 48. Alternative 1-B inundation depths, at 12 hours, m.

Figure 49. Alternative 1-B inundation depths, at 24 hours, m.

7.2 Alternative 2

For Alternative 2-A the simulation did not have the berm downstream of the ditch. Without the berm for the 24 hr, 20 yr event, the ditch is filled, spilling out in several locations (see Figure 50). The primary location of concern is the center of the ditch south of the gate opening (see Figure 19). Here, the topography forms a valley funneling the flow toward the gate opening. Other spillage locations are further east and were somewhat mitigated by existing defensive measures. The Alternative 2-A ditch is successful in reducing the peak flow, which minimizes the impact to the downstream network. However, the flow that passes the ditch and is diverted through wall openings is sufficient to flood the camp and airfield, as shown in Figure 50.

An additional concern is the amount of material that is required for excavation. As indicated in Figure 51 and Table 5, significant cut volumes are required to obtain the required ditch grade.

Alternative 2-B built on Alternative 2-A by adding a berm downstream of the ditch. Adding the 2.5 m berm further reduces flooding (Figure 52). The only portion of the berm that is overtopped is located in the center of the ditch where the topography is such that a valley reduces both the ditch slope and berm top elevation. Here, due to the volume and subsequent momentum, the flow runs up-hill in this portion, creating a back-water
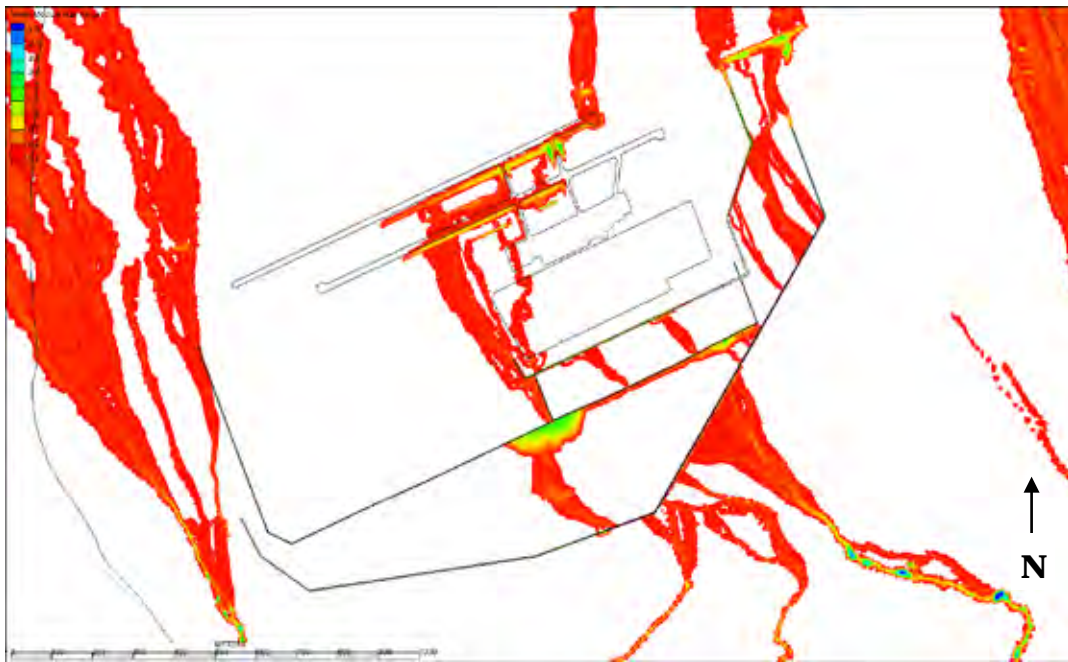
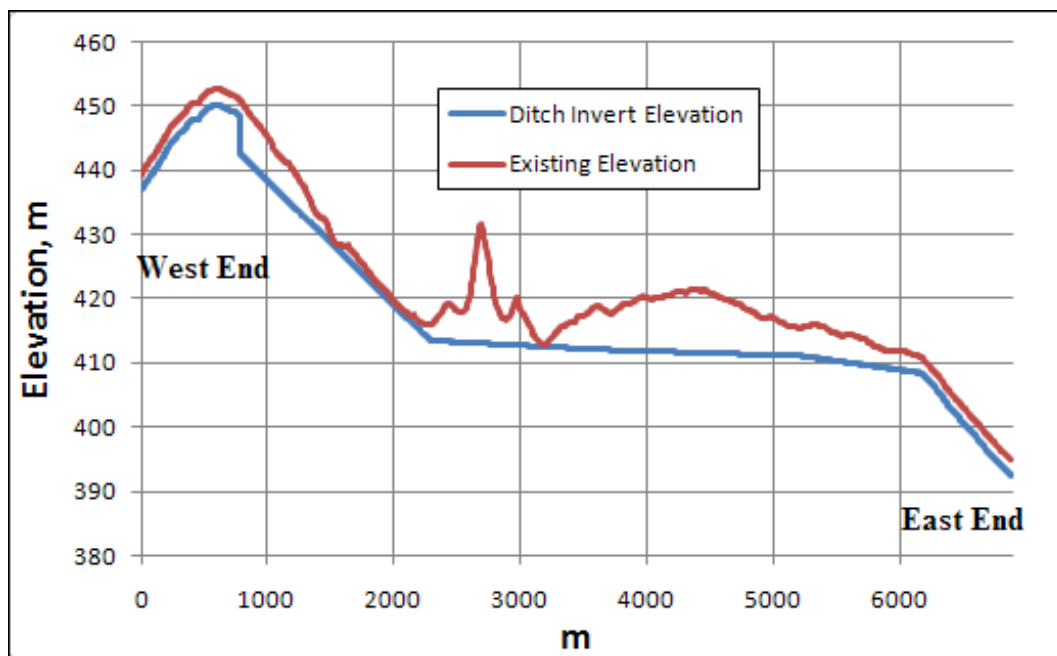Figure 50. Alternative 2-A maximum inundation depth, m.

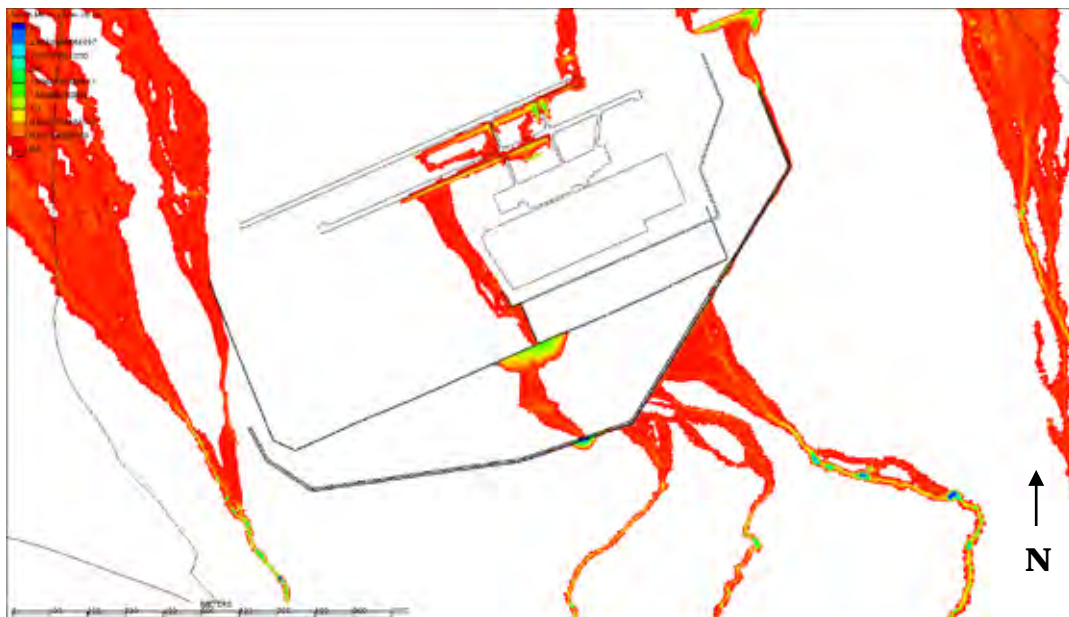Figure 51. Profile views of ditch invert and existing elevation grade.

Figure 52. Alternative 2-B maximum inundation depth, m.

effect which overtops the berm. The simulation indicates that an additional berm height of 2 meters will be required at this location. Figure 52 also indicates that the ditch section that slopes toward the west is unnecessary. Removal of this portion would take out the portion of the ditch and berm that is overtopped.

Figures 53 – 59 present a series of time lapse contour plots illustrating the dynamic behavior of the Alternative 2-B.

Figure 53. Alternative 2-B inundation depths, at 3 hours, m.
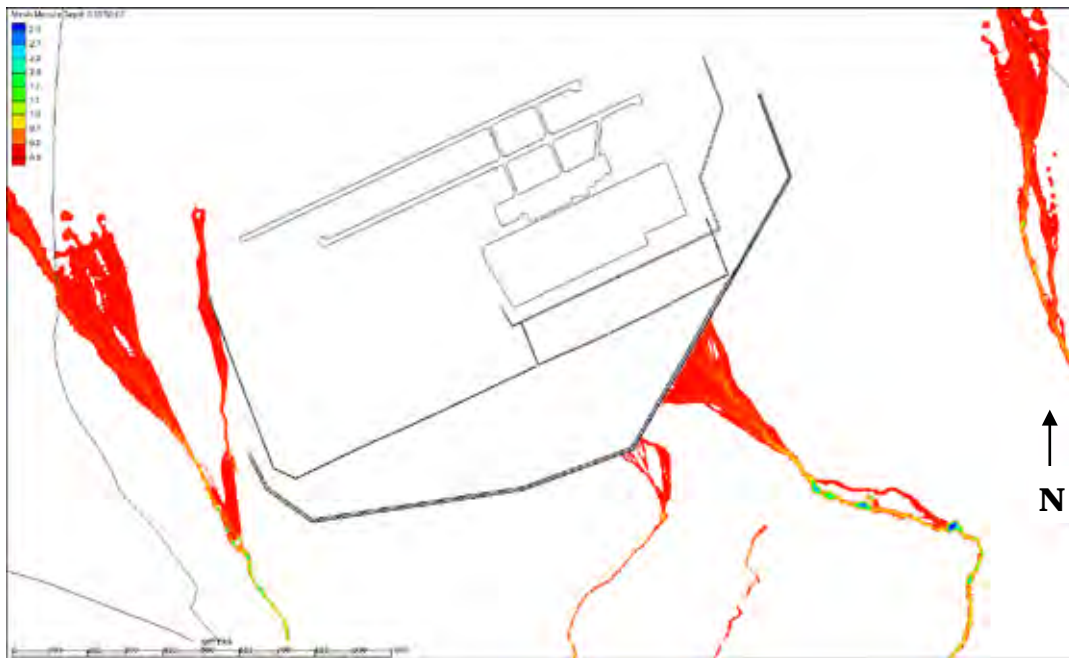
Figure 54. Alternative 2-B inundation depths, at 3.5 hours, m.
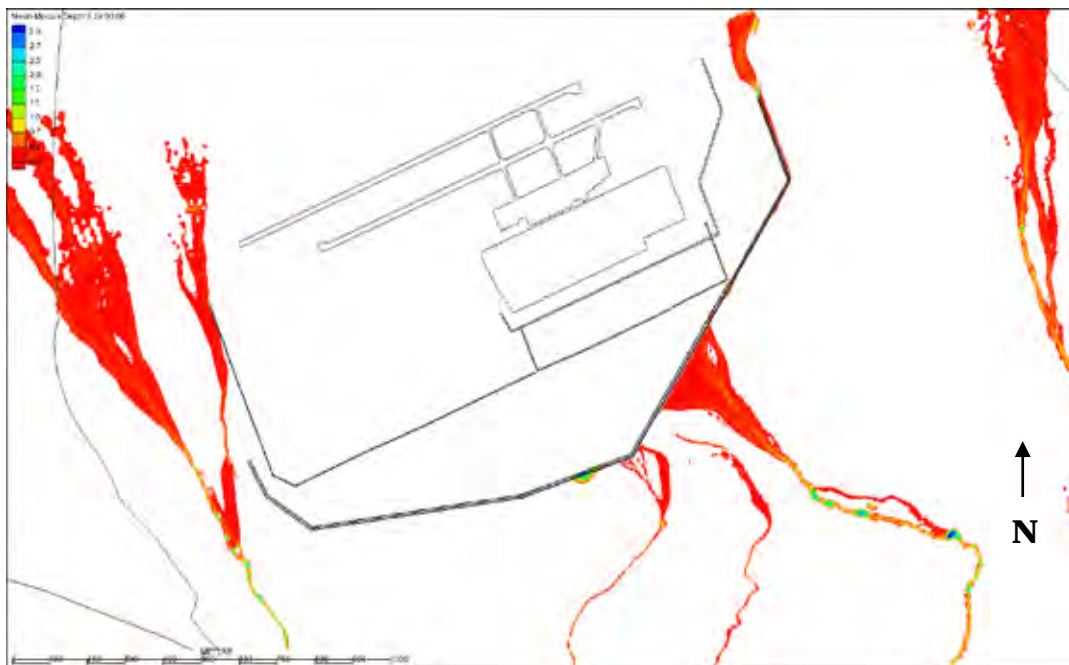
Figure 55. Alternative 2-B inundation depths, at 4 hours, m.
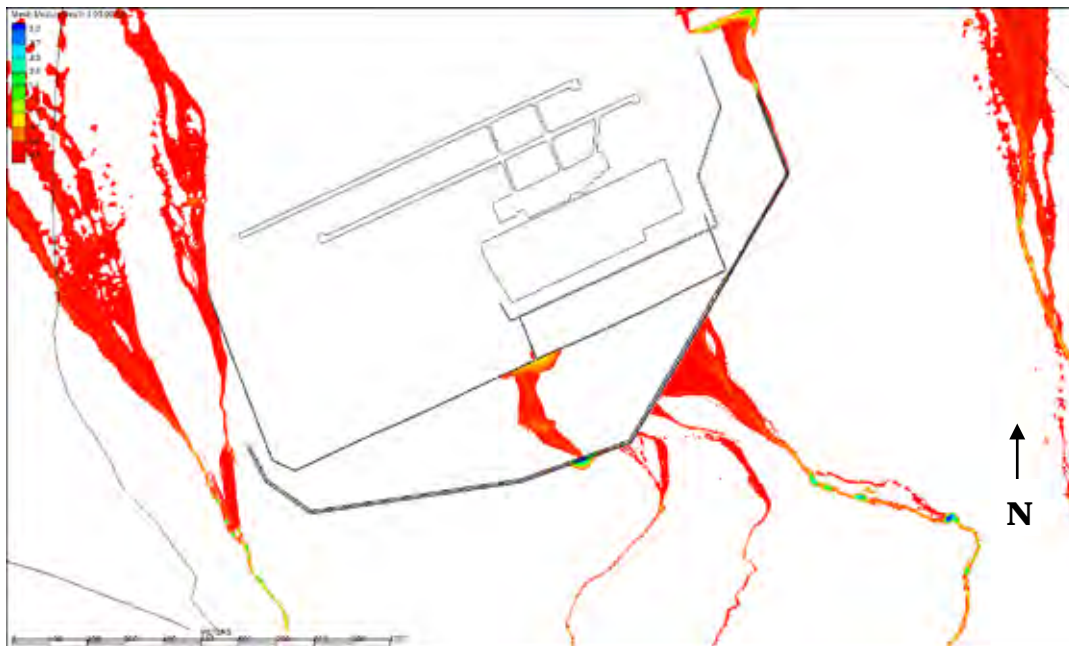
Figure 56. Alternative 2-B inundation depths, at 5 hours, m.

Figure 57. Alternative 2-B inundation depths, at 7.5 hours, m.
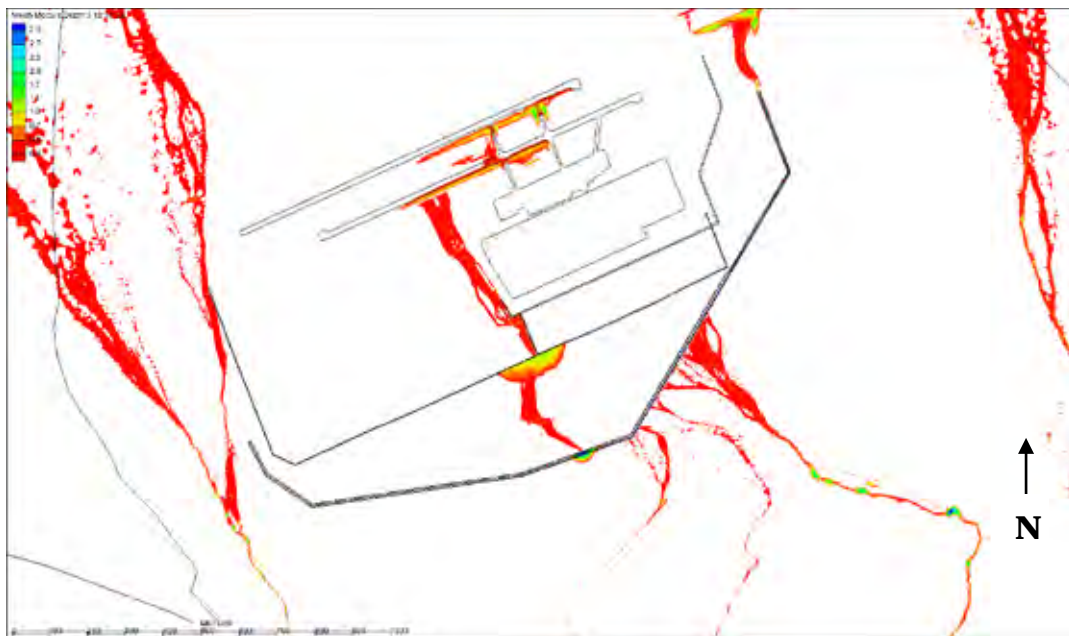
Figure 58. Alternative 2-B inundation depths, at 12 hours, m.

Figure 59. Alternative 2-B inundation depths, at 24 hours, m.

7.3   Alternative 3

As shown in Figure 60, Alternative 3-A successfully defends against the 24 hr, 20 year, indicating that implementing Alternative 3-A will potentially mitigate flooding from upstream sources. This insures that the in-Base drainage system is not overwhelmed, allowing for drainage of local run-off. There is one location that additional height on the berm is needed to contain the flood flow (see Figures 60 and 61).
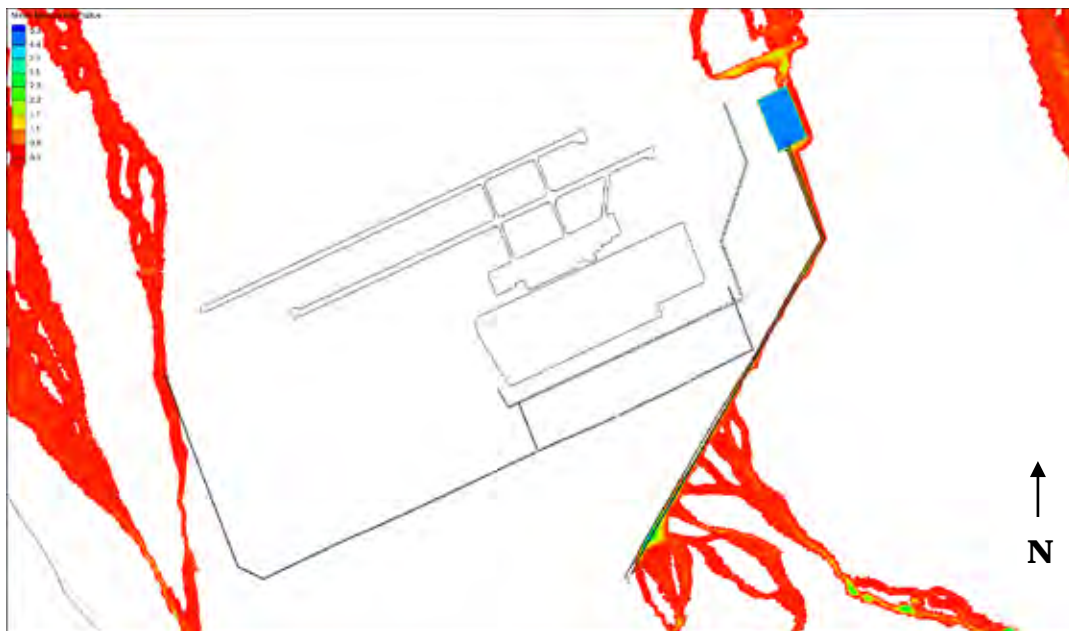
Figure 60. Alternative 3-A maximum inudation depth, m.
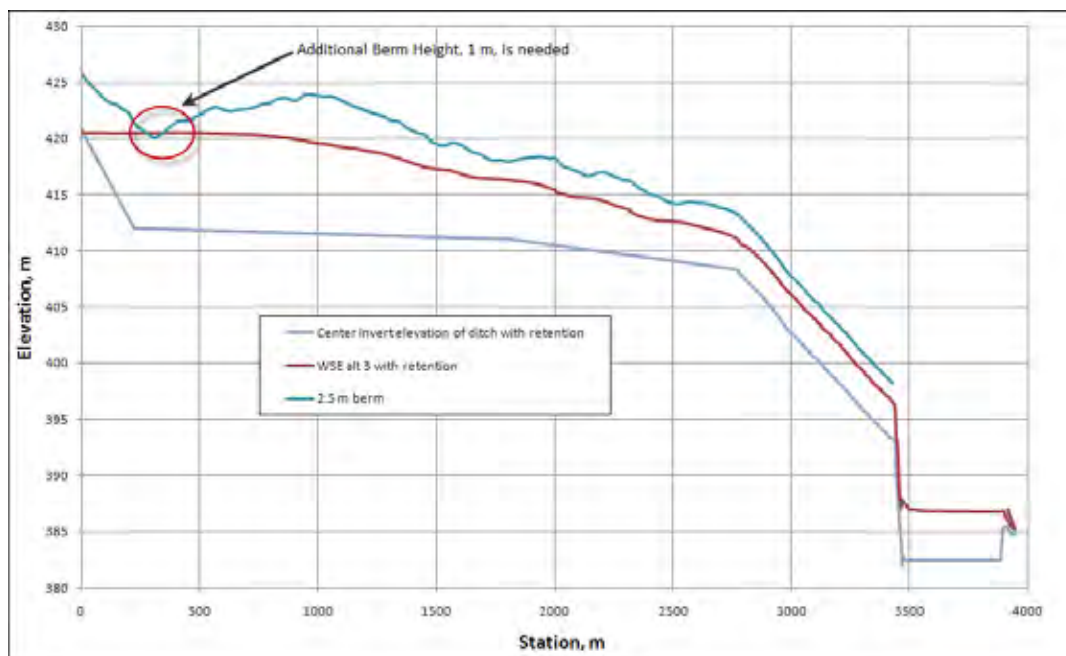
Figure 61. Alternative 3-A maximum water surface elevation profile.

The discharge of the retention basin was simulated by means of a broad-crested weir built into the topography of the mesh. There is 0.5 m of freeboard and the width of the weir is 30 m. This configuration does not have a base flow structure, and only discharges when the retention basin is filled. Discharge, as shown in Figure 62, is peaking at 27 m^3 and quickly tails off to a much lower discharge that averages 15 m^3.
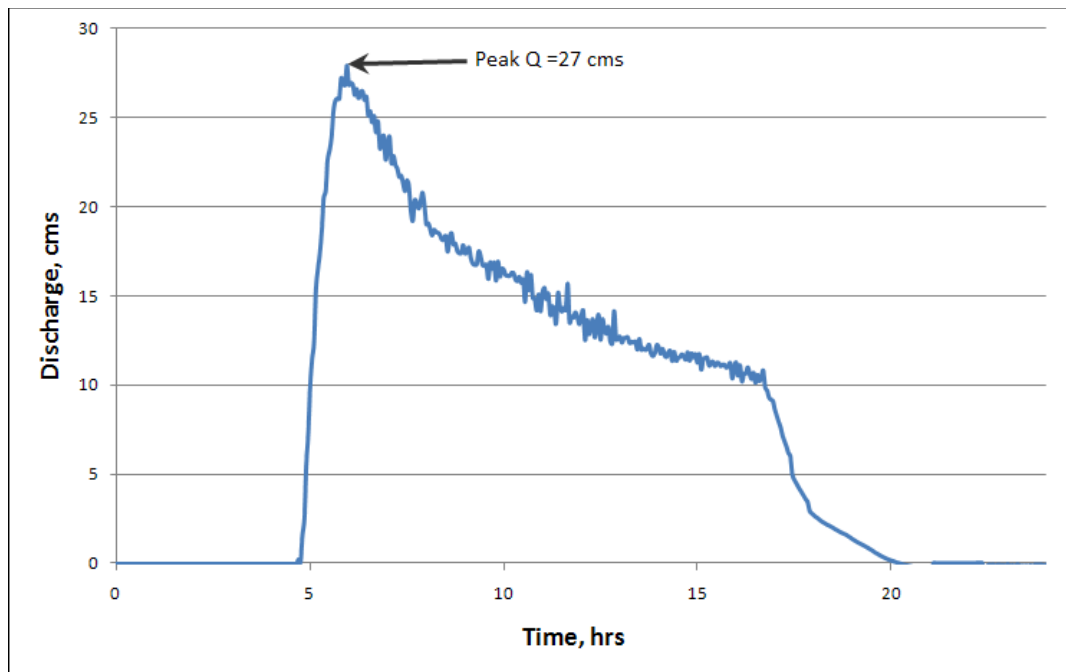
Figure 62. Alternative 3-A retention basin dowstream discharge.

Figures 63 – 69 present a series of time lapse contour ploots illustrating the dynamic behavior of the design event simulation for Alternative 3-A.
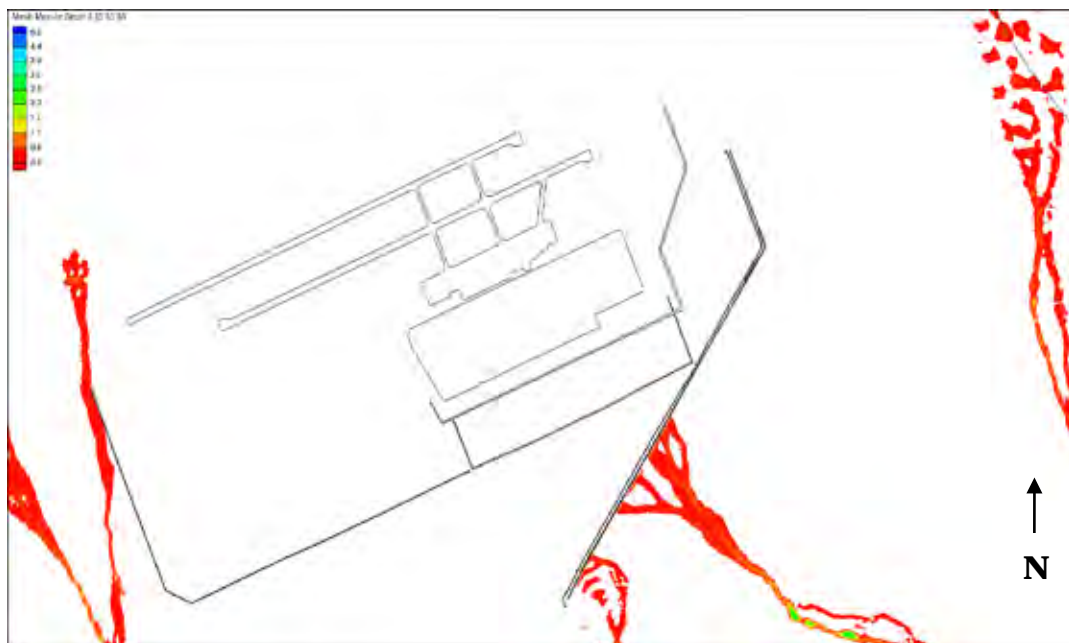
Figure 63. Alternative 3-A inundation at 3 hours into simulation, m.
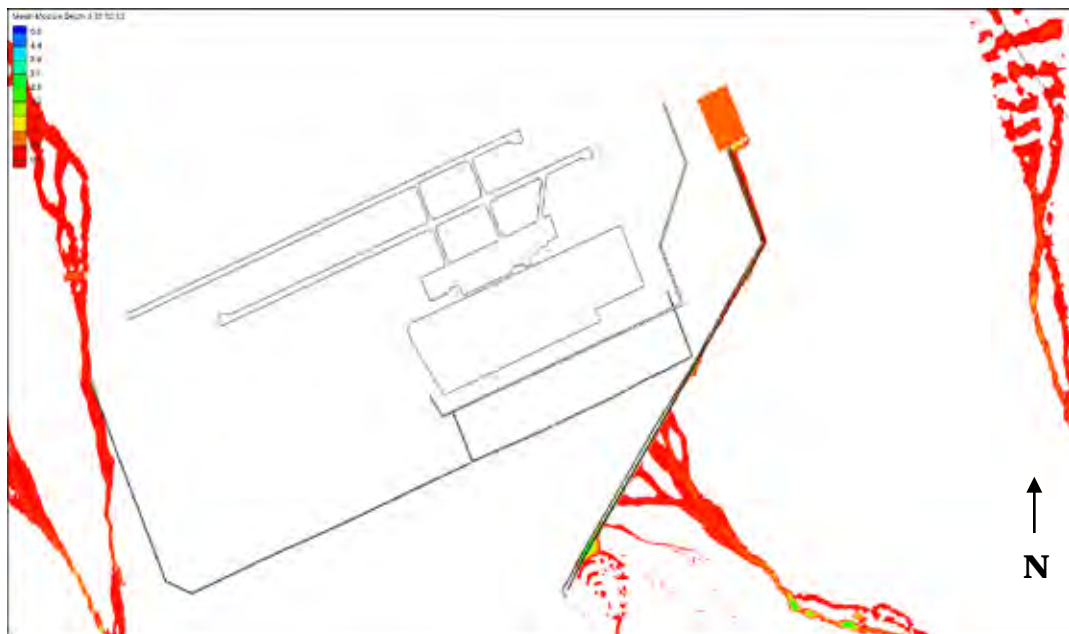
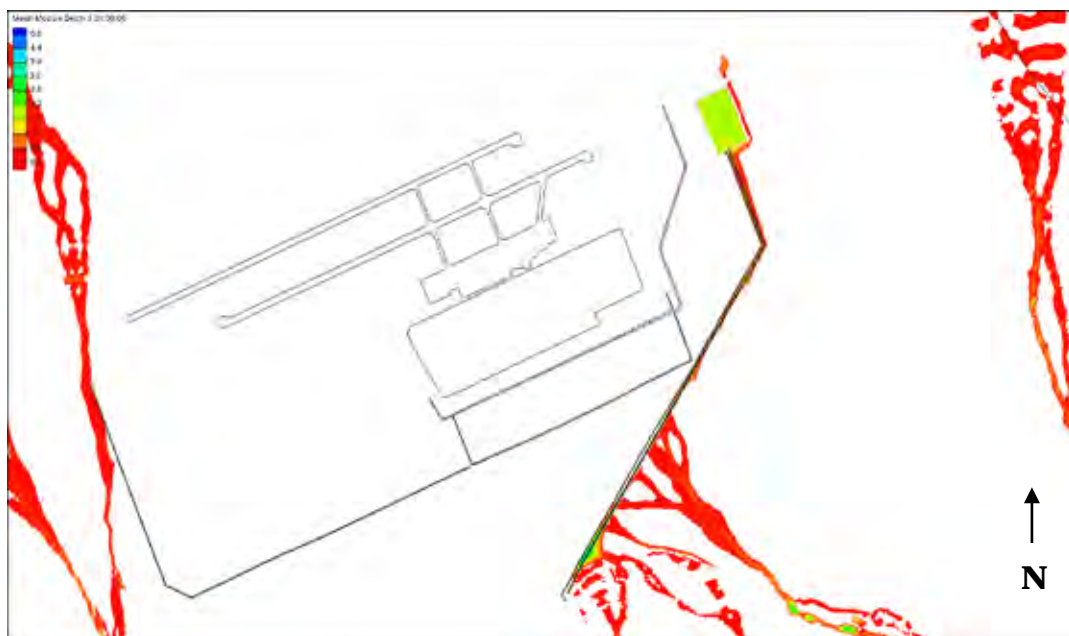Figure 64. Alternative 3-A inundation at 3.5 hours into simulation, m.

Figure 65. Alternative 3-A inundation at 4 hours into simulation, m.
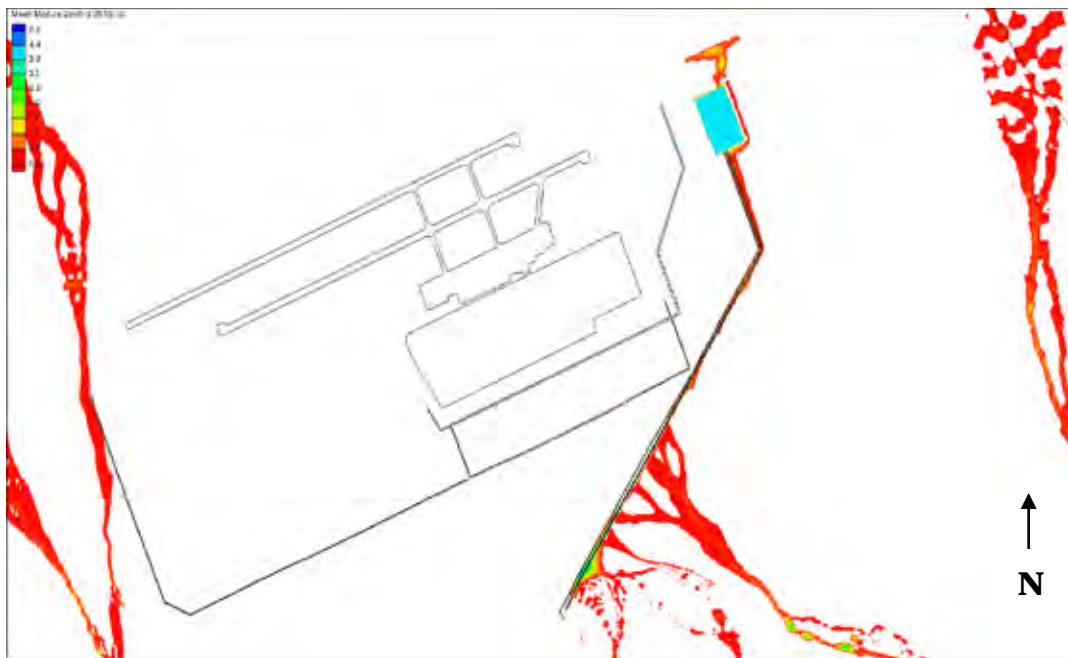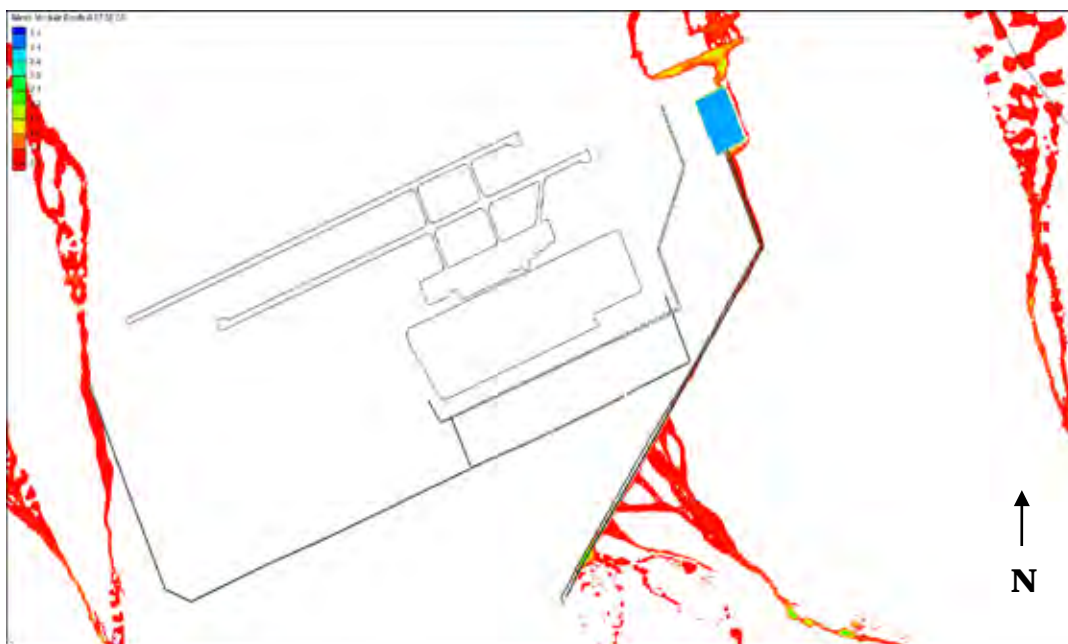
Figure 66. Alternative 3-A inundation at 5 hours into simulation, m.

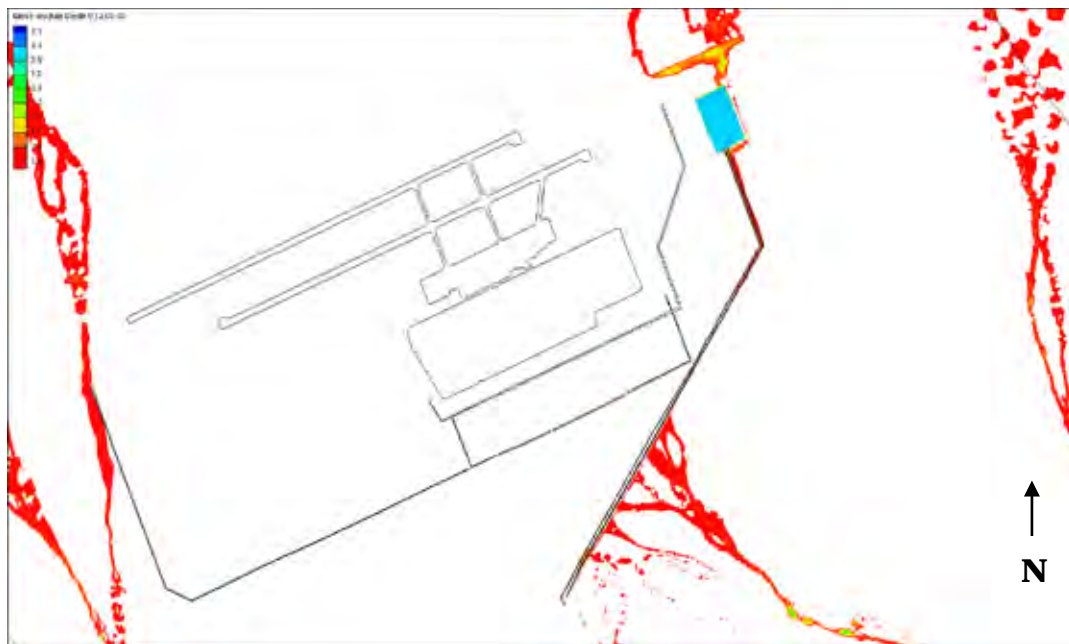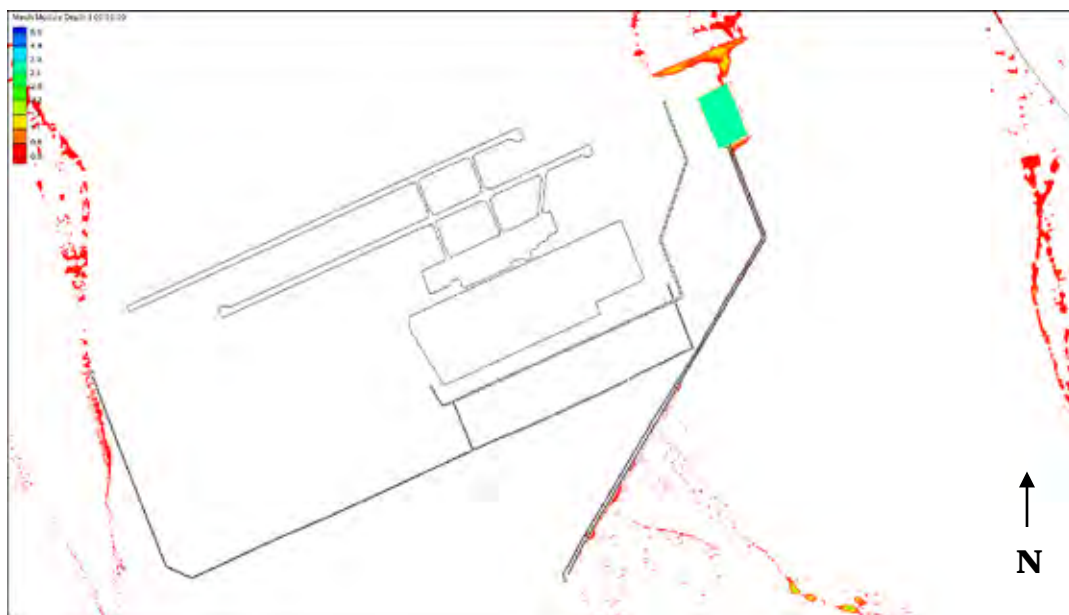Figure 67. Alternative 3-A inundation at 7.5 hours into simulation, m.

Figure 68. Alternative 3-A inundation at 12 hours into simulation, m.

Figure 69. Alternative 3-A inundation at 24 hours into simulation, m.

Alternative 3-B was just as effective as Alternative 3-A (see Figure 70). However, Alternative 3-B simulated a higher peak discharge, 64 m³, released downstream, as shown in Figure 71. In addition, the berm, as noted in Figure 72, will require greater height to provide the protection shown in Figure 70. As shown in Figure 71 all flooding is mitigated on the camp. Figures 73 – 79 present a series of time lapse contour plots illustrating the dynamic behavior of design event simulation for the Alternative 3-B.
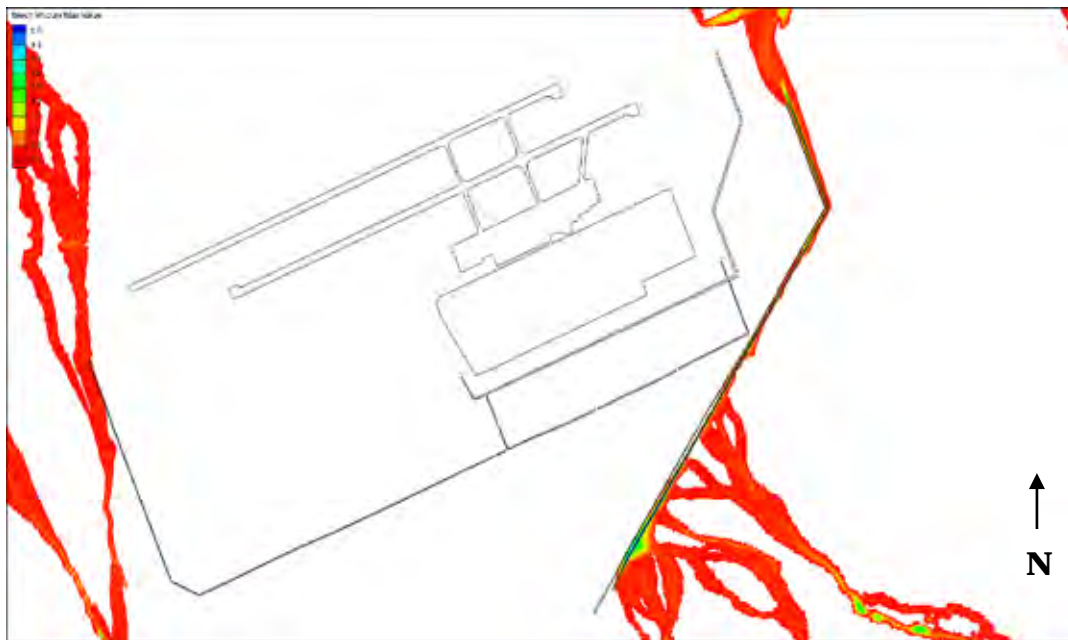
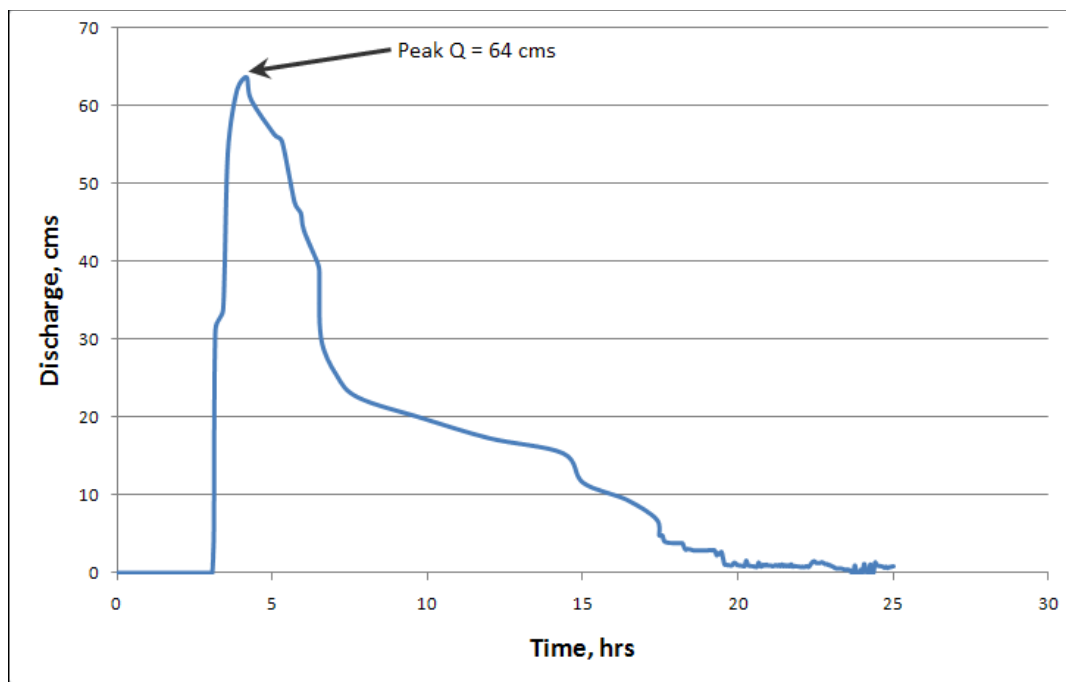Figure 70. Maximum depth flood inundation map for Alternative 3-B, m.

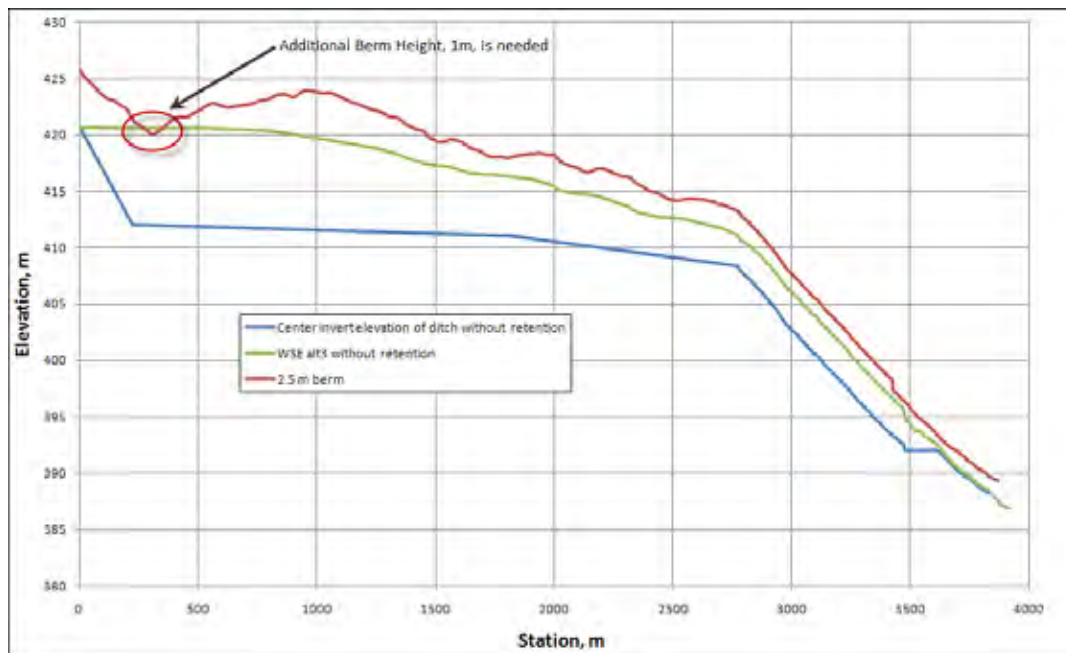Figure 71. Alternative 3-B discharge at downstream end of ditch.

Figure 72. Alternative 3-B maxium water surface elevation.
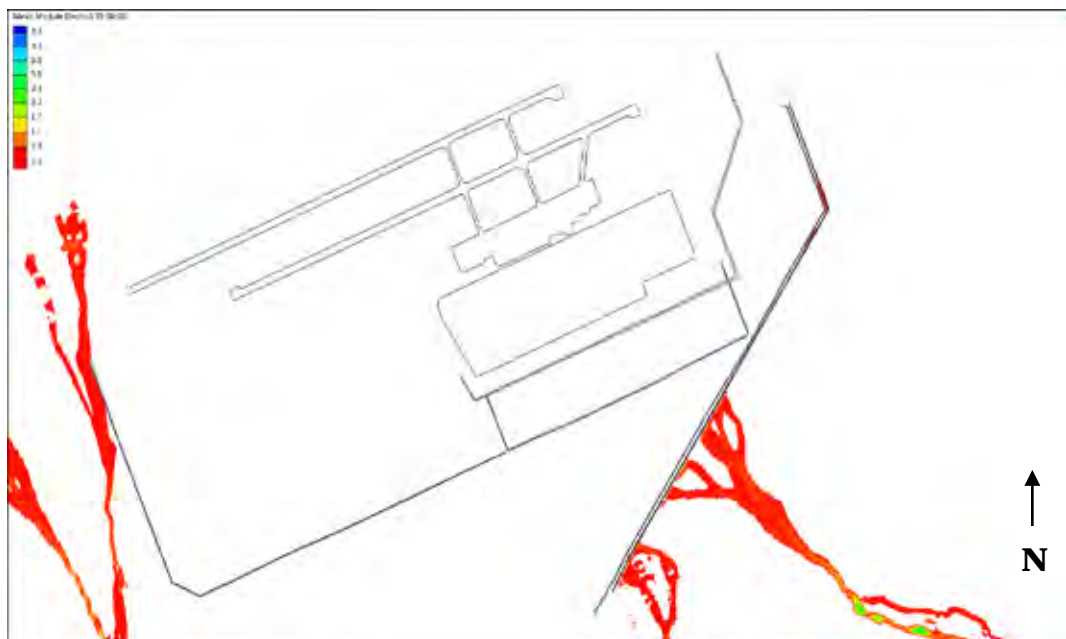

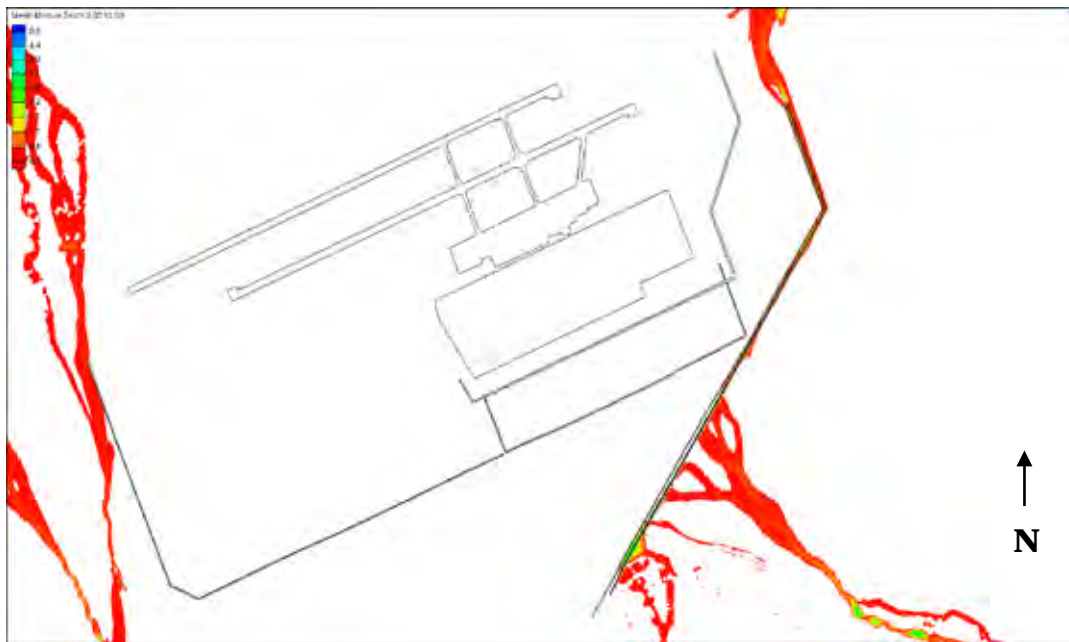Figure 73. Alternative 3-B inundation at 3 hours into simulation, m.

Figure 74. Alternative 3-B inundation at 3.5 hours into simulation, m.
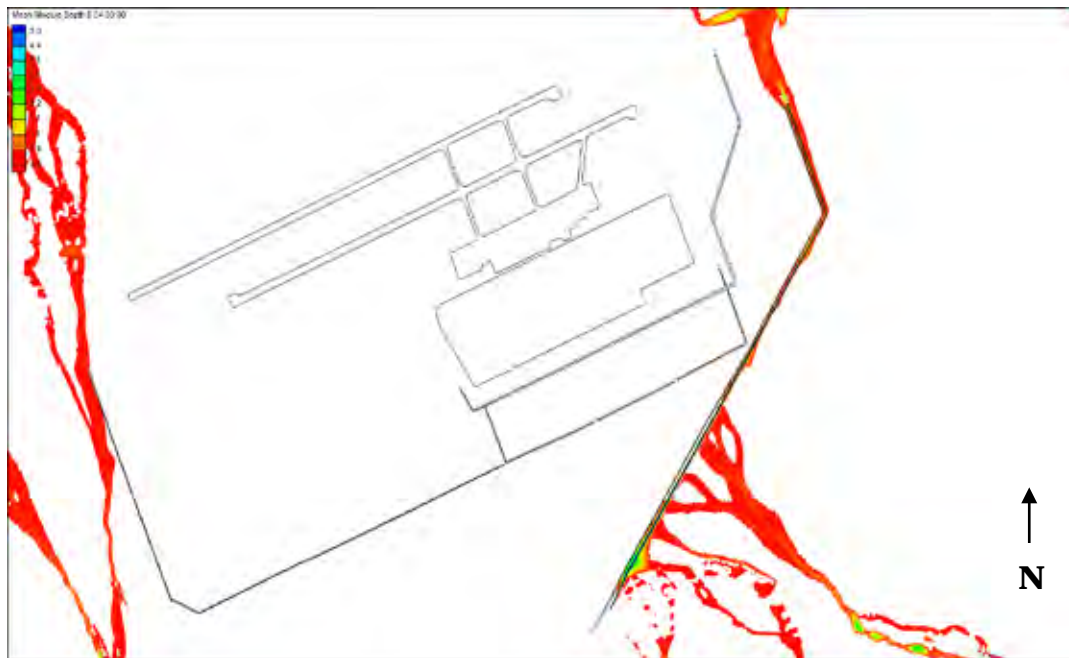

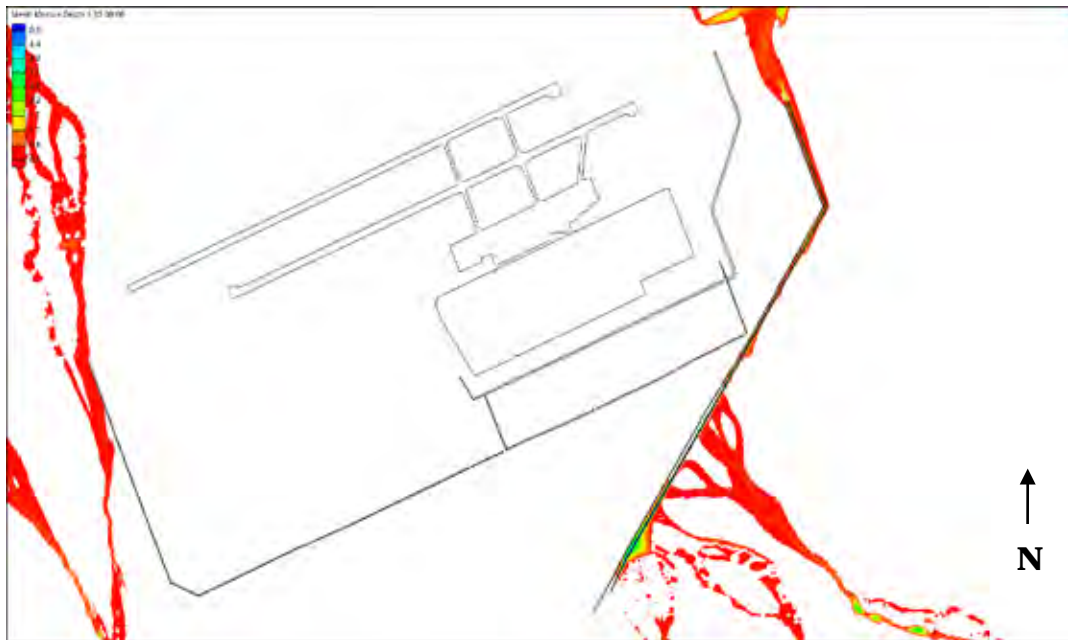Figure 75. Alternative 3-B inundation at 4 hours into simulation, m.

Figure 76. Alternative 3-B inundation at 5 hours into simulation, m.
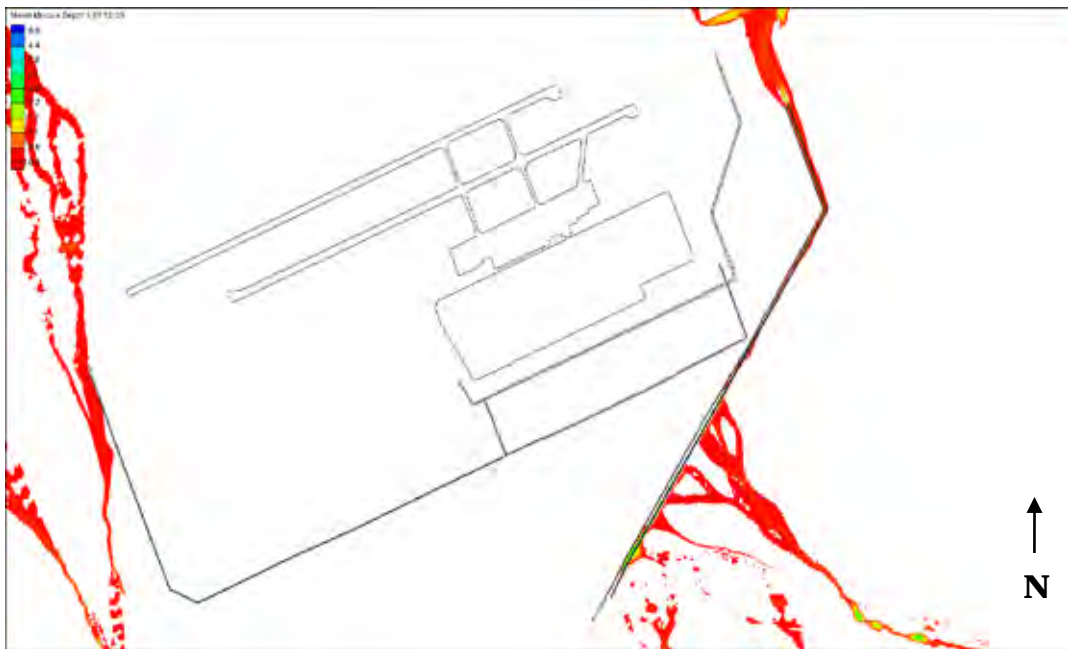

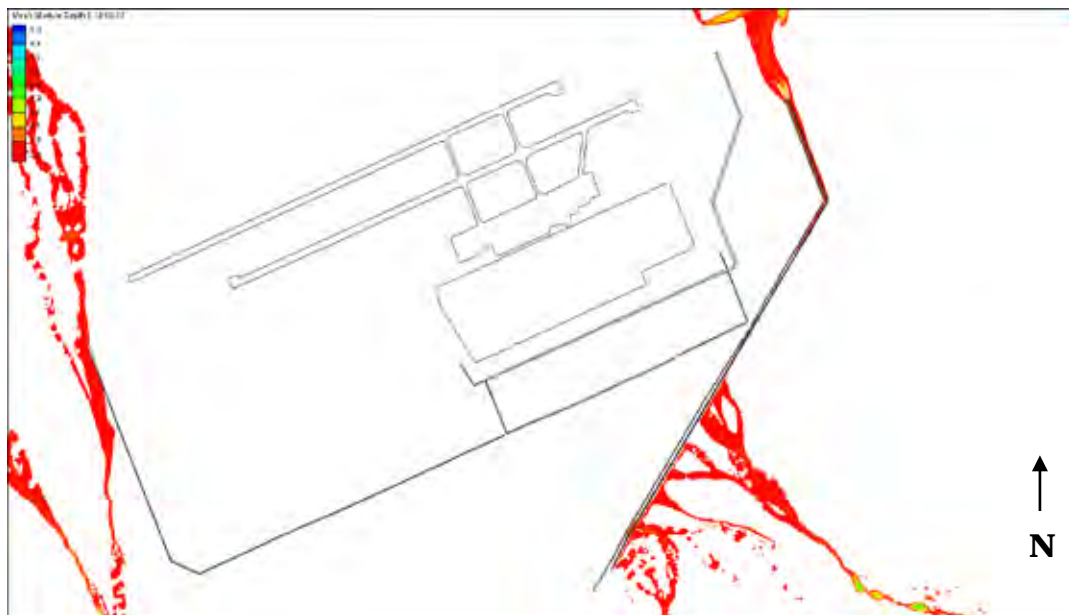Figure 77. Alternative 3-B inundation at 7.5 hours into simulation, m.

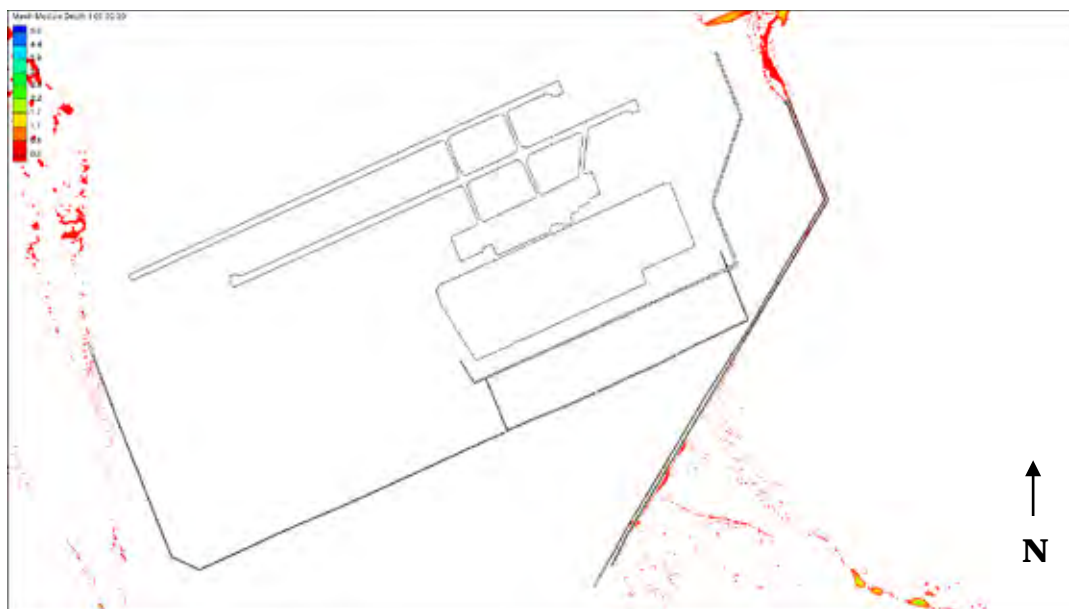Figure 78. Alternative 3-B inundation at 12 hours into simulation, m.

Figure 79. Alternative 3-B inundation at 24 hours into simulation, m.

Likewise, Alternative 3-C was just as effective as Alternatives 3-A and 3-B (see Figure 80). Even with less retention basin volume, Alternative 3-C does prevent flooding of the camp, as shown in Figure 81. The peak discharge from the retention basin is still 27 m³, as shown in Figure 81, but has a higher sustained flow averaging 18 m³. Similar to the other Alternative 3 simulations, the berm will need to be raised, as shown in Figure 82.
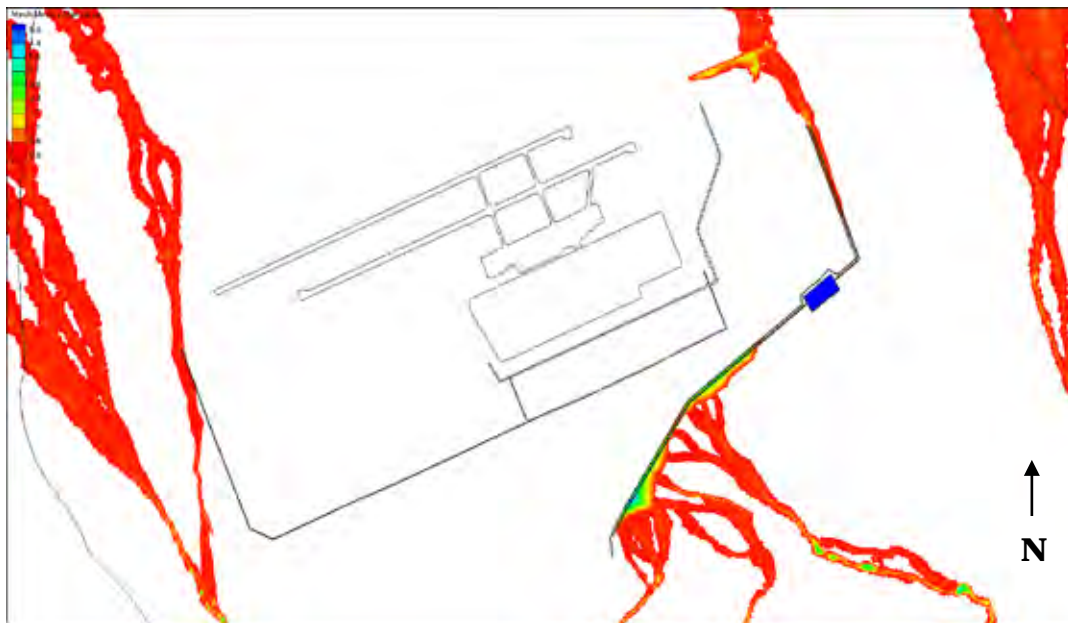
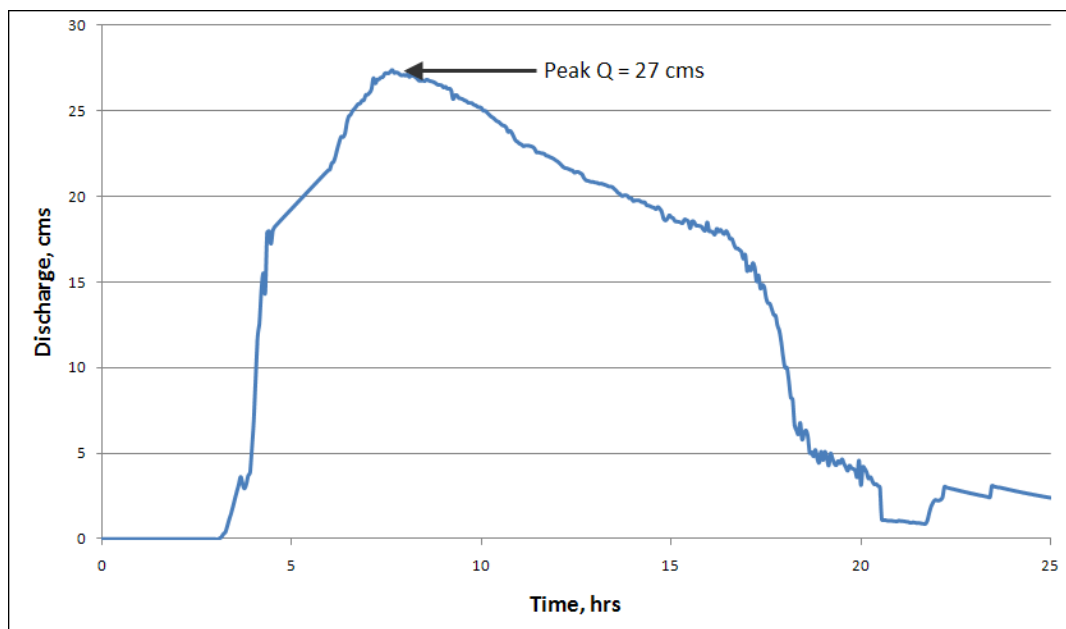Figure 80. Alternative 3-C maximum flood inundation depth, m.

Figure 81. Alternative 3-C discharge at downstream end of retention basin.

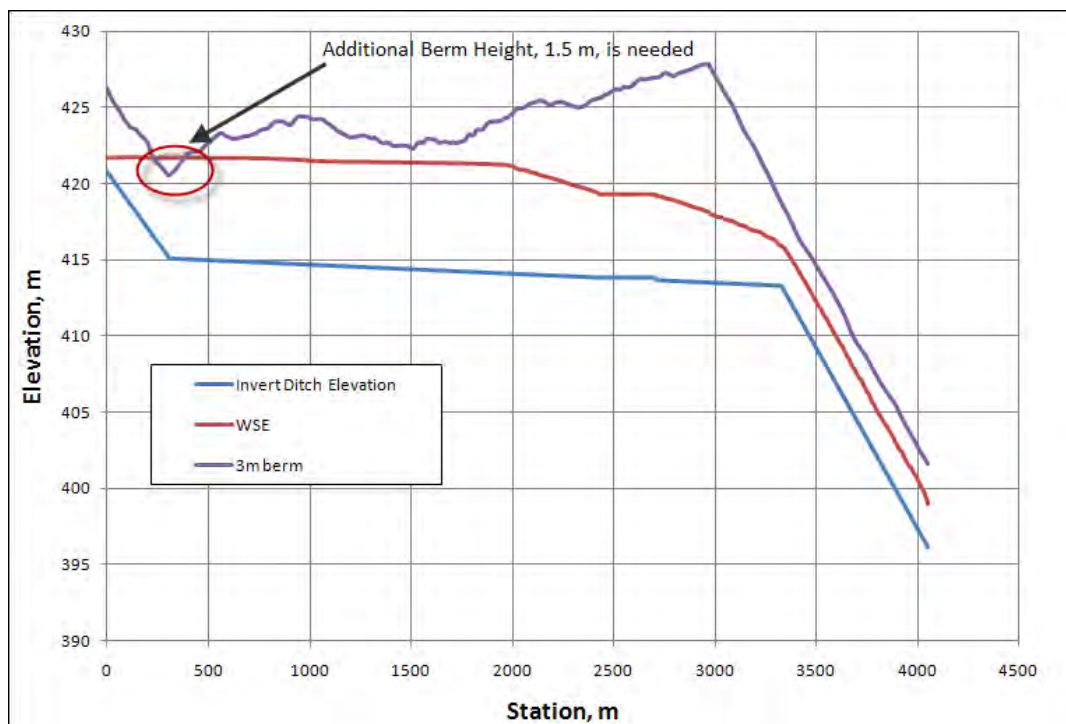Figure 82. Alternative 3-C A maximum water surface elevation profile.

Figures 83 - 89, present a series of time lapse contour plots illustrating the dynamic behavior of the Alternative 3-B.

Figure 83. Alternative 3-C inundation at 3 hours into simulation, m.

Figure 84. Alternative 3-C inundation at 3.5 hours into simulation, m.

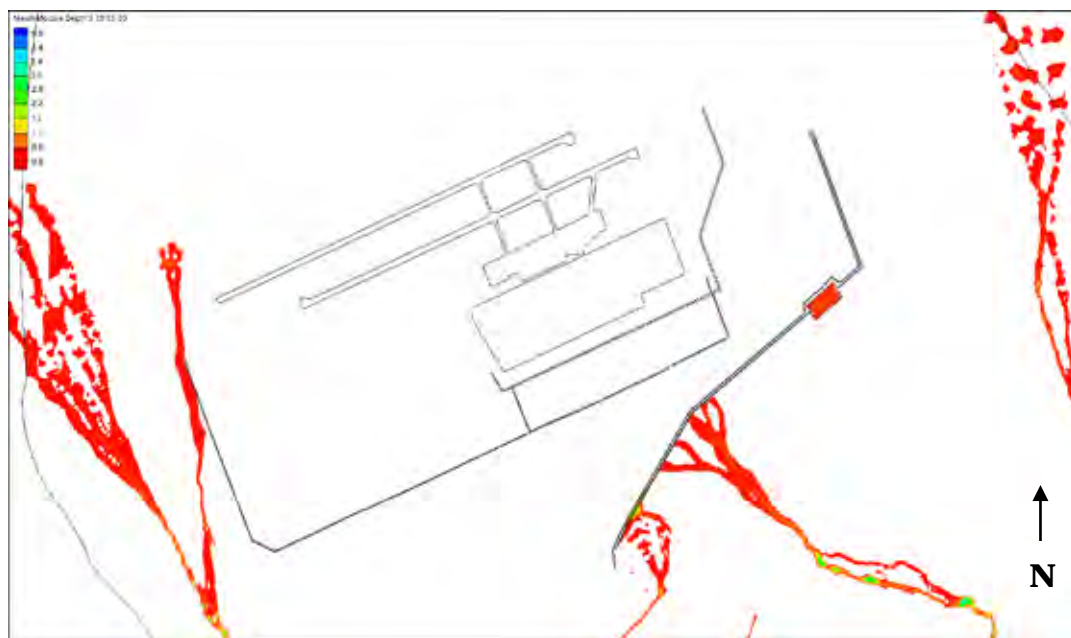Figure 85. Alternative 3-C inundation at 4 hours into simulation, m.

Figure 86. Alternative 3-C inundation at 5 hours into simulation, m.
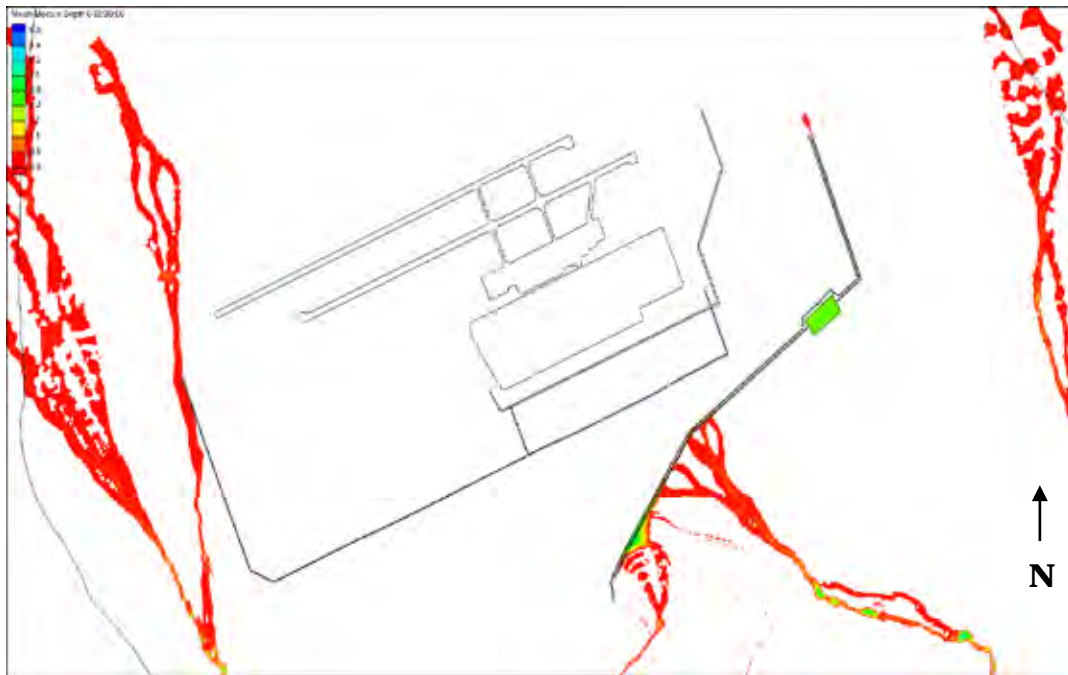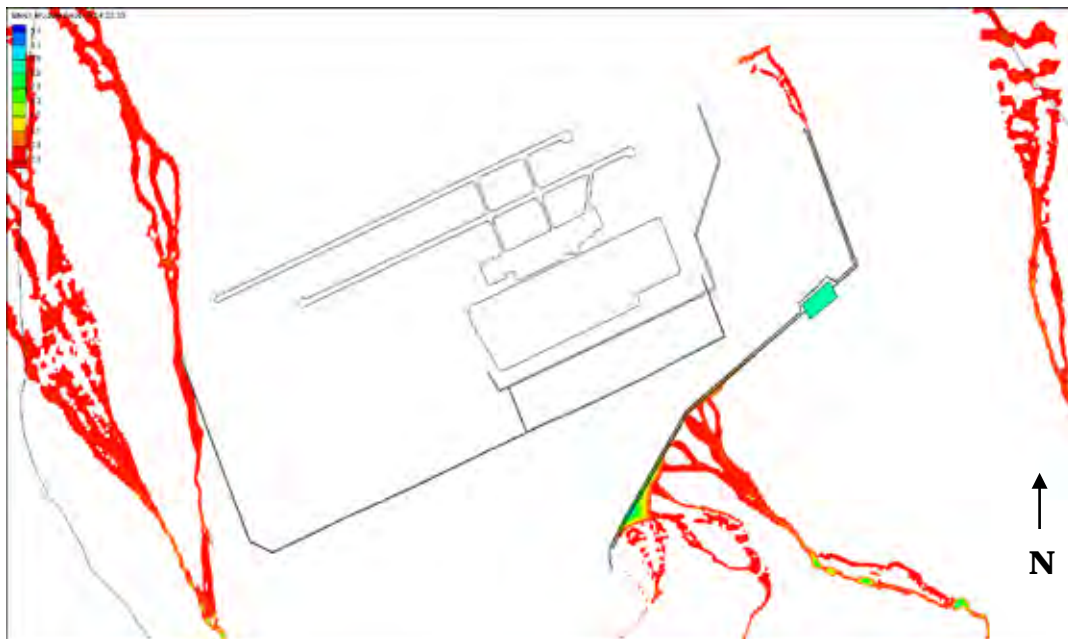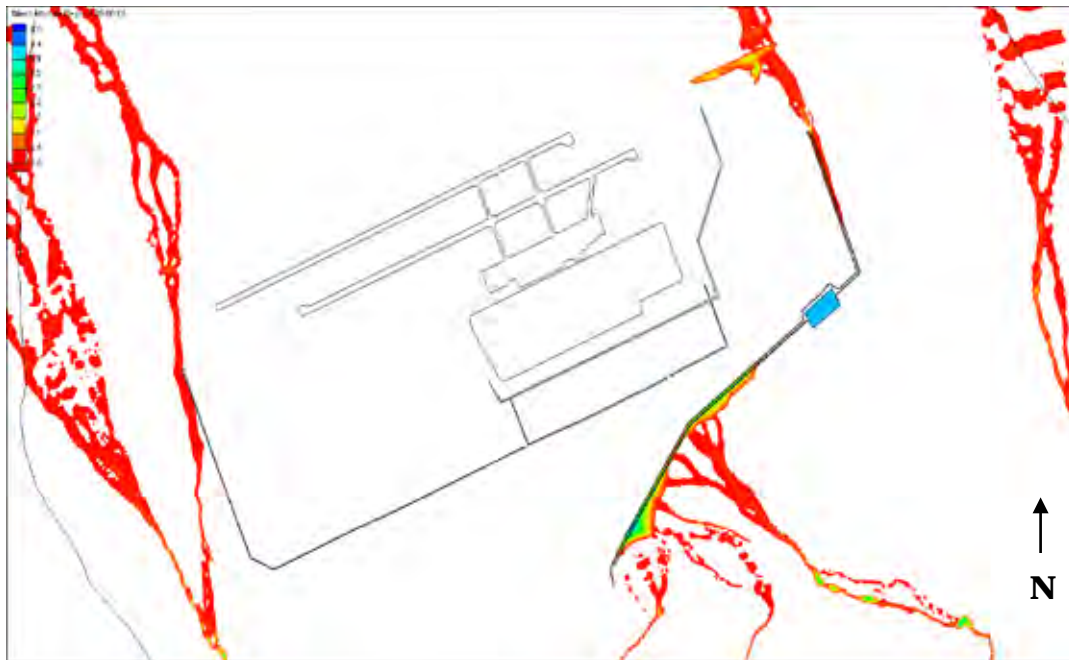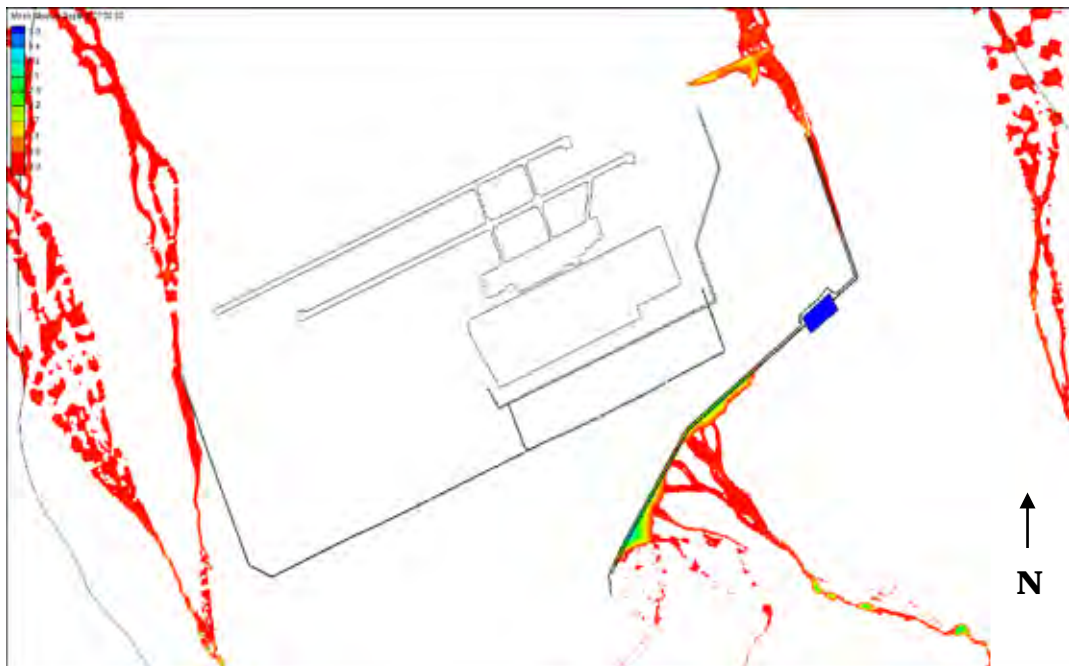

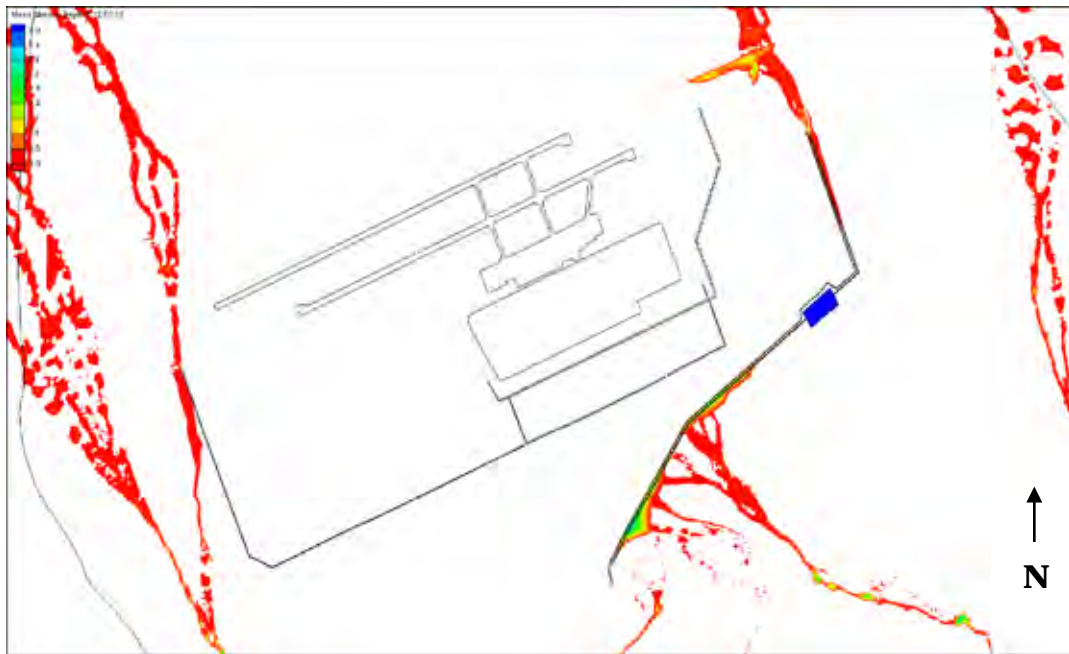Figure 87. Alternative 3-C inundation at 7.5 hours into simulation, m.

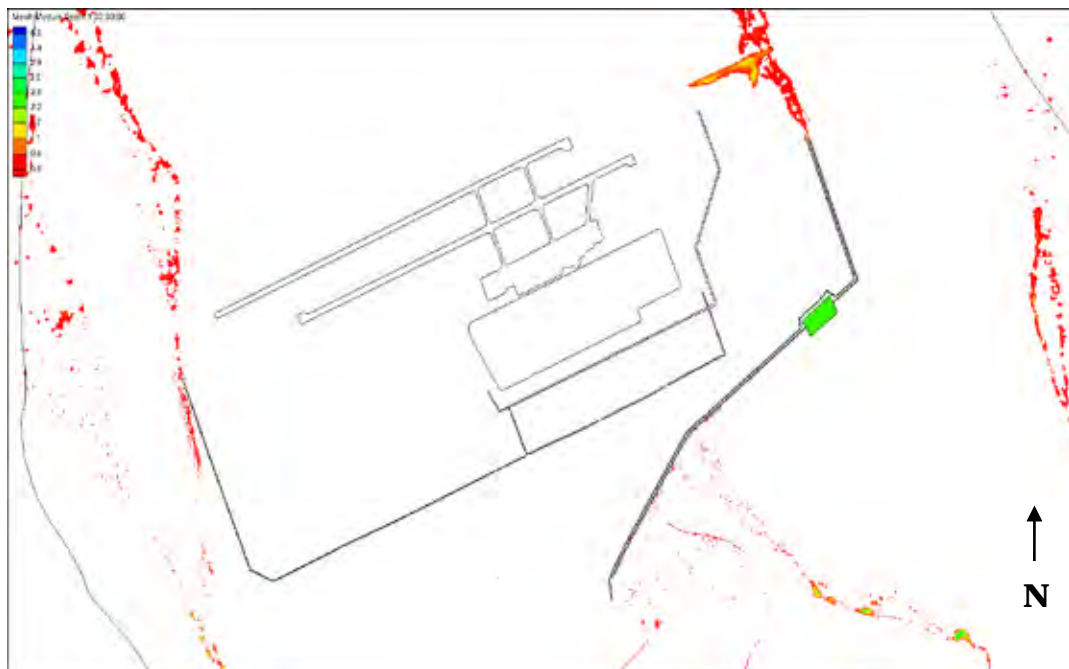Figure 88. Alternative 3-C inundation at 12 hours into simulation, m.

Figure 89. Alternative 3-C inundation at 24 hours into simulation, m.

8 German Alternative

At the request of TAN, a German alternative measure was simulated and compared to the three TAN alternatives. It is shown to be effective in delaying and reducing the hydrograph peak and for having the potential for eliminating flooding in sensitive areas.

The German alternative includes the addition of a solid wall to Alternative A-2, both on the east and west side of the entrance gate, located on the southeast wall (see Figure 90). These two additional walls flank the entrance and prevent flow from entering the camp. As illustrated in Figure 91, the eastern wall must be extended further than its western counterpart. The eastern wall is approximately 610 meters long while the western is 285 meters. The walls provide the necessary area for storage and are aligned such that flow cannot enter the gate. The culverts through which flow passes should have control structures such that a manageable discharge can be accommodated by the in-Base drainage system. Note that no control at these other locations is implemented in the simulation. However, the model effectively shows the flood mitigation potential for this plan (see Figure 91).

Figures 92 – 98, present a series of time lapse contour plots illustrating the dynamic behavior of the simulation of the design event for German alternative.
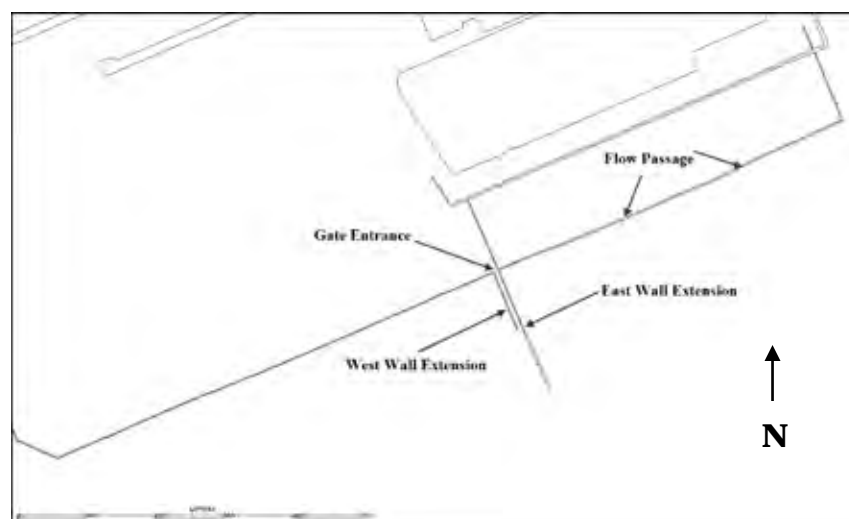
Figure 90. German alternative configuration.
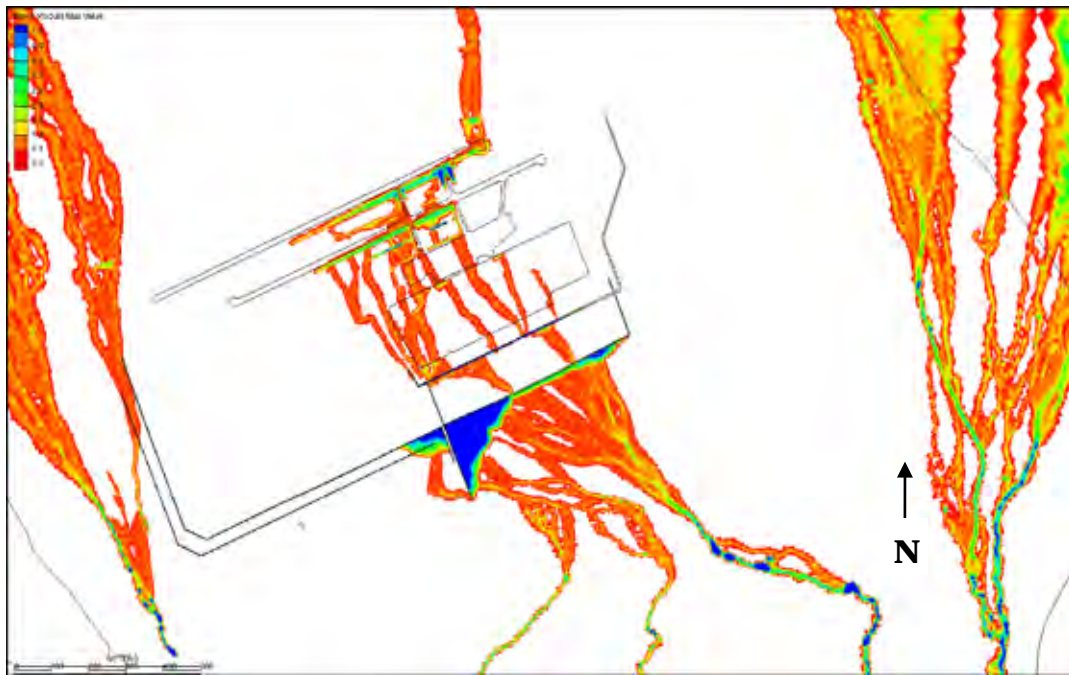
Figure 91. Maximum flood inundation depth, German alternative, m.

Figure 92. German alternative A-2 inundation depths, at 3 hours, m.

Figure 93. German alternative A-2 inundation depths, at 3.5 hours, m.

Figure 94. German alternative A-2 inundation depths, at 4 hours, m.

Figure 95. German alternative A-2 inundation depths, at 5 hours, m.

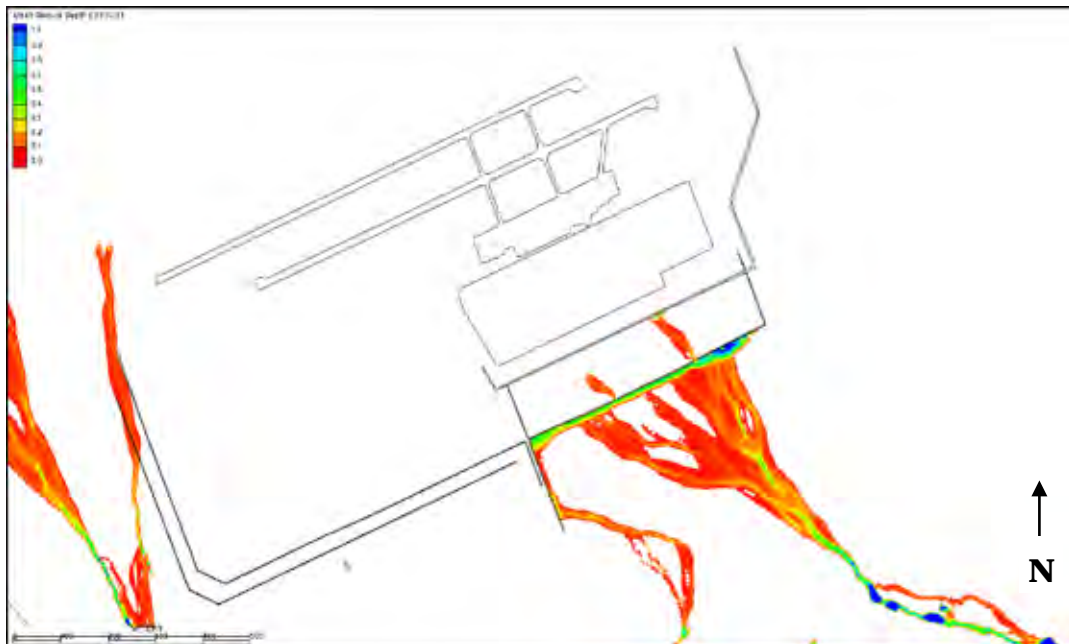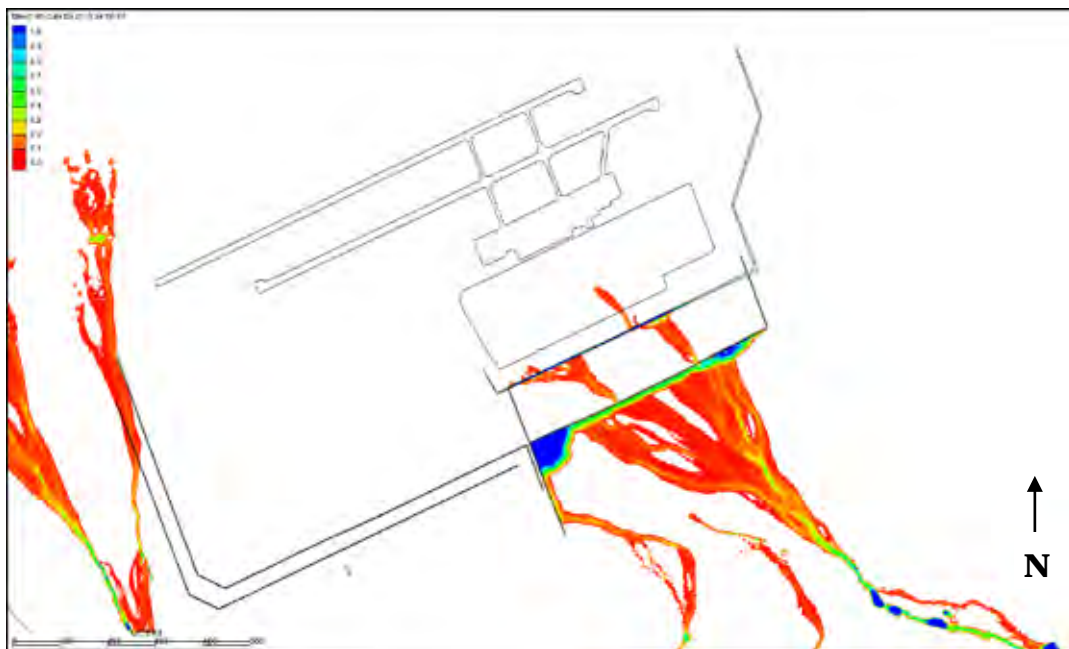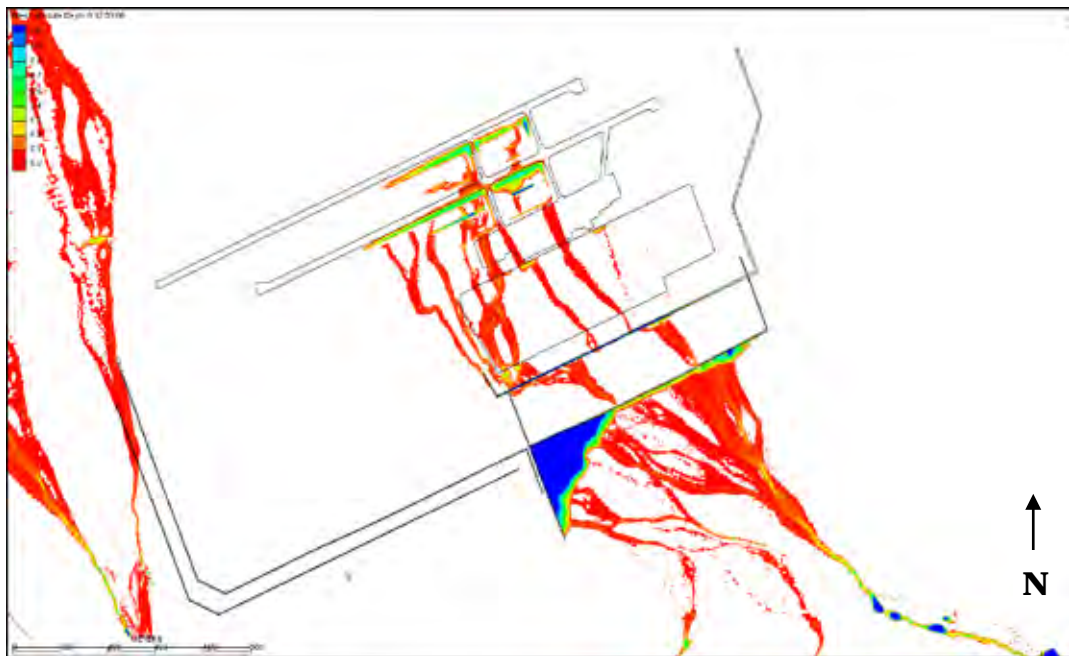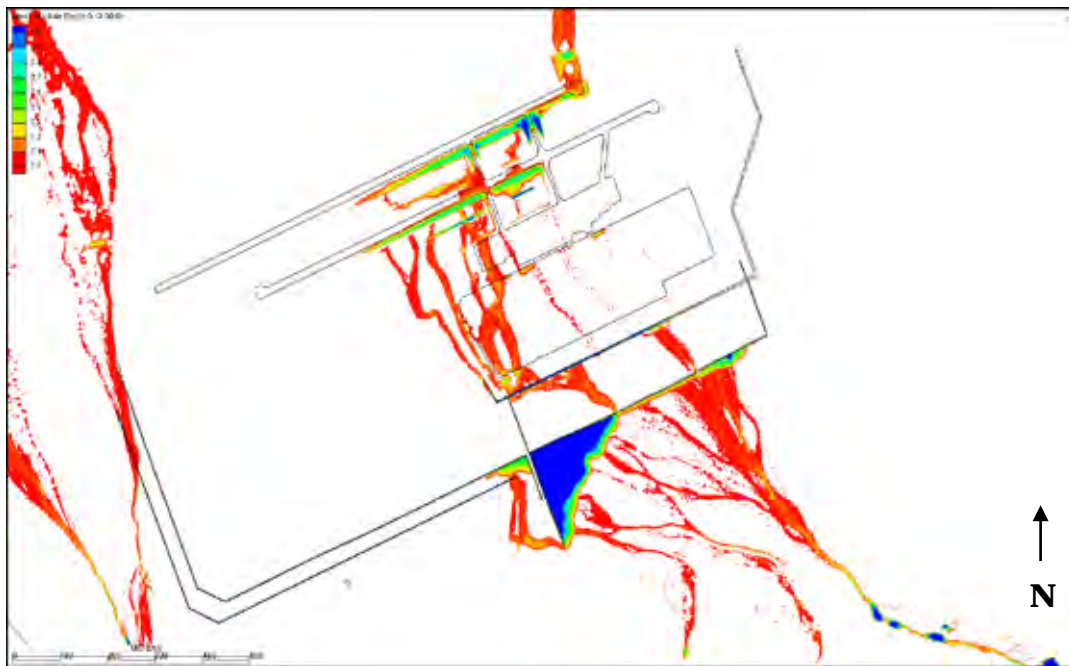Figure 96. German alternative A-2 inundation depths, at 7.5 hours, m.

Figure 97. German alternative A-2 inundation depths, at 12 hours, m.
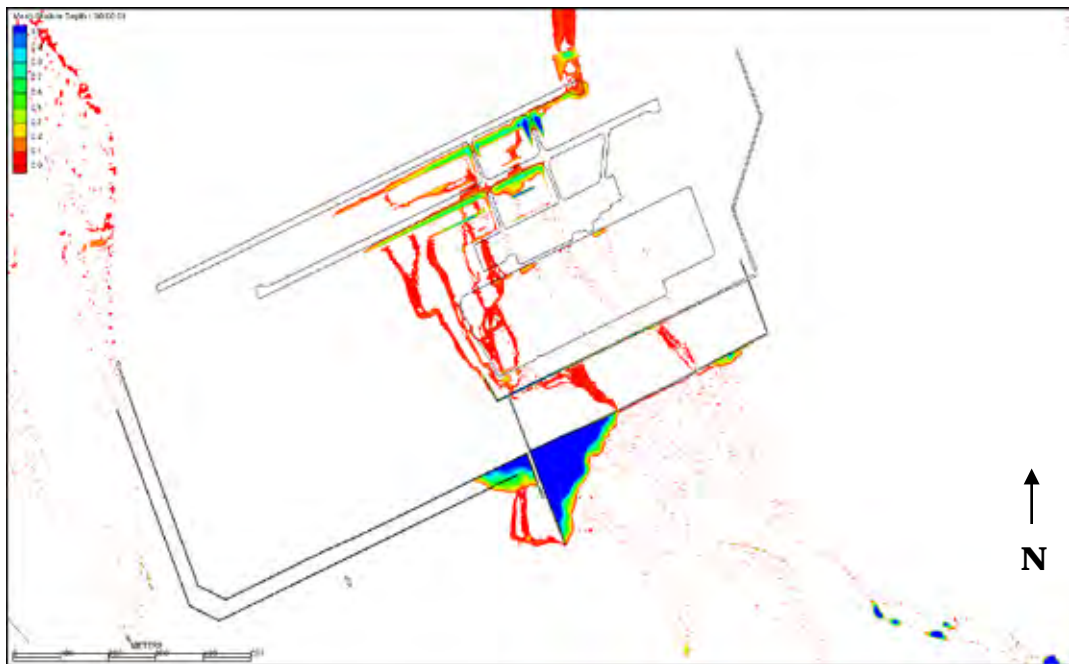
Figure 98. German alternative A-2 inundation depths, at 24 hours.

9 Conclusions

The existing condition and alternative measure model simulations provided insight to several key issues:

- Existing condition simulations showed extensive flooding of Camp Marmal due to upstream watersheds;
- Sensitivity analysis showed changes in flooding extents from variations in Manning's n roughness coefficients and runoff return periods;
- Greater flooding occurred with a higher Manning's n and larger runoff event;
- Four alternatives were simulated with the 20 year, 24 hour event with Manning's n equal to 0.03 over the majority of the domain;
- The simulation for Alternative 1 showed it to be unsuccessful in protecting the camp from flooding;
- The simulation for Alternative 2 showed that half of the protective ditch upstream of the camp was un-necessary;
- Three configurations were simulated for Alternative 3;
- All three Alternative 3 configurations potentially provided comprehensive protection;
- A German recommended alternative was simulated and shown to potentially provide protection for smaller events.

10 Recommendations

Based on the alternative simulations, Alternative 3 provided the most comprehensive protection. This alternative will potentially mitigate flooding on the camp and adjoining airfield. Regardless of the selected alternative, it is recommended that the final design should be simulated with the AdH model prior to construction.

References

Berger, R. C. 1997. HIVEL 2D v2.0 Users Manual. Vicksburg, MS: Waterways Experiment Station, U.S. Army Corps of Engineers.

Chow, V. T. 1959. *Open channel hydraulics*. New York, NY: McGraw-Hill.

HEC_HMS. http://hec.usace.army.mil/software/hec-hms/

Reeve, D. E., A. Soliman, and P. Z. Lin. 2008. *Numerical study of combined overflow and wave overtopping over a smooth impermeable seawall*. Coastal Engineering. 55, 155-166.

Rodi, W. 1993. Turbulence models and their application in hydraulics – a state of the art review, Balkema: Leiden.

Savant, G., C. Berger, T. McAlpin, and J. Tate. 2010. *Application of Adaptive Hydraulics (ADH) to Rapidly Evolving Hydrodynamic Flows*. Vicksburg, MS: System Wide Water Resource Program, U.S. Army Engineer Research and Development Center. (https://swwrp.usace.army.mil/portal/alias__swwrp/lang__en-US/tabID__3637/DesktopDefault.aspx)

Savant, G., C. Berger, T. O. McAlpin, and J. N. Tate. 2011. Efficient implicit finite-element hydrodynamic model for dam and levee breach. *J. Hydraul. Eng.* 137, 1005.

REPORT DOCUMENTATION PAGE

1. REPORT DATE *(DD-MM-YYYY)*	2. REPORT TYPE	3. DATES COVERED *(From - To)*
March 2012	Final report	

4. TITLE AND SUBTITLE	5a. CONTRACT NUMBER
Camp Marmal Flood Study	5b. GRANT NUMBER
	5c. PROGRAM ELEMENT NUMBER

6. AUTHOR(S)	5d. PROJECT NUMBER
Jeremy A. Sharp, Steve H. Scott, Mark R. Jourdan, and Gaurav Savant	5e. TASK NUMBER
	5f. WORK UNIT NUMBER

7. PERFORMING ORGANIZATION NAME(S) AND ADDRESS(ES)	8. PERFORMING ORGANIZATION REPORT NUMBER
U.S. Army Engineer Research and Development Center Coastal and Hydraulics Laboratory 3909 Halls Ferry Road Vicksburg, MS 39180-6199	ERDC/CHL TR-12-5

9. SPONSORING / MONITORING AGENCY NAME(S) AND ADDRESS(ES)	10. SPONSOR/MONITOR'S ACRONYM(S)
U.S. Army Corps of Engineers, Afghanistan Engineer District - North Attn: Qalaa House Kabul, Afghanistan, APO, AE 09356 441 G Street NW , Washington, DC 20314-1000	11. SPONSOR/MONITOR'S REPORT NUMBER(S)

12. DISTRIBUTION / AVAILABILITY STATEMENT

Approved to public release; distribution is unlimited.

13. SUPPLEMENTARY NOTES

14. ABSTRACT

The ERDC-CHL conducted the Camp Marmal Flood Study at the request of the Afghanistan District. Major flooding at the camp occurs from upland sources. The purpose of the study was to determine the effectiveness of flood mitigation alternatives. The AdH 2-D shallow water finite element model was implemented for the study. Boundary conditions for AdH were generated with HEC-HMS. The HEC model used local rainfall data to generate the routed run-off hydrograph from upstream watersheds. Existing conditions were simulated with the generated hydrographs to determine the potential flood characteristics of the facility and for the comparison of the alternatives. Additionally, a sensitivity analysis was conducted to determine the effect of variations in Manning's n and run-off return periods. The 20 year, 24 hour event was selected for simulation in the alternatives. The District provided three alternatives for evaluation in the model. Alternative 1 provided minimum protection. Alternative 2 showed increased protection, but there were several issues of concern that made it less ideal. Alternative 3 potentially provided the most flood mitigation. However, prior to construction of any alternative it is recommended that the final design be simulated in the AdH model.

15. SUBJECT TERMS	Flood plain	Inundation	
Flooding	Flood protection	Multi-dimensional modeling	Wetting and drying
Flood diversion	Hydrograph	Streams and retention	

16. SECURITY CLASSIFICATION OF:			17. LIMITATION OF ABSTRACT	18. NUMBER OF PAGES	19a. NAME OF RESPONSIBLE PERSON
a. REPORT	b. ABSTRACT	c. THIS PAGE			19b. TELEPHONE NUMBER *(include area code)*
UNCLASSIFIED	UNCLASSIFIED	UNCLASSIFIED		78	